THE SURFACE BEHAVIOR AND POLYMERIZATION OF ANILINE CONTAINING SURFACTANTS IN LANGMUIR MONOLAYERS

By

LEROY JOSEPH KLOEPPNER

A DISSERTATION PRESENTED TO THE GRADUATE SCHOOL
OF THE UNIVERSITY OF FLORIDA IN PARTIAL FULFILLMENT
OF THE REQUIREMENTS FOR THE DEGREE OF
DOCTOR OF PHILOSOPHY

UNIVERSITY OF FLORIDA

1998

This dissertation is dedicated to my loving wife, Jennifer
and child, Alexandra.

ACKNOWLEDGEMENTS

The author would like to acknowledge the following people for their help and kindness in conducting and preparing the work within this document. I would like to acknowledge and thank my research advisor, Dr. Randy Duran, for his support. I would also like to acknowledge the members of the Duran research group, especially Dr.Tim Herod for many hours of help and friendship. A special thanks needs to be given to Mark Watson for his help in synthesizing 1,22-bis(2-aminophenyl)docosane, Dr. Hiep Ly for his help in determining the electrochemical potentials of various compounds, Don Cameron for his help with molecular weight determinations, and Christy Nixon for editing this document. Most of all, I would like to thank Jennifer Batten whose help and support made much of this work possible.

Financial and technical support was given by the Office of Naval Research, the National Science Foundation, KSV Instruments, Microcal Software, and E. M. Separations.

TABLE OF CONTENTS

ACKNOWLEDGMENTS ii

LIST OF TABLES vi

LIST OF FIGURES vii

ABSTRACT xiii

1 INTRODUCTION 1

1.1 Langmuir Films 1
1.1.1 Surface Pressure 3
1.1.2 Surface Potential 5
1.1.3 Langmuir-Blodgett Films 7
1.2 Monolayer Reactions 9
1.2.1 Electrical Factors 10
1.2.2 Interfacial Pressure Factors 11
1.2.3 Kinetic Studies 13
1.3 Monolayer Polymerizations 14
1.3.1 Langmuir Film Polymerization 17
1.3.2 Aniline Monolayer Polymerization 18
1.4 Polyaniline 20
1.4.1 History 21
1.4.2 Synthesis 24
1.4.3 Mechanism 24
1.4.4 Degradation of Polyaniline 29
1.5 Oxidative Polymerization 30
1.6 Overview of Dissertation 30

2 EXPERIMENTAL 33

2.1 Introduction 33
2.2 Materials 34

2.2.1 Pentadecylaniline 34
2.2.1.1 Pentadecyltriphenylphosphonium bromide 34
2.2.1.2 General procedure for the synthesis of pentadecylaniline 35
2.2.1.3 2-Pentadecylaniline 36
2.2.1.4 3-Pentadecylaniline 36
2.2.1.5 4-Pentadecylaniline 36
2.2.2 (1-Octadecynyl)aniline 37
2.2.2.1 General procedure for the synthesis of (1-octadecynyl)aniline 37
2.2.2.2 2-(1-octadecynyl)aniline 38
2.2.2.3 3-(1-octadecynyl)aniline 38
2.2.3 Methyl 17-(2-aminophenyl) heptadecanoate and 17-(2-aminophenyl)heptadecanoic acid 39
2.2.3.1 Methyl 16-hydroxyhexadecanoate 39
2.2.3.2 Methyl 16-bromohexadecanoate 40
2.2.3.3 15-(Carbomethoxy)pentadecyltriphenylphosphonium bromide 41
2.2.3.4 Methyl 17-(2-nitrophenyl)-16-heptadecenoate 42
2.2.3.5 Methyl 17-(2-aminophenyl)heptadecanoate 42
2.2.3.6 17-(2-Aminophenyl)heptadecanoic acid 43
2.2.4 1,22-Bis(aminophenyl)docosane 44
2.2.4.1 10-Undecenyltriphenylphosphonium bromide 45
2.2.4.2 1-(2-Nitrophenyl)-1,11-dodecadiene 45
2.2.4.3 1,22-Bis(2-nitrophenyl)-1,11,21-docostriene 46
2.2.4.4 1,22-Bis(2-aminophenyl)docosane 47
2.3 Langmuir Film Preparation 48
2.4 Monolayer Characterization 49
2.4.1 Surface Pressure vs. Mean Molecular Area Isotherms 49
2.4.2 Isobaric Stabilities 50
2.4.3 Surface Potential vs. Mean Molecular Area Isotherms 50
2.5 Polymerization 53
2.6 Additional Characterizations Methods 54
2.6.1 UV-vis 54
2.6.2 Size Exclusion Chromatography 54
2.6.3 FT-IR 54
2.6.4 Cyclic Voltammetry 55

3 THE POLYMERIZATION AND SURFACE BEHAVIOR OF ALKYL SUBSTITUTED ANILINE SURFACTANTS AT THE AIR-AQUEOUS INTERFACE 56

3.1 Introduction 56

3.2 Monolayer Characterization 57
3.3 Polymerization of Pentadecylaniline 69
3.4 Kinetics of Polymerization 74
3.5 Conclusions 90

4 SURFACE BEHAVIOR AND POLYMERIZATION OF 2- AND 3-(1-OCTADECYNYL)ANILINE AT THE AIR-AQUEOUS INTERFACE .. 92

4.1 Introduction 92
4.2 Monolayer Characterization 94
4.3 Polymerization of 1-Octadecynylaniline 101
4.4 Polymerization Kinetics 104
4.5 Conclusions 111

5 DIPOLAR ANILINE SURFACTANTS 113

5.1 Introduction 113
5.2 Synthesis 115
5.3 Monolayer Characterization 115
5.3.1 π-*A* Isotherms 116
5.3.2 ΔV-*A* Isotherms 119
5.4 Polymerization 126
5.5 Conclusions 128

6 LANGMUIR FILM POLYMERIZATION OF 1,22-BIS(2-AMINOPHENYL) DOCOSANE 130

6.1 Introduction 130
6.2 Synthesis of 1,22-Bis(2-aminophenyl)docosane 131
6.3 Monolayer Characterization 136
6.4 Polymerization 139
6.5 Conclusions 145

7 CONCLUSIONS 147

LIST OF REFERENCES 151

BIOGRAPHICAL SKETCH 161

LIST OF TABLES

Table		page
3.1	ΔG values determined from the π-*A* isotherms of 2-, 3-, and 4-pentadecylaniline between 0 and 10 mN m^{-1} surface pressures at 25 °C	69
3.2	k and k' for 2- and 3-pentadecylaniline at different surface pressures	86
4.1	The rate constant k' for 2-(1-octadecynyl)aniline at surface pressures of 5, 10, and 15 mN m^{-1} and at 25°C	107
4.2	The rate constants k' and k for 3-(1-octadecynyl)aniline at surface pressures 5 and 10 mN m^{-1} and at 25°C	107
4.3	Oxidation potentials of aniline containing surfactants in acetonitrile.	111
5.1	Comparison of the electrical properties of 17-(2-aminophenyl)heptadecanoic acid and methyl 17-(2-aminophenyl)heptadecanoate	123
6.1	The surface compressional modulus at surface pressures of 2, 5, 10, and 15 mN m^{-1} for 2-pentadecylaniline and 1,22-bis(2-aminophenyl)docosane on a 0.10 M H_2SO_4 subphase at 25 °C	138

LIST OF FIGURES

Figure		page
1.1	Langmuir trough	2
1.2	The reduced and oxidized forms of polyaniline	23
1.3	The four resonance structures of the anilinium cation radical	24
1.4	Structures of p-aminodiphenylamine, benzidine, and N, N-diphenylhydrazine	25
1.5	Formation of 4-aminodiphenylamine from aniline	26
1.6	Mechanism for the oxidative polymerization of aniline as proposed by Duic[129]	27
1.7	The mechanism for the autoacceleration proposed by Shim and Park	28
1.8	Proposed oxidative decomposition pathway of polyaniline	29
2.1	Synthetic scheme for pentadecylaniline	35
2.2	Synthetic scheme for (1-octadecynyl)aniline	38
2.3	Synthetic scheme for methyl 17-(2-aminophenyl)heptadecanoate and 17-(2-aminophenyl)heptadecanoic acid	40
2.4	Synthetic scheme for 1,22-bis(2-aminophenyl)docosane	44
2.5	Surface potentiometer	52
3.1	Surface pressure, π, vs. mean molecular area, *A*, isotherms of 2-, 3-, and 4-pentadecylaniline on deionized water at 25 °C.	57
3.2	Surface pressure, π, vs. mean molecular area, *A*, isotherms of 2-, 3-, and 4-pentadecylaniline on 0.10 M H_2SO_4 at 25 °C	58

3.3 Surface pressure, π, vs. mean molecular area, *A*, isotherms of 3-pentadecylaniline on a H_2SO_4 subphase at 10, 17.5, 25, 32.5, 40 °C 60

3.4 Surface Pressure, π, vs. mean molecular area, *A*, isotherms of 2-, 3-, and 4-pentadecylaniline on 0.20 M HCl at 25 °C 61

3.5 Surface pressure, π, potential, ΔV, and dipole moment, μ_n, vs. mean molecular area, *A*, for 2-pentadecylaniline on a 0.20 M HCl subphase at 25 °C 62

3.6 Surface pressure, π, potential, ΔV, and dipole moment, μ_n, vs. mean molecular area, *A*, for 3-pentadecylaniline on a 0.20 M HCl subphase at 25 °C 62

3.7 Surface pressure, π, potential, ΔV, and dipole moment, μ_n, vs. mean molecular area, *A*, for 4-pentadecylaniline on a 0.20 M HCl subphase at 25 °C 63

3.8 Plot of surface dipole moments, μ_n, of 2-, 3-, and 4-pentadecylaniline at their corresponding surface pressures, π 65

3.9 Predicted surface behavior of the head group of 2-, 3-, and 4-pentadecylaniline at changing surface pressures. Arrows show the predicted conformation change of the anilinium head group when going from low to higher pressures 67

3.10 Absorption spectra of poly(2-pentadecylaniline) just after completion of the polymerization reaction (spectrum A) and after the polymer is allow to remain at the interface for 4 h (spectrum B). Absorption spectrum of poly(3-pentadecylaniline) just after completion of the polymerization reaction (spectrum C). 70

3.11 Infrared spectra of a) poly(2-pentadecylaniline) base and b) poly(2-pentadecylaniline) base after remaining on trough for five hours 73

3.12 ξ and dξ/dt vs. time for the polymerization of 2-pentadecylaniline at an applied surface pressure of 10 mN m^{-1} 75

3.13 *A* and R_p vs. time for the polymerization of 2-pentadecylaniline at an applied surface pressure of 10 mN m^{-1} 76

3.14 ξ and dξ/dt vs. time for the polymerization of 3-pentadecylaniline at an applied surface pressure of 10 mN m^{-1} 78

3.15 *A* and R_p vs. time for the polymerization of 3-pentadecylaniline at an applied surface pressure of 10 mN m^{-1}. 78

3.16 m vs. π for 2-pentadecylaniline on a 0.10 M H_2SO_4 subphase and poly(2-pentadecylaniline) on a 0.10 M H_2SO_4 and 0.03 M $(NH_4)_2S_2O_8$ subphase at 25 °C 80

3.17 R_p vs. time for the polymerization of 2-pentadecylaniline at 5, 10, 15, 20, 25, and 30 mN m^{-1} applied surface pressure, temperature held constant at 25 °C. .. 80

3.18 R_p vs. time for the polymerization of 3-pentadecylaniline at 5, 10, 15, and 20 mN m^{-1} applied surface pressure, temperature held constant at 25 °C. 81

3.19 k^{app} vs. poly(2-pentadecylaniline) concentration at the air-aqueous interface. Plot shows up to 80 % completion 82

3.20 k^{app} vs. poly(3-pentadecylaniline) concentration at the air-aqueous interface. Plot shows up to 80 % completion 83

3.21 k^{app} vs. poly(3-pentadecylaniline) concentration at the air-aqueous interface. Plot shows up to 15 % completion 84

3.22 ln k' vs. ln π for the formation of poly(2-pentadecylaniline) and poly(3-pentadecylaniline) at 25 °C. 87

3.23 lnk' vs. 1/T plot for the polymerization of 2- and 3-pentadecylaniline a 15 mN m^{-1}. 88

3.24 lnk vs. 1/T plot for the polymerization of 2- and 3-pentadecylaniline at 15 mN m^{-1}. 89

4.1 Cartoon of the predicted conformational change of 2- and 3-(1-octadecynyl)aniline at the air-aqueous interface during compression 93

4.2 Surface pressure, π, vs. mean molecular area, *A*, isotherms of 2- and 3-(1-octadecynyl)aniline on a 0.10 M H_2SO_4 at 25 °C. 94

4.3 Surface pressure, π, potential, ΔV, and dipole moment, μ_m, vs. mean molecular area, *A*, for 2-(1-octadecynyl)aniline on a 0.20 M HCl subphase at 25 °C. 95

4.4 Surface pressure, π, potential, ΔV, and dipole moment, μ_n, vs. mean molecular area, *A*, for 3-(1-octadecynyl)aniline on a 0.20 M HCl subphase at 25 °C 96

4.5 Plot of surface dipole moments, μ_n, of 2- and 3-(1-octadecynyl) aniline at their corresponding surface pressures, π 97

4.6 Surface pressure, π, potential, ΔV, and m vs. mean molecular area, *A*, for 2-(1-octadecynyl)aniline on a 0.10 M H_2SO_4 subphase at 25 °C 98

4.7 Surface pressure, π, potential, ΔV, and m vs. mean molecular area, *A*, for 3-(1-octadecynyl)aniline on a 0.10 M H_2SO_4 subphase at 25 °C 99

4.8 Plot of m of 2- and 3-(1-octadecynyl) aniline at their corresponding surface pressures, π 100

4.9 The absorption spectra of the polymerization products of 2- and 3-(1-octadecynyl)aniline 102

4.10 Infrared spectra of poly[2-(1-octadecynyl)aniline] base 103

4.11 *A* and R_p vs. time for the polymerization of 2-(1-octadecynyl)aniline at an applied surface pressure of 5 mN m^{-1} 104

4.12 *A* and R_p vs. time for the polymerization of 3-(1-octadecynyl)aniline at an applied surface pressure of 5 mN m^{-1} 105

4.13 k^{app} vs. poly[2-(1-octadecynyl)aniline] concentration at the air-aqueous interface. The plot shows polymerization up to 50 % completion 106

4.14 k^{app} vs. poly[3-(1-octadecynyl)aniline] concentration at the air-aqueous interface. The plot shows polymerization up to 50 % completion 106

5.1 Structures of the dipolar molecules 17-(2-aminophenyl)heptadecanoic acid and methyl 17-(2-aminophenyl) heptadecanoate 114

5.2 Surface pressure, π, potential, ΔV, and dipole moment, μ_n, vs. mean molecular area, *A*, for 17-(2-aminophenyl)heptadecanoic acid on water subphase at 25 °C 116

5.3 Surface pressure, π, potential, ΔV, and dipole moment, μn, vs. mean molecular area, *A*, for methyl 17-(2-aminophenyl)heptadecanoate on water subphase at 25 °C 117

5.4 The proposed surface behavior of 17-(2-aminophenyl)heptadecanoic acid and methyl 16-hydroxyhexadecanoate on a water surface at different surface areas 119

5.5 Three proposed mechanisms for the phase transition of the dipolar compounds 17-(2-aminophenyl)heptadecanoic acid and methyl 17-(2-aminophenyl)heptadecanoate on water. 120

5.6 Surface pressure, π, potential, ΔV, and dipole moment, μ_n, vs. mean molecular area, *A*, for 2-pentadecylaniline on water subphase at 25 °C 121

5.7 Surface pressure, π, vs. mean molecular area, *A*, isotherm of methyl 17-(2-aminophenyl)heptadecanoate on 0.10 M H_2SO_4 subphase at 25 °C 125

5.8 Cartoon of the methyl 17-(2-aminophenyl)heptadecanoate polymerization. .. 127

5.9 Change of surface area for the polymerization of 17-(2-aminophenyl)heptadecanoic acid monolayer at 5 and 25 mN m^{-1}. 128

6.1 Structure of 1,22-bis(2-aminophenyl)docosane. 131

6.2 Ruthenium alkylidene catalyzed methathesis coupling of 1-(2-nitrophenyl)-1,11-dodecdiene. 132

6.3 ^1H NMR spectra of 1-(2-nitrophenyl)-1,11-dodecadiene and 1,22-bis(2-nitrophenyl)-1,11,21-docostriene between 4.8 and 7.0 ppm 133

6.4 An alternative route for the synthesis of 1,22-bis(2-aminophenyl)docosane. .. 135

6.5 Surface pressure, π, vs. mean molecular area, *A*, isotherms of 2-pentadecylaniline and 1,22-bis(2-aminophenyl)docosane on 0.10 H_2SO_4 at 25 °C. 136

6.6 *A* vs. time for the polymerization of 1,22-bis(2-aminophenyl)docosane and R_p vs. time for the polymerization of 1,22-bis(2-aminophenyl)docosane and 2-pentadecylaniline 10 mN m^{-1} and 25 °C. 139

6.7 Surface pressure, π, vs. mean molecular area, *A*, isotherms of poly(1-22-bis[2-aminophenyl]docosane) and poly(2-pentadecylaniline) on 0.10 M H_2SO_4 and 0.03 M $(NH_4)_2S_2O_8$ subphase at 25 °C. 141

6.8 The removal of poly[1,22-bis(2-aminophenyl)docosane] from the trough's surface and a single fiber of poly[1,22-bis(2-aminophenyl)docosane] 142

6.9 Absorption spectra of poly[1,22-bis(2-aminophenyl)docosane] film on a quartz slide 143

6.10 Two possible polymerization pathways of 1,22-bis(2-aminophenyl)docosane. 144

Abstract of Dissertation Presented to the Graduate School
of the University of Florida in Partial Fulfillment of the
Requirements for the Degree of Doctor of Philosophy

THE SURFACE BEHAVIOR AND POLYMERIZATION
OF ANILINE CONTAINING SURFACTANTS IN
LANGMUIR MONOLAYERS

By

Leroy Joseph Kloeppner

December 1998

Chairperson: Randolph S. Duran
Major Department: Chemistry

The surfactants pictured below were synthesized and their surface behavior and polymerization rates in a Langmuir monolayer studied.

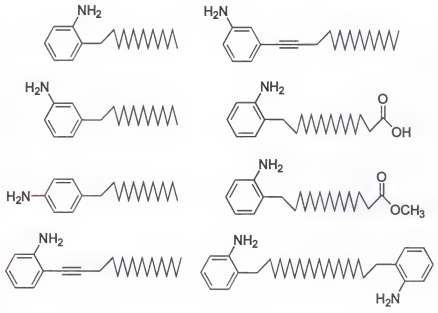

Surface pressure and potential vs. mean molecular area isotherms of the substituted anilines were generated and the results were attributed to the orientation of the aromatic rings at the interface. Alkyl substituted aniline has been shown, in this and previous studies, to polymerize at the air-aqueous interface when a strong chemical oxidant and acid are present in the subphase. The reactivities of the aniline derivatives were studied under different conditions. When the polymerizations of 2- and 3-pentadecylaniline were compared, the rate of reactivity of 2-pentadecylaniline was more dependent on the applied surface pressure than 3-pentadecylaniline. Further, there was a more significant autoacceleration effect present during the 2-pentadecylaniline polymerization. Reaction rates of 2- and 3- (1-octadecynyl)aniline were then compared under the same polymerization conditions. The initial rate constant for 2-(1-octadecynyl)aniline was significantly greater than that of 2-pentadecylaniline, and autoacceleration was not detected. The initial rate constant of 3-(1-octadecynyl)aniline polymerization was similar to that of 3-pentadecylaniline. Reaction rates were explained in terms of electronic and orientational differences in the monomers at the air-aqueous interface.

On a water subphase, methyl 17-(2-aminophenyl)heptadecanoate and 17-(2-aminophenyl)heptadecanoic had multi-phase behavior. The results suggest that at low surface pressures, both polar ends of the molecules were adsorbed to the water surface, but at high surface pressures only one polar group per molecule was adsorbed to the subphase. Surface potential data indicated that, in the case of methyl 17-(2-aminophenyl)heptadecanoate, the anilinium groups were oriented away from the interface, while in the case of 17-(2-aminophenyl)heptadecanoic, ion pairs were formed

and a mixture of the head groups was adsorbed to the interface. When these monomers were reacted at low surface pressure (π=5mN m^{-1}), only low molecular weight oligomers were produced, which was attributed to the hinderance of the non-reactive polar end.

1,22-Bis(2-aminophenyl)docosane was polymerized at the air-aqueous interface to produce a unique, 2-dimensional network polymer. The material produced was the characteristic blue of polyaniline and was insoluble in the solvents that usually dissolve polyaniline and poly(pentadecylaniline). Further, the material could be lifted from the Langmuir trough in essentially one piece, indicating mechanical strength not usually observed in materials produced in Langmuir films. The surface and polymerization behavior of this polymer mirrored many of the properties of 2-pentadecylaniline.

CHAPTER 1

INTRODUCTION

1.1 Langmuir Films

It was noted early in the scientific literature by American statesman Benjamin Franklin that when a small amount of oil was applied to the surface of a pond, the oil spontaneously spread over the water and had a calming effect on the surface.[1,2] It was not until the late nineteenth century that this observation was studied in a more scientific manner[3-7] when Lord Rayleigh (John William Strutt, 3rd Baron Rayleigh) discover that the surface tension of water was reduced when a superficial layer of olive oil was placed on its surface.[4] In these early publications, Lord Rayleigh hypothesized that the film that he produced was only one molecule thick or a monolayer.[8] This discovery, together with the work done by Agnes Pockels on developing what is known today as the Langmuir trough,[9-11] laid much of the groundwork for what later became known as Langmuir film techniques.

In 1915, Irving Langmuir began developing the experimental and theoretical concepts that are used to understand the behavior of molecules in a monolayer.[12] Langmuir demonstrated that films of long-chain fatty acids at the air-water interface were only one molecule thick and that the molecules oriented such that the long alkyl chain

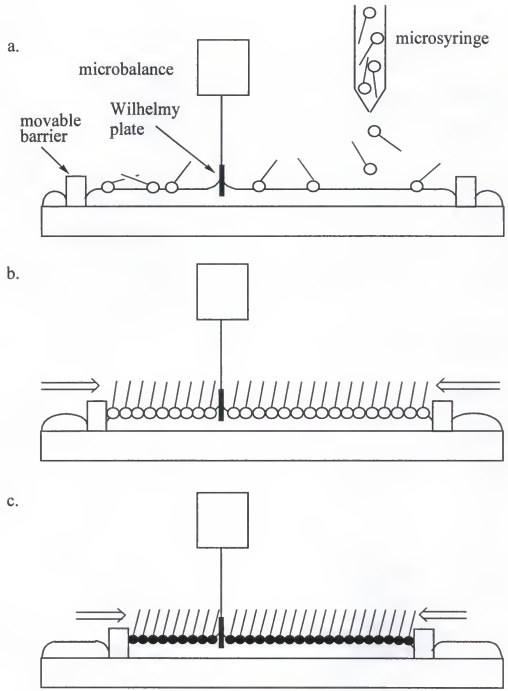

Figure 1.1. Langmuir trough. Monolayer experiment (a) before compression, (b) after compression, and (c) after reaction.

was directed nearly vertical from the surface and that the polar group was immersed into the water phase. Langmuir also developed a number of new techniques, including a surface balance that measured the force needed to deflect a movable float separating a clean water surface from a surface that contained a monomolecular film.[13] This force could be directly related to the surface pressure of the film side of the float.

A diagram of a typical Langmuir trough is shown in Figure 1(a). The trough is normally made of a polymeric material such as Teflon™ and is equipped with movable barriers which are used to control the surface area. Normally, the trough is equipped with a Wilhelmy or Langmuir balance that can monitor the surface pressure of an interface. Many Langmuir troughs are also equipped with channels underneath the trough that can be used to control the temperature of the subphase. The temperature is controlled by pumping cooling or heating solution through this jacket.

1.1.1 Surface Pressure

A surface active molecule (surfactant) can be spread at the surface of water by first dissolving it in a water-immiscible, volatile solvent, such as chloroform or benzene, and then placing the solution at the surface of the interface (Figure 1(a)). Once placed on the surface, the surfactant can rapidly spread to cover the available area. A surfactant is decrease the surface energy of the interface. Consider this simple model for describing the free energy of an interface:[14] a solid or a liquid that is composed of spherical molecules in a closed packed arrangement has a cohesive energy, ϵ, that binds each molecule to its nearest neighbors. If the molecule is bound to twelve other molecules, then the binding energy between each molecule is $\epsilon/12$. If that molecule is taken from the

bulk of the material and moved to the outer surface, the number of molecules that it is bound to is only nine and its total binding energy is $9\epsilon/12$ or $\frac{3}{4}\epsilon$. In this crude model, it is apparent that the molecule at the surface of the material has only ¾ of the binding energy that an interior molecule has, which means that it has higher free energy. It is this difference in the free energies that gives rise to the surface tension ,γ_0, of a material. For a homogeneous material, surface tension can be defined as the change in the Gibbs free energy of the material with the change in interfacial area, A, at constant temperature, T, volume, V, and number of moles, n[12]:

$$\gamma_0 = \left(\frac{\delta G}{\delta A} \right)_{T,V,n} \tag{1.1}$$

Equation 1.1 relates the amount of work required to increase the amount of surface area of a material.

The surface tension of a material can be changed by the adsorption of a second component at its surface. For example, adding a small amount of butanol to water decreases the surface tension of the water. This decrease is due to the formation of an oriented monomolecular layer of butanol at the surface of the water, which formed by random molecular motion. If there were no reduction in the Gibbs free energy of the surface after the butanol reached the interface, there would be no preferential adsorption and the composition of the surface would be no different from that of the bulk of the material. By forming a monolayer at the interface of the water, the surface tension of the

interface decreases. It is this decrease in the overall energy of the system that drives the adsorption process. The decrease in the surface tension is defined as the surface pressure, π, and is given by Equation 1.2:

$$\pi = \gamma_0 - \gamma \tag{1.2}$$

where γ_0 is the surface tension of a clean surface and γ is the surface tension with a monolayer. Surface pressure can be expressed in terms of mN m^{-1} and is considered a 2-dimensional analog of 3-dimensional pressure.[15]

1.1.2 Surface Potential

Another important physical property of Langmuir films is the surface potential, ΔV. Surface potential refers to the change in the phase boundary potential produced by the addition of an interfacial film. A monolayer film at the air-aqueous interface can be treated as an assembly of molecular dipoles that can shift the potential across an interface.[12] ΔV can be related to an apparent or surface dipole moment, μ_n, using the Helmholtz equation:[12, 16]

$$\Delta V = \frac{\mu_n N}{\epsilon_0} \tag{1.3}$$

where ϵ_0 is the permittivity of a vacuum and N is the concentration of dipoles at the interface. μ_n is the dipole moment normal to the interface, and hence, its value is affected

by the orientation of the surfactant. Davies and Rideal proposed that μ_n is made up of three components: μ_1, the reorientation of the water molecules at the interface, μ_2, the dipole moment from the head group, and μ_3, the dipole moment from the hydrophobic group.[17,18] μ_n is defined by equation 1.4:

$$\mu_n = \left(\frac{\mu_1}{\epsilon_1} + \frac{\mu_2}{\epsilon_2} + \frac{\mu_3}{\epsilon_3} \right) \tag{1.4}$$

where ϵ_1, ϵ_2, and ϵ_3 are the local dielectric constants of each of the three layers.[19]

When an ionized monolayer is spread at the interface, an additional term needs to be added to the Helmholtz equation that accounts for the electrical potential in the plane of the ionized groups, ψ_0, which is called the double-layer potential. ψ_0 can be estimated by the Gouy-Chapman equation[20, 21]

$$\psi_0 = \left(\frac{2kT}{e} \right) \sinh^{-1} \left[\frac{\alpha e}{\left(5X10^{-7} c \epsilon_0 T \right)^{1/2} A} \right] \tag{1.5}$$

where ***k*** is the Boltzmann constant, T is the absolute temperature, *e* is the electron charge, α is the degree of ionization of the monolayer, and *c* is the concentration monovalent ions

in the subphase. The Helmholtz equation can now be written for the surface potential of an ionic monolayer as

$$\Delta V = \frac{\mu_{\perp} N}{\epsilon_0} + \psi_0 \qquad (1.6)$$

One popular method by which the surface potential of a Langmuir film can be determined is by the vibrating plate or vibrating capacitor method, which will be described in Chapter 2.[12, 22, 23] Other common methods are the static-capacitor[24,25] and ionizing-probe.[26-28]

1.1.3 Langmuir-Blodgett Films

An important derivative of Langmuir films is the Langmuir-Blodgett (LB) film, which is formed by lowering or raising a substrate, such as glass, silica, or quartz, through a Langmuir film at the water surface while maintaining a constant surface pressure. This technique is also referred to as film deposition and was first developed by Irving Langmuir[29] and Katharine Blodgett.[30,31] The first layer of the monolayer is transferred onto a hydrophilic substrate by vertically pulling the substrate upwards through the insoluble monolayer such that the head groups directly adsorbed onto the substrate. If the substrate is hydrophobic, the monolayer is deposited by lowering the substrate vertically through the monolayer so that the tail groups directly adsorb to the substrate. Repeating this process can lead to the formation of multilayer films. The quality of the film deposition is characterized by Equation 1.7:[12,32,33]

$$\tau = \frac{A_l}{A_s} \tag{1.7}$$

where τ is the transfer ratio, and A_l and A_s are the decrease in the area of the monolayer and the amount of area of the substrate that is coated during the deposition at constant surface pressure, respectively.

LB films of small molecules are usually mechanically, chemically, and thermally unstable, which has prevented their industrial application. LB film polymerization has been used to stabilize the films while still maintaining their structure.[34-39] Usually the polymerization is carried out by irradiation, but other methods such as polycondensation and oxidative polymerizations have been studied.[40]

The another means by which ultrathin organic films can be prepared is by self-assembly. Self-assembled monolayers (SAMs) are formed by the immersion of an appropriate substrate in a solution containing a functionalized surfactant. The interaction of the surfactant and the substrate results in an adsorption of the surfactant on to the surface of the substrate by either chemisorption or physical adsorption.[41] Many types of SAMs are known today, but organosilicon on hydroxylated surfaces,[42-44] alkanethiol[45-52] and disulfides[53-56] on gold, and carboxylic acids on aluminum oxide and silver surfaces[57-59] are some of the more common types reported in the literature.[60, 61]

1.2 Monolayer Reactions

One of the main advantages of studying chemical reactions in Langmuir films is that the orientation of the monolayer forming molecules can be controlled and hence, the reactivity of the molecules and in some cases the products can be controlled. For example, the solution oxidation of *cis* and *trans*-13-docosenoic acid (erucic and brassidic acid) resulted in the *cis* and *trans* dihydroxy isomers when the reaction was done in an acidic solution of potassium permanganate. However, when the same oxidation was done in a Langmuir film with permanganate in the subphase, both the *cis* and *trans*-13-docosenoic acids produced the same stereo isomer of the dihydroxy acid.[62]

According to Gaines, concentration and orientation are the major factors that affect the reactivity of molecules at an air-water interface.[12] In addition to these factors, the reactivity of a monolayer film can also be affected by factors that can be unique to reactions done in organized films such as electrical potential (electrical factors) and the effect of interfacial pressure (steric effects).[12, 15]

For insoluble surfactants, the concentration of adsorbed molecules at the interface is easily determined from the amount of material placed on the interface and the total area of the interface. For a soluble surfactant, the distribution of molecules between the bulk and the interface can be expressed in the following equation when surface pressure, π, and electrostatic potential at the interface, ψ, are held constant:[15]

$$\frac{c_i}{c_b} = K_0 \exp\left(\frac{-\pi A}{kT}\right) \tag{1.8}$$

where c_i and c_b are the concentration of the species at the interface and in the bulk, respectively, K_0 is a distribution coefficient when π is equal to zero, A is the mean molecular area of the interface, k is the Boltzmann constant, and T is the absolute temperature.[15]

1.2.1 Electrical Factors

At an interface, charged surfactants can have a significant effect on the reaction kinetics.[18] This effect, which is not observed in a three dimensional solution, is caused by an increase in the concentration of charged species due to an adsorption phenomenon that creates a very steep electrical gradient just below the surface of the interface. It is this increase in the charged species at the interface that gives rise to the electrostatic potential at the interface, ψ.[18] Further, the electrical field created by the adsorption of charged species at the interface gives rise to changes in the concentration of soluble ions near the interface. If the ions in the subphase are involved in the reaction at the interface, the reaction kinetics can also be affected. Gouy solved the Boltzmann equation for the distribution of cations ($_sc^+$) and anions ($_sc^-$) near the interface in terms of a positively charged surface relative to the bulk of the solution using the equations.[18, 20]

$$_sc^+ = {}_bce^{-e\psi/kT} \tag{1.9a}$$

$$_sc^- = {}_bce^{+\epsilon\psi/kT} \quad (1.9b)$$

where $_bc$ is the concentration of ions in the bulk, **k** is the Boltzmann constant, T is the absolute temperature, and ϵ is the electronic charge. As a consequence, a positively charged surface will have a higher concentration of negatively charged ions just below the interface as compared to the rest of the solution. In principle this method could be highly useful, but the actual calculation requires the assignment of a 'depth' to the surface phase, which can only be crudely estimated.[12]

1.2.2 Interfacial Pressure Factors

The effect that surface pressure has on the rate of a reaction at the interface is interpreted in terms of different steric and orientational factors. Mittelmann and Palmer showed that the rate of the permanganate oxidation of (Z)-9-octadecenoic acid was affected by the surface pressure applied to the reaction.[63] It was determined that at higher surface pressures, the rate of the reaction was slower than when the same reaction was done at lower surface pressures. It was concluded that the double bond, which was in the middle of the hydrophobic chain, was more accessible to the permanganate ions when the film was more expanded. As the accessibility was decreased, the rate of the reaction also decreased.

Davies reported a similar effect in the lactonization of γ-hydroxystearic acid in a monolayer.[64] He concluded that the rate of the reaction was directly proportional to the number of hydroxyl groups forced out of the interfacial phase at higher surface pressures.

Another example of a reaction that is affected by steric effects is the hydrolysis of long-chain esters by acid in the subphase.[65] It was reported that the hydrolysis of ethyl palmitate molecules at high surface pressure is much slower relative to reactions done at low surface pressures. It was concluded (from surface potential measurements) that at lower surface pressures, the ester was more accessible to the acid, but at higher pressures the ethyl group on the ester shifted downward into the subphase, which hindered the approach of the acid.

In the case of 3-dimensional reactions, collision theory expresses the rate constant by equation 1.10a:

$$k = pZ\exp\left(-\frac{E_a}{RT}\right) \qquad (1.10a)$$

where Z is the collision rate, E_a is the activation energy, and p is the probability factor. In a monolayer in which the molecules are confined to the interface, the probability factor becomes very important. It has been proposed that term p in Equation 1.10a could be separated into an accessibility factor (φ) and a probability factor (p') which accounts for the steric factors, energy exchange, and other reaction probability effects that are typical to reactions done in 3-dimensions:[12]

$$k = \varphi p' Z \exp\left(-\frac{E_a}{RT}\right) \tag{1.10b}$$

Therefore, if the reactive portion of the surfactant is completely accessible to reactants in the subphase, φ is unity. As the accessibility decreases, φ also decreases.

1.2.3 Kinetic Studies

Generally, reactions done at an interface are accompanied by physical changes in the interfacial properties like molecular area, surface pressure, interfacial potential, surface dipole moments, interfacial viscosity, or elasticity. Therefore, interfacial reaction rates can be monitored by measuring the changes in one or more of these physical properties. A popular method of monitoring the reaction kinetics is by the film balance technique, which can be used if there is a difference in the surface area of the products compared to the reactants at a specific surface pressure.[66-72] In this technique, the film area change is monitored while the surface pressure is held constant. If there is a molecular area change during the course of a reaction, the extent of a reaction, ξ, is assumed to be equal to the change in the molecular area compared to the total change in area from the beginning to end of the reaction. Equation 1.11,[15]

$$\xi = \frac{A_0 - A}{A_0 - A_\infty} \tag{1.11}$$

where A, A_0 and A_∞ are the molecular areas at a given time during the reaction, at the beginning, and at the end of a reaction, respectively, relates area to the extent of the reaction. If the molecular area of the product is greater than that of the reactant, the order of the terms in the denominator is simply reversed. It should be noted that equation 1.11 is only valid if the molecular areas of the reactants and the products are additive and if the products and reactants are not lost to desorption. If a plot of $\log(A - A_\infty)$ versus time is a straight line, then the reaction is first order and Equation 1.11 can be rewritten as

$$\exp(-kt) = \frac{A_0 - A}{A_0 - A_\infty} \tag{1.12}$$

where k is a first order rate constant and t is time. Similar to the change in molecular area, other parameters that show a change during reaction, such as surface potential, ΔV, can also be substituted into equation 1.11 in order to determine the extent of the reaction.[15]

1.3 Monolayer Polymerizations

The construction of a Langmuir monolayer is one way in which molecules can be organized before polymerization. Other methods that have been used include template polymerizations, [73, 74] liquid crystalline polymerizations,[75] the polymerization of micelle-

forming monomers,[76] and the polymerizations of microemulsions.[77] Monolayer polymerizations fall into three different categories: Langmuir film, LB (Section 1.1.3), and SAM polymerizations.[40] It should be noted that Langmuir film polymerization generally refers to the polymerization of a monomer at the gas-liquid or liquid-liquid interface and LB and SAM polymerizations are normally polymerizations of materials that have been transferred to a solid substrate. Due to the control of molecular orientation and film thickness, Langmuir monolayer polymerization has proven to be a powerful method to form ultrathin polymer films.

As was noted in Section 1.1.3, the polymerization of reactive LB films can lead to highly oriented films with controlled thickness; however, polymerization can lead to molecular reorganization that can cause defects in the films. This problem can be overcome by two techniques: (1) by spreading of preformed polymer at the interface or (2) by the in-situ polymerization of amphiphilic molecules in a Langmuir film. The resulting polymeric Langmuir films can then be transferred to solid substrates to give a stable layered structure.

Preformed polymers are spread into monolayers in much the same way as monomer surfactants. The most important structural requirement for these types of films is that a hydrophilic group must be present at regular, short intervals along the backbone. The most significant problem associated with this technique is that one must assume that the polymer chains are extended at the interface and that every monomer unit interacts with the subphase.

Studies done by Lando et al. showed that Langmuir films polymerized in situ had a higher compressional modulus and a smaller area per molecule when compared to bulk prepared polymer.[78, 79] These and other results led to the conclusion that Langmuir polymerized films have better packing order due to structural differences that result from this type of polymerization. Another benefit of monolayer polymerization is that overlapping chains are eliminated.

Many applications have been proposed for ultrathin films in the past 20 years, such as nonlinear optical applications,[80, 81] integrated circuit technology,[82] sensors,[83] lubricants,[84, 85] and microlithography[86] to name a few. Most applications for ultrathin organic films require the films to be mechanically, thermally, and chemically stable under environmental conditions. Since polymeric systems are, in general, more stable than monomeric ones due to the covalent bonding in the film plane, polymeric systems are usually preferred over monomeric systems.[87] One application that uses ultrathin polymeric films is microlithography. It was shown that LB films of ω-tricosenoic acid are excellent negative resist materials. 22-Tricosenoic acid can be photopolymerized in an ultrathin film with line resolutions as low as 60 nm, which is much smaller than that achieved with conventional methods.[86]

The remainder of this section will focus primarily on the polymerization of Langmuir films, but an excellent review on the polymerization of LB and SAM films as well as Langmuir films was written by Bernd Tieke.[40]

1.3.1 Langmuir Film Polymerization

Unlike most chemical reactions studied in Langmuir films, which involve only the reaction between subphase and surfactant, polymerization reactions involve the chemical reaction between several neighboring molecules that are confined to a monolayer. Therefore, the orientation of the reactive group and the concentration of the surfactant at the interface become even more important. One example of a monolayer polymerization involved the maleic anhydride compound of β-elasostearin reported by Gee.[88, 89] Gee determined that the reaction rate increased with increasing surface pressure and temperature. [89]

Surface pressure can also affect the relative orientation of the surfactant at the interface, which is very important when studying reactions between two or more molecules adsorbed at the interface. For example, the reactivity of the photoinduced polymerization of octadecylacrylate at the nitrogen-water interface depends on the surface pressure at which the polymerization was performed.[67, 90] It was reported that the polymerization rate reaches a maximum at a molecular area of 20 $Å^2$ $molecule^{-1}$ or at a surface pressure of 14 mN m^{-1}, and it is proposed that the optimum orientation was achieved at this surface pressure.

The photopolymerization of diacetylenes in Langmuir films has generated a great deal of interest. Tamura and co-workers discovered that the polymerization rate of 10,12-pentacosadiynoic acid at the interface was dependent on molecular arrangement and density.[91] At higher surface densities the photopolymerization was slower than at lower surface densities, which was attributed to differences in the orientation at the interface.

Further, due to the topochemical nature of these polymerizations, the polymerization is believed to only occur in the condensed state.

There have been a number of reports on the formation of oriented polymeric monolayers by polycondensation.[40] For example, α-octadecylamino acid underwent spontaneous polycondensation at surface pressures between 2 and 5 mN m^{-1}.[92]

1.3.2 Aniline Monolayer Polymerization

In order to polymerize aniline in a monolayer, it is necessary to add a long chain alkyl group to the conventional aniline monomer to make it insoluble in the aqueous subphase. In addition to stabilizing the monomeric film, the pendant alkyl group improves the solubility of the polymer in common organic solvents such as chloroform and allows the polymer to be characterized by techniques such as gel permeation chromatography and UV-vis with such solvents.

Early work done in the Duran group found that the Langmuir film polymerization rate of 2-pentadecylaniline was dependent on the applied surface pressure.[93, 94] The polymerization of 2-pentadecylaniline at the air-aqueous interface was done in the presence of the strong chemical oxidant, ammonium peroxydisulfate and an acid.[93] The polymerization was monitored by observing the barrier movement needed to maintain a specific applied surface pressure. The area change per molecule was attributed to the replacement of van der Waals radii by covalent bonds between monomer molecules and conformational differences between monomer and polymer.[93, 95] At higher applied surface pressures, the polymerization rate was faster than at lower pressures, suggesting

that the reactive group conformation at the interface might have a significant effect on the polymerization rate at an interface.

The polymerization rate of 2-pentadecylaniline at the air-aqueous interface was determined and a single rate constant assigned.[93, 95] This constant was assigned from the point of a maximum reaction rate, which is normally 10 to 30 minutes into the polymerization. The rate constant was calculated from the following equation:[95]

$$k = \frac{(BS_{MAX})W(A_0 - A_\infty)}{N(A_0 - A)(A - A_\infty)} \qquad (1.13)$$

where BS_{MAX} is the maximum barrier speed during the polymerization, W is the width of the trough, and N is the number of monomer molecules spread at the interface. These previous studies showed the effect that surface pressure has on the rate of the reaction, but the effect that autoacceleration has on the complex polymerization kinetics was not explored. Further, the polymerization was considered to be first order in terms of the monomer concentration during the course of the reaction, which is contrary to what is observed in the polymerization of aniline by chemical and electrochemical oxidation, in which the concentration of the polymer affects the rate of the reaction.[96-98] Bodalia et al. furthered this work by addressing autoacceleration and assigning a second rate constant to the overall rate of the polymerization.[99] However, this method was accurate only when

the initial polymerization rate was orders of magnitude slower than the maximum rate, which is not always the case for aniline surfactant polymerizations.[100]

1.4 Polyaniline

Polyaniline, which is one of the oldest known synthetic organic polymers, has attracted a considerable amount of interest in the past decade as a conductive material. Historically, synthetic polymers have been known more for their ability to act as excellent electrical insulators and not as electrical charge carriers. It was not until 1977, when MacDiarmid et al. showed that polyacetylene, a highly conjugated synthetic organic polymer, could be doped with an electron-attracting species such as chlorine, bromine, iodine, or AsF_5, which increased the materials conductivity up to $5.6 \times 10^2\ \Omega^{-1}\ cm^{-1}$, a 10^{11} increase.[101-103] This discovery gave rise to an increased interest in discovering other materials that were both polymeric and conductive in nature. Of these materials, doped polyaniline exhibits many of the same conductive characteristics as the doped polyacetylene.

Since the discovery that organic polymers could be made conductive, many applications have been proposed for these materials.[104-106] Some of the proposed applications are for rechargeable batteries, corrosion protection, electrochromic devices, chemical sensors, catalysis in redox reactions, indicators, and ion exchange resins.

1.4.1 History

In 1835, "aniline black" was the term that was given to the oxidative product of aniline. It was not until 1862, that Letheby performed the first extensive study of the product of this oxidation.[107] He showed that aniline, oxidized at the surface of a platinum electrode in the presence of aqueous sulfuric acid solution, gave a dark brown precipitate. However, the structure of polyaniline was not determined until the twentieth century, when Willstätter and co-workers proposed that the oxidative product of aniline was regarded as a octameric structure coupled in the para-position (leucoemeraldine).[108, 109] A few years later, Green and Woodhead clarified this proposed structure by proposing that the octameric structure could have different oxidative states, or be made up of two different repeat units that were dependent on the octamers oxidation state.[110, 111] On the following pages the five oxidative states of polyaniline as proposed by Green and Woodhead are presented, as are some of the physical properties of the octamers. The nomenclature, put forth by Green and Woodhead, to describe the different oxidation states of the octamer of aniline is still used today.

Leucoemeraldine, which is the completely reduced form of the polymer, is a pale brown substance that slowly oxidizes to the protoemeraldine form when exposed to air.

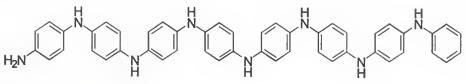

The protoemeraldine is a violet material that is yellowish-green in the salt form.

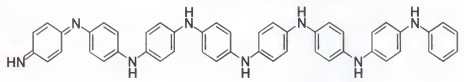

The emeraldine form is a material that is violet-blue in the base form and green in the salt form. The salt of the emeraldine is stable in air, but the base form slowly oxidizes to the niganiline base.

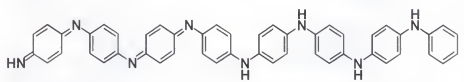

The salt of the emeraldine base is what most research groups report in the literature as the oxidative state that is closest to what is produced during synthesis of the polymer.[112]

The nigraniline is a blue substance in both the base and salt form. The base form of the nigraniline is stable in air; however, the salt form is very unstable.

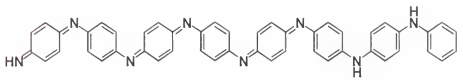

Finally, the pernigraniline is the fully oxidized form of the octamer. Both the base and the salt forms are purple in color. The pernigraniline in the salt and base form are very unstable and quickly decompose.

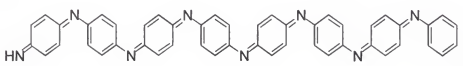

An alternative way of expressing the structure of polyaniline is to express the polymer in terms of being made up of two principal units: (i) the completely reduced form of a repeat unit containing two benzenoid rings and (ii) the completely oxidized form of a repeat unit containing one benzenoid ring and one quionoid ring.[104]

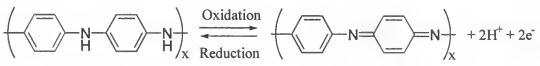

Figure 1.2. The reduced and oxidized forms of polyaniline.

1.4.2 Synthesis

Though several methods have been reported in the literature,[113-115] polyaniline is usually synthesized by the direct oxidation of monomeric aniline in an acidic solution. In solution chemistry, aniline is normally polymerized by the oxidation of the monomer with classical oxidants like ammonium peroxydisulfate or potassium dichromate[116] or by electrochemical methods[117, 118] under acidic conditions (0-2 pH).

1.4.3 Mechanism

The mechanism of polyaniline formation has been the subject of much debate in the past 30 years, which is in part due to the short-lived nature of the intermediates involved in the polymerization. What is known today about the polymerization mechanism is based mostly on the evidence obtained from the electrochemical polymerization of aniline .

Most researchers believe that the first step in the formation of polyaniline under oxidative and acidic conditions is the formation of an anilinium radical cation.[117, 119-124] This anilinium cation radical gives four resonance forms as shown in Figure 1.3.

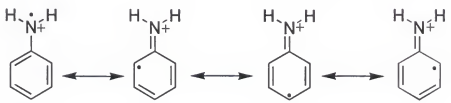

Figure 1.3. The four resonance structures of the anilinium cation radical.

There is also evidence that shows that this anilinium radical cation can undergo an additional loss of an electron and a proton to form a nitrenium cation.[125]

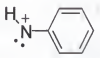

Because the anilinium radical ion and the nitrenium cation are short-lived, direct observation is difficult, leading to considerable debate over which species is involved in the polymerization mechanism. It is believed that two anilinium radical cations or two nitrenium ions then couple, and the loss of protons follows to form either p-aminodiphenylamine, benzidine, or N, N-diphenylhydrazine (Figure 1.4).[117, 119-124]

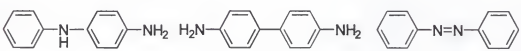

Figure 1.4. Structures of p-aminodiphenylamine, benzidine, and N, N-diphenylhydrazine.

Of the three dimers that form, 4-aminodiphenylamine is the primary product under oxidative conditions when the pH is 0-2 and is the intermediate that subsequently polymerizes.[126]

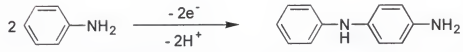

Figure 1.5. Formation of 4-aminodiphenylamine from aniline.

Earlier work done by Genies and co-workers suggests that the p-aminodiphenylamine oxidizes to form a new cation radical that can couple with a new molecule of aniline which was also oxidized to the cation radical to form a trimer. This process is repeated over and over again to form polymer.[117] Other researchers have proposed that the p-aminodiphenylamine then undergoes a rapid oxidation to form a quinoidal diimine which deprotonates, resulting in a nitrenium cation intermediate which can react as an electrophile with aniline.[127, 128] Once the new molecule of aniline is added to the oligomer, it is easily oxidized and deprotonated to form a new nitrenium cation which can react with a new aniline monomer. This process is repeated over and over to form polymer.

An alternative mechanism proposed by Duic and co-workers, suggests that a cation radical of aniline couples with a neutral molecule of aniline, with the loss of two electrons and two protons to form a new cation radical that can couple with additional aniline to propagate the polymer (Figure 1.6).[129] The polymerization is terminated when two radicals of a monomer or oligomer combine

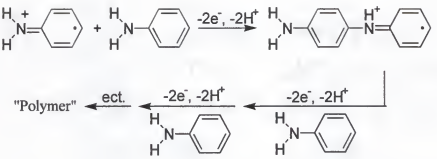

Figure 1.6. Mechanism for the polymerization of aniline proposed by Duic.[129]

Once the polymerization is initiated, normally the polymer formation rate autoaccelerates or has an autocatalytic effect.[95-98] Wei and co-workers showed that the rate increase in an electrochemical polymerization of aniline at a Pt electrode surface is directly proportional to the amount of polymer present.[96] This effect was also observed in aniline polymerization by a chemical oxidant in an aqueous medium.[98] It was suggested by Shim and Park that autoacceleration is due to the newly formed polymer or oligomers assisting the monomeric aniline oxidation; therefore, the propagation of the polymerization accelerates.[97] They concluded that the polymer, which is more easily oxidized than the monomer, can oxidize additional monomer (Figure 1.7).

The electropolymerization of aniline in a sulfuric acid medium (pH<3) showed that monomeric aniline begins to oxidize at 0.9 to 1.0 V vs. SCE.[130] The oxidation potential of the dimer, 4-aminophenylamine, was lower than that of the monomer and is believed to oxidize faster.[127] The polymer itself can be oxidized at ca. 0.15 and 0.80 V for the emeraldine and pernigraniline oxidative states, respectively.[131]

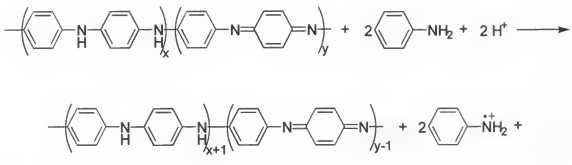

Figure 1.7. The mechanism for the autoacceleration proposed by Shim and Park.[97]

Another proposed theory suggests that when the polymer and oligomers are in the pernigraniline form, its highest oxidative state, neutral aniline monomers can easily add to the polymer by an electrophilic substitution reaction.[128, 129] Therefore, once polymer/oligomer is formed and is oxidized to the pernigraniline oxidative state, the rate of polymerization should accelerate. It is still not clear, however, whether an oxidized polymer directly reacts with a neutral aniline or if it catalytically oxidizes the neutral aniline, followed by the coupling of the momomer with polymer. Both of these routes have been suggested, but neither has been confirmed.[95]

A number of different derivatives of aniline have been shown to undergo oxidative polymerization. The kinetics of the polymerization of two such derivatives, *o*-toluidine and *m*-toluidine, were reported and compared to the polymerization of aniline under similar conditions.[128] It was reported that *o*-toluidine and *m*-toluidine, during the initial stages of an electrochemical polymerization, were less reactive than aniline. It was concluded that this reduced reactivity was due to steric hinderence from the methyl group towards the formation of the dimer during the early stages of the polymerization. After the initial stages of the polymerization, the rate of polymer formation for both *o*-toluidine

and *m*-toluidine were about the same, but greater than that of aniline. This result was attributed to the electron donating behavior of the methyl groups which may have increased electrochemical substitution. It is expected that there would be a difference in the polymerization rate of the two toluidine monomers due to the differences in the electron donating character of a methyl group at the *meta* and *ortho* positions, but none was observed.

1.4.4 Degradation of Polyaniline

Yoneyama and co-workers found that polyaniline undergoes irreversible changes when left under a potential greater than 0.5 volts (versus SCE) in a 1.0 M HCl solution.[131] They demonstrated that the polymer decomposed and that the product of the degradation was *p*-benzoquinone. The reversible cyclic voltammogram peak Yoneyama observed at ca. 0.5 volts was attributed to the redox chemistry of the *p*-benzoquinone. Hand and Nelson proposed, based on their work involving the electrochemical oxidation

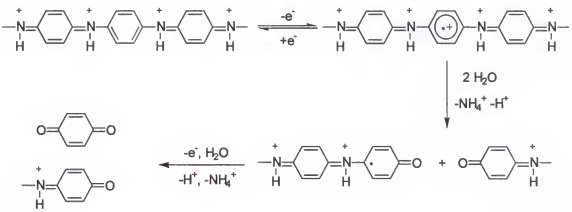

Figure 1.8. Proposed oxidative decomposition pathway of polyaniline

of aniline, that once the polymer is oxidized to the pernigraniline form, water can attack and cleave the backbone (Figure 1.8).[123, 124]

1.5 Oxidative Polymerization

Oxidative polymerization is frequently used to prepare conjugated polymers that have conductive properties, like polypyrrole, polyaniline, and polythiophene. Like polyaniline, these polymers are formed by the oxidation of the monomer by either electrochemical or chemical means. It has been shown that the oxidative polymerization rate is sensitive to the oxidation potential of the monomer. For example, the co-polymerization of pyrrole and N-(2-bromophenyl)pyrrole, with a 50:50 feed ratio, produced a polymer containing only 2.1% of the N-(2-bromophenyl)pyrrole.[132] The low reactivity of N-(2-bromophenyl)pyrrole was attributed to its higher oxidation potential compared to pyrrole.

1.6 Overview of Dissertation

The effects on reactivity and polymerization kinetics that result from the organization of aniline monomers at the air-aqueous interface are presented in this dissertation. The polymerizable units that were studied in this work were all derivatives of aniline. The structure of the monomer and its orientation at the interface is related to its subsequent reactivity.

Chapter 2 includes the characterization and synthetic procedures used to prepare the monomers used in this investigation. This chapter also includes a description of the procedures and instrumentation used to characterize the monomers and polymers in the Langmuir film environment.

In Chapter 3, a method of determining the polymerization rate, R_p, of *ortho* and *meta* alkyl substituted polyaniline in a Langmuir film is proposed. This method monitors the change in the mean molecular area of the initial surfactant at a constant applied surface pressure and predicts the concentrations of the monomer and polymer at the interface. A quantitative study of the effect that surface pressure and reactive group orientation have on polymer formation rate for the two isomers is presented. Surface pressure and potential measurements were used to determine the relative effect that different surface areas have on the reactive group conformation of the monomers. The R_p of the two monomers are related to these conformational and steric differences.

Langmuir films of 2- and 3-(1-octadecynyl)aniline were formed, characterized, and the oxidative reaction kinetics are reported in Chapter 4. The R_p of the two monomers were calculated and the reactivities of these monomers are compared with the alkyl substituted surfactants.

Chapters 5 and 6 present information on the Langmuir films of surfactants with functionalities at both ends of their aliphatic chains. The films (both before and after subjection to oxidative coupling conditions) of methyl 17-(2-aminophenyl) heptadecanoate and 17-(2-aminophenyl) heptadecanoic acid are discussed in Chapter 5. Chapter 6 presents a study on the Langmuir films of 1,22-bis(aminophenyl)docosane.

This dipolar surfactant has two polymerizable aniline groups attached to the same alkyl chain. The polymerization of this monomer led to the formation of a unique film with promising properties.

CHAPTER 2

EXPERIMENTAL

2.1 Introduction

Chapter 2 describes the equipment, procedures, and synthesis of the materials used in this work. Details of the KSV 5000 LB trough system and how it was used to gain information about monolayer properties and polymerization kinetics are given. Procedures and conditions are described such that the experiments can be easily reproduced.

The synthetic pathways to the monomers rely on known organic reactions; however, with the exception of the pentadecylaniline synthesis, the routes are original. The synthesis of 2-pentadecylaniline was previously carried out in our group via a Grignard reaction. The overall yields were not reported and are assumed to be quite low due to the fact that the Grignard reagent used in the synthetic route is a strong base that most probably deprotonated the amino functionality before it underwent nucleophilic attack on the cyano group of 2-aminobenzonitrile. The synthetic route reported herein was previously proposed for C_7 and C_{11} side chains.[134] The alkyltriphenylphosphonium salts used in that study were commercially available, but the C_{15} length side chains required for this study had to be synthesized. Therefore, considerable effort was put forth

in finding the optimum conditions for this reaction. Each compound was characterized using appropriate standard techniques (^{1}H and ^{13}C NMR, FTIR, MS, melting point, and elemental analysis) that prove both structure and purity.

2.2 Materials

All of the materials used for the monomer and polymer syntheses, unless otherwise stated, were purchased from the Aldrich and Fisher Chemical Companies and were used without further purification.

2.2.1 Pentadecylaniline

The three isomers of pentadecylaniline were synthesized by the route indicated in Figure 2.1. Modifications of reported literature procedures were used to prepared the monomers.[92, 122]

2.2.1.1 Pentadecyltriphenylphosphonium bromide. Tetradecylbromide (50.0 g, 0.180 mol) and triphenylphosphine (50.0 g, 0.190 mol) were dissolved in 200 mL of acetonitrile and refluxed overnight. The acetonitrile was removed under reduced pressure and the product was allowed to solidify. The solid was recrystallized in diethyl ether and a white crystalline material was collected in 80% yield. The melting point was 89.5-90.0 °C. ^{1}H NMR (DMSO): δ = 0.85 (t, 3H); 1.22 (bs, 22H); 1.45 (bs, 2H); 3.61 (t, 2H); 7.75-7.95 (m, 15H). ^{13}C NMR (DMSO): δ = 13.81, 19.85, 20.51, 21.67, 21.98, 28.06, 28.60, 28.78, 28.92, 29.57, 29.79, 31.18, 117.95, 119.08, 130.02, 130.19, 133.43, 133.56,

134.72. Anal. Calcd. for $C_{32}H_{44}BrP$: C, 71.23; H, 8.22; Br, 14.81. Found: C, 71.25; H, 8.20; Br, 14.78.

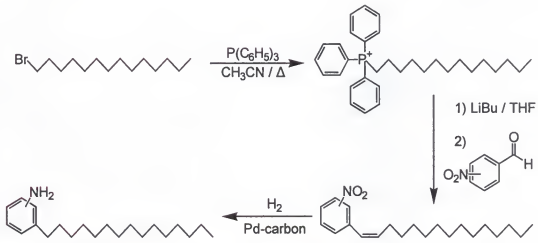

Figure 2.1. Synthetic scheme for pentadecylaniline.

2.2.1.2 General procedure for the synthesis of pentadecylaniline. Pentadecyltriphenylphosphonium bromide (1 equivalent) was dissolved in potassium dried tetrahydrofuran under an argon atmosphere and cooled in an ice bath to 0 °C. One equivalent of 2.5 M n-butyl lithium in hexanes was added dropwise over 15 min while stirring. The dark red mixture was stirred for an additional hour at 0 °C, then 1 equivalent of the appropriate isomer of nitrobenzaldehyde in potassium dried tetrahydrofuran was added dropwise. The solution was warmed to room temperature and mixed for 12 h. The solution was poured into water, extracted with three portions of methylene chloride, and dried over anhydrous magnesium sulfate. The solvent was removed under reduced pressure to yield a yellow oil. The yellow oil (a mixture of *cis* and *trans* isomers) was purified by column chromatography (silica/methylene chloride).

1-(Nitrophenyl)-1-pentadecene (6.1 g) was placed in 20 mL of 95% ethanol with

0.8 g of 10% palladium on carbon. The solution was mixed with a pure hydrogen gas atmosphere until no more gas was consumed (1-3 days). The hydrogenation was done at atmospheric pressure and room temperature. The mixture was filtered and the solvent was removed under reduced pressure yielding a solid, pentadecylaniline, which was purified by column chromatography (silica/methylene chloride). Purity was verified by gas chromatography (only one peak was observed) and elemental analysis.

2.2.1.3 2-Pentadecylaniline. The light yellow solid melted at 34.0-34.5 °C. The yield was 75%. ^{1}H NMR ($CDCl_3$): δ = 0.80 (t, 3H); 1.27 (bs, 24H); 1.60 (m, 2H); 2.48 (t, 2H); 3.60 (bs, 2H); 6.65-6.77 (m, 2H); 7.00-7.05 (m, 2H). ^{13}C NMR ($CDCl_3$): δ = 14.11, 22.68, 28.74, 29.35, 29.66, 31.29, 31.91, 115.46, 118.72, 126.77, 126.96, 129.39, 143.98. FTIR (KBr, cm^{-1}): 3433, 3308 (*v* NH); 1276 (*v* NAr). HRMS: Calcd for $C_{21}H_{37}N$ (M^+): 303.2926. Found: 303.2937. Anal. Calcd. for $C_{21}H_{37}N$: C, 83.10; H, 12.29; N, 4.61. Found: C, 83.06; H, 12.30; N, 4.57.

2.2.1.4 3-Pentadecylaniline. The white solid melted at 44.0-44.5 °C. The yield was 43%. ^{1}H NMR ($CDCl_3$): δ = 0.90 (t, 3H); 1.28 (bs, 24H); 1.60 (m, 2H); 2.53 (t, 2H); 3.60 (bs, 2H); 6.50-6.64 (m, 3H); 7.08 (t, 1H). ^{13}C NMR ($CDCl_3$): δ = 13.92, 22.49, 29.48, 31.18, 31.72, 35.78, 112.31, 144.99, 118.58, 128.87, 144.05, 146.03. FTIR (KBr, cm^{-1}): 3409, 3336 (*v* NH); 1278 (*v* NAr). HRMS: Calcd for $C_{21}H_{37}N$ (M^+): 303.2926. Found: 303.2931. Anal. Calcd. for $C_{21}H_{37}N$: C, 83.10; H, 12.29; N, 4.61. Found: C, 83.14; H, 12.30; N, 4.62.

2.2.1.5 4-Pentadecylaniline. The light yellow solid melted at 51.0-52.0°C. The yield was 29%. ^{1}H NMR ($CDCl_3$): δ = 0.90 (t, 3H); 2.50 (bs, 24H); 1.55 (m, 2H); 2.50 (t,

2H); 3.50 (bs, 2H); 6.65 (d, 2H); 6.95 (d, 2H). ^{13}C NMR ($CDCl_3$): δ = 13.92, 22.50, 29.11, 29.37, 31.64, 34.89, 114.94, 128.93, 132.92, 143.76. FTIR (KBr, cm^{-1}): 3394, 3315 (ν NH); 1272 (ν NAr). HRMS: Calcd for $C_{21}H_{37}N$ (M^+): 303.2926. Found: 303.2934. Anal. Calcd. for $C_{21}H_{37}N$: C, 83.10; H, 12.29; N, 4.61. Found: C, 83.14; H, 12.28; N, 4.62.

2.2.2 (1-Octadecynyl)aniline.

The *ortho* and *meta* isomers of (1-octadecynyl)aniline were synthesized by the route indicated in Figure 2.2. Modifications of reported literature procedures were used to prepare the monomers.[135] 1-Octadecyne was provided by Farchan Laboratories, Gainesville, Florida.

2.2.2.1 General procedure for the synthesis of (1-octadecynyl)aniline.

Bromoaniline (2.22 g, 12.9 mmol), 1-octadecyne (3.59 g, 14.4 mmol), triphenylphosphine (171 mg, 0.653 mmol), cupric acetate dihydrate (42.6 mg, 0.235 mmol), and palladium dichloride (22.7 mg, 0.128 mmol) were suspended in 50 mL of diisopropylamine. The flask was flushed with argon and heated to 80° C for 4 h. Upon completion (determined by TLC), the reaction mixture was cooled and the white precipitate that formed was filtered and discarded. The solvent was removed under reduced pressure and the crude mixture was passed through silica gel using methylene chloride as the eluant. Further purification was achieved by column chromatography (silica gel/ hexane:methylene chloride, 60:40).

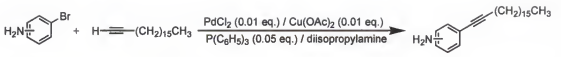

Figure 2.2. Synthetic scheme for (1-octadecynyl)aniline.

2.2.2.2 2-(1-Octadecynyl)aniline. The yield was 41 % (1.84 g, 5.26 mmol). The white solid melted at 29.5 - 30.0 °C. ^{1}H NMR($CDCl_3$) δ= 0.90 (t, 3H), 1.28 (bs, 24H), 1.47 (m, 2H), 1.63 (m, 2H), 2.47 (t, 2H), 4.00 (bs, 2H), 6.70 (m, 2H), 7.09 (t, 1H), 7.25 (d, 1H). ^{13}C NMR ($CDCl_3$) δ= 14.09, 19.62, 22.67, 28.97, 29.15, 29.35, 29.54, 29.68, 31.91, 95.79, 108.99, 114.09, 117.81, 128.74, 131.98, 147.55. FTIR (KBr) 3483, 3389, 2919, 2837, 1607, 1484, 1454, 1302, 1266, 1149, 743 cm^{-1}. MS(FAB) exact mass calcd. (m+1) 342.3161. Found 342.3179. Anal. Calcd. for $C_{24}H_{39}N$: C, 84.39; H, 11.51; N, 4.10. Found: C, 84.43; H, 12.09; N, 3.89.

2.2.2.3 3-(1-Octadecynyl)aniline. The yield was 36% (1.62g, 4.68 mmol). The white solid melted at 36.4 - 38.6 °C. ^{1}H NMR($CDCl_3$) δ= 0.90 (t, 3H), 1.28 (bs, 24H), 1.45 (m, 2H), 1.63 (m, 2H), 2.39 (t, 2H), 3.64 (bs, 2H), 6.61 (d, 1H), 6.74 (s, 1H), 6.81 (d, 1H), 7.08 (t, 1H). ^{13}C NMR ($CDCl_3$)δ= 14.15, 19.42, 22.73, 28.82, 28.96, 29.21, 29.40, 29.59, 29.73, 31.95, 80.70, 89.89, 114.57, 117.93, 122.02, 124.80, 129.11, 146.15. FTIR (KBr) 3425, 3307, 3189, 2919, 2848, 1610, 1600, 1470, 1314, 1196, 1161, 861, 782, 714, 685 cm^{-1}. MS(FAB) exact mass calcd. (m+1) 342.3161. Found 342.3205. Anal. Calcd. for $C_{24}H_{39}N$: C, 84.39; H, 11.51; N, 4.10. Found: C, 84.48; H, 11.41; N, 4.08.

2.2.3 Methyl 17-(2-aminophenyl) heptadecanoate and 17-(2-aminophenyl)heptadecanoic acid.

Methyl 17-(2-aminophenyl)heptadecanoate and 17-(2-aminophenyl)heptadecanoic acid were synthesized by the route indicated in Figure 2.3.

2.2.3.1 Methyl 16-hydroxyhexadecanoate. Two mL of conc. H_2SO_4 were added to 600 mL of methanol and cooled to 0 °C. One gram of 16-hydroxyhexadecanoic acid was added and the solution was mixed at 0 °C. Once the 16-hydroxyhexadecanoic acid completely dissolved, another gram of acid was added. This procedure was repeated until all of the starting material (5.215 g, 19.14 mmol) was added. The solution was mixed for an additional 8 h at 0 °C and was then allowed to warm to room temperature. The solution volume was reduced to ca.100 mL under reduced pressure, and then 200 mL of deionized water was added to the mixture, which resulted in precipitation. The solid was collected and then dissolved in 50 mL of methylene chloride. The organic solution was extracted with 5% $NaHCO_3$ and water. After drying with anhydrous magnesium sulfate, the methylene chloride was removed under reduced pressure leaving 4.994 g (17.43 mmol) of methyl 16-hydroxyhexadecanoate. The yield was 91 %. The white solid melted at 53.0 - 54.0 °C. ^1H NMR ($CDCl_3$): δ = 1.23 (bs, 22H); 1.57 (m, 4H); 2.28 (t, 2H); 3.61 (t, 2H); 3.64 (s, 3H). ^{13}C NMR ($CDCl_3$): δ = 24.90, 25.70, 29.10, 29.20, 29.39, 29.56, 32.74, 34.06, 51.40, 62.95, 174.35. FTIR (KBr, cm^{-1}): 1743 (stretch, C=O). MS (CI) exact mass calcd. (m+1): 287.2586. Found: 287.2554. Anal. Calcd. for $C_{17}H_{34}O_3$: C, 71.28; H, 11.96. Found: C, 71.28; H, 11.87.

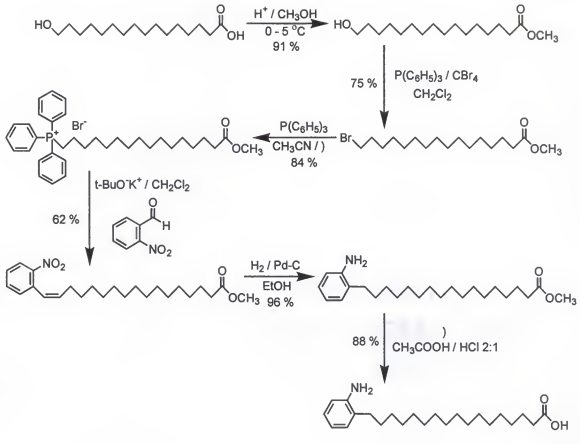

Figure 2.3. Synthetic route for methyl 17-(2-aminophenyl)heptadecanoate and 17-(2-aminophenyl)heptadecanoic acid.

2.2.3.2 Methyl 16-bromohexadecanoate. Methyl 16-hydroxyhexadecanoate (4.892 g, 17.71 mmol) and tetrabromomethane (11.70 g, 35.42 mmol) were dissolved in 12 mL of dry methylene chloride and mixed at room temperature under an argon atmosphere. Triphenylphosphine (4.65 g, 17.7 mmol), dissolved in 10 mL of dry methylene chloride, was added dropwise over the next 4 h, and then the mixture was allowed to stir for an additional 8 h. The solution was treated with 200 mL of n-pentane

in order to precipitate the triphenylphosphine oxide. The precipitate was filtered and washed several times with n-pentane. The combined n-pentane extracts were washed with 5% $NaHCO_3$, water, and then dried over anhydrous magnesium sulfate. The n-pentane was removed under reduced pressure and the residue was crystallized from absolute ethanol. The yield was 75 % (4.49 g) and the white solid melted at 30.0 - 30.5 °C. ^1H NMR ($CDCl_3$): δ = 1.26 (bs, 20H); 1.42 (m, 2H); 1.62 (m, 2H); 1.85 (m, 2H); 2.30 (t, 2H); 3.40 (t, 2H); 3.66 (s, 3H). ^{13}C NMR ($CDCl_3$): δ = 24.92, 28.14, 28.73, 29.11, 29.21, 29.40, 29.49, 29.57, 32.81, 33.92, 34.06, 51.35, 174.23. MS(FAB) exact mass calcd. (m+1): 349.1742. Found: 349.1756. Anal. Calcd. for $C_{17}H_{33}O_2Br$: C, 58.44; H, 9.52; Br, 22.87. Found: C, 58.67; H, 9.45; Br, 22.64.

2.2.3.3 15-(Carbomethoxy)pentadecyltriphenylphosphonium bromide. Methyl 16-bromohexadecanoate (4.237 g, 12.13 mmol) and triphenylphosphine (3.181 g, 12.13 mmol) were placed in 30 mL of acetonitrile and refluxed for 10 h under an argon atmosphere. The solvent was removed under reduced pressure, leaving a thick yellow oil. n-Pentane (40 mL) was added to the oil and the mixture was cooled in an ice bath. The precipitate that formed was isolated and dried under vacuum, yielding 6.214 g of white solid that melted at 97 - 99 °C. The yield was 84 %. ^1H NMR ($CDCl_3$): δ = 1.97 (bs, 22H); 1.62 (bs, 4H); 2.29 (bs, 2H); 3.65 (s, 2H); 3.72 (bs, 2H); 7.72 - 7.83 (m, 15H). ^{13}C NMR ($CDCl_3$): δ = 22.37, 23.03, 24.80, 29.05, 29.27, 29.42, 30.19, 30.40, 33.96, 51.27, 117.63, 118.76, 130.31, 130.47, 133.45, 133.59, 134.91, 174.20. Anal. Calcd. for $C_{35}H_{48}O_2BrP$: C, 68.73; H, 7.91; Br, 11.75. Found: C, 68.33; H, 7.88; Br, 12.40.

2.2.3.4 Methyl 17-(2-nitrophenyl)-16-heptadecenoate. In a 200 mL round bottom flask, 15-(carbomethoxy)pentadecyltriphenylphosphonium bromide (6.194 g, 10.13 mmol) and 2-nitrobenzaldehyde (1.530 g, 10.13 mmol) were placed in 100 mL of dry tetrahydrofuran and mixed under an argon atmosphere. The solution was cooled to -78 °C, then potassium *tert*-butoxide (1.14 g, 10.1 mmol) was added all at once. The solution was stirred under argon at -78 °C for an hour and was then allowed to slowly warm to room temperature and stir for an additional 8 h. The solution was poured into 100 mL of water and extracted with methylene chloride (3 x 50 mL). The combined methylene chloride extracts were washed with water, dried over anhydrous magnesium sulfate, and the solvent was removed under reduced pressure. The product was purified by column chromatography (silica/methylene chloride/hexanes, 70:30). The light yellow solid product was a mixture of *cis* and *trans* isomers (2.552 g) with a melting point at 39-41 °C. The yield was 62 %. ^{1}H NMR ($CDCl_3$): δ = 1.22 (bs, 22H); 1.62 (m, 2H); 2.04 - 2.33 (m, 4H); 3.67 (s, 3H); 5.78 - 6.27 (m, 1H); 6.67 - 6.86 (m, 1H); 7.34 - 7.59 (m, 3H); 7.85 - 8.00 (m, 1H). ^{13}C NMR ($CDCl_3$): δ = 24.92, 28.39, 28.96, 29.11, 29.22, 29.36, 29.41, 29.45, 29.45, 29.49, 29.58, 33.16, 34.07, 124.30, 124.38, 124.77, 124.89, 127.25, 127.54, 128.33, 131.84, 132.50, 132.72, 132.92, 134.81, 136.94, 174.35 MS(FAB) exact mass calcd. (m+1): 404.2801. Found: 404.2830. Anal. Calcd. for $C_{24}H_{37}O_4N$: C, 71.43; H, 9.24; N, 3.46. Found: C, 71.14; H, 9.73; N, 3.57.

2.2.3.5 Methyl 17-(2-aminophenyl)heptadecanoate. Methyl 17-(2-aminophenyl)-16-heptadecenoate (2.361 g, 5.850 mmol) and 10% palladium on carbon (0.45 g) were placed in 30 mL of 95% ethanol and stirred under a hydrogen atmosphere

for 12 h at room temperature and atmospheric pressure. The solution was filtered through a glass fritted funnel to remove the catalyst, which was then washed with several portions of methylene chloride. The ethanol and methylene chloride washings were combined and the solvents were removed under reduced pressure leaving a white solid. The product was purified by column chromatography (silica/methylene chloride). The melting point was 56-57 °C and the yield was 96% (2.106 g). ^{1}H NMR ($CDCl_3$): δ = 1.25 (bs, 24H); 1.61 (m, 4H); 2.30 (t, 2H); 2.47 (t, 2H); 3.61 (bs, 2H); 3.66 (s, 3H); 6.65 - 6.75 (m, 2H); 7.00 - 7.04 (m, 2H). ^{13}C NMR ($CDCl_3$): δ = 24.92, 28.71, 29.12, 29.22, 29.42, 29.63, 29.68, 31.27, 34.08, 51.39, 115.44, 118.64, 126.74, 126.90, 229.35, 143.97, 174.29. MS(FAB) exact mass calcd. (m+1): 376.3216. Found: 376.3226. Anal. Calcd. for $C_{24}H_{41}O_2N$: C, 76.75; H, 11.00; N, 3.73. Found: C, 76.74; H, 11.08; N, 3.71.

2.2.3.6 17-(2-Aminophenyl)heptadecanoic acid. Methyl 17-(2-aminophenyl) heptadecanoate (1.013 g, 2.697 mmol) was placed in 24 mL of 2:1 glacial acetic acid and concentrated hydrochloric acid. The slurry was refluxed for 3 h under an argon atmosphere and then transferred to a beaker containing saturated $NaHCO_3$ and ice. Solid $NaHCO_3$ was slowly added to the slurry until the pH of the solution was neutral. The solution was extracted with methylene chloride (5 x 100 mL), then the combined organic extracts were extracted once with deionized water, dried over anhydrous magnesium sulfate, and the organic solvent was removed under reduced pressure. The product was purified by column chromatography (silica/methylene chloride) and was a white solid with a melting point at 82.0 - 83.0 °C. The yield was 88% (0.840 g). ^{1}H NMR ($CDCl_3$): δ = 1.25 (bs, 24H); 1.61 (m, 4H); 2.34 (t, 2H); 2.48 (t, 2H); 6.70 - 6.76 (m, 2H); 7.01 -

7.05 (m, 2H). ^{13}C NMR ($CDCl_3$): δ = 24.67, 28.77, 29.04, 29.22, 29.40, 29.55, 29.62, 29.69, 31.27, 34.04, 115.64, 118.88, 126.78, 127.12, 129.39, 143.79, 179.82. MS(FAB) exact mass calcd. (m+1): 362.3059. Found: 362.3047. Anal. Calcd. for $C_{23}H_{39}O_2N$: C, 76.47; H, 10.87; N, 3.87. Found: C, 76.21; H, 10.81; N, 3.70.

2.2.4 1,22-Bis(2-aminophenyl)docosane

1,22-Bis(2-aminophenyl)docosane was synthesized by the route indicated in Figure 2.4. 11-Bromo-1-undecene was graciously provided by Mr. Mark Watson and Dr. Kenneth Wagener of the University of Florida. The ruthenium catalyst mediated metathesis step in this synthetic route was carried out by Mark Watson.

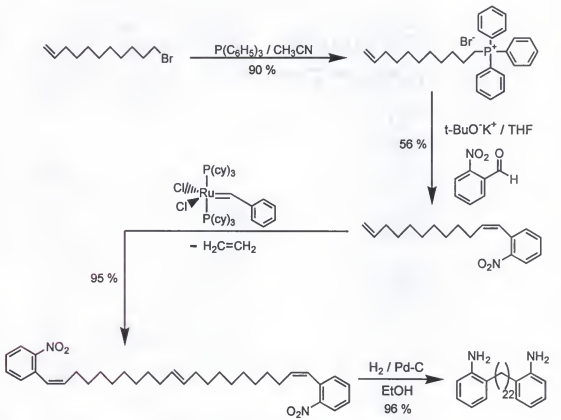

Figure 2.4. Synthetic scheme for 1,22-bis(2-aminophenyl)docosane.

2.2.4.1 10-Undecenyltriphenylphosphonium bromide. 11-Bromo-1-undecene (5.760 g, 24.70 mmol) was placed in a 100 mL round bottom flask with triphenylphosphine (6.802 g, 25.94 mmol) and 20 mL acetonitrile. The mixture was refluxed for 12 h and then allowed to cool to room temperature. The solvent was removed under reduced pressure, leaving a thick oil. The product was purified by column chromatography (silica) by first using methylene chloride as the mobile phase and eluting all of the mobile impurities, then the silica was remove from the column and mixed with methanol for 8 h. The silica was filtered and the methanol was removed under reduced pressure leaving a thick oil. The yield was 90 % (10.97 g). ^{1}H NMR($CDCl_3$) δ= 1.15 (bs, 10H), 1.57 (bs, 4H), 1.95 (m, 2H), 3.66 (bs, 2H), 4.87 (m, 2H), 5.71 (m, 1H), 7.66 - 7.78 (m, 15H). ^{13}C NMR ($CDCl_3$) δ= 22.33, 22.44, 22.99, 28.66, 28.83, 28.95, 29.00, 29.15, 30.16, 30.36, 33. 58, 113.96, 117.58, 118.72, 130.29, 130.46, 133.42, 133.55, 134.89, 134.93, 138.99. Anal. Calcd. for $C_{29}H_{36}PBr$: C, 70.30; H, 7.32; Br, 16.13. Found: C, 68.81; H, 7.45; Br, 18.58.

2.2.4.2 1-(2-Nitrophenyl)-1,11-dodecadiene. 10-Undecenyltriphenyl-phosphonium bromide (10.44 g, 21.06 mmol) was placed in a 250 mL round bottom flask with 2-nitrobenzaldehyde (3.183 g, 21.06 mmol) and 70 mL dry tetrahydrofuran. The solution was mixed under argon at -78 °C, then potassium *tert*-butoxide (2.363 g, 21.06 mmol) was added in one portion to the solution. The mixture was stirred for 3 h at -78 °C, then mixed for 8 h at room temperature. The mixture was poured into a 100 mL solution of ice and water, then extracted with methylene chloride (3 x 50 mL). The combined extracts were washed with deionized water and then dried over anhydrous

magnesium sulfate. The solvent was removed under reduced pressure and the product was purified by column chromatography (silica/1:1 hexanes and methylene chloride) to give 3.41 g of a light yellow oil. The yield was 56 %. The product was a mixture of *cis* and *trans* isomers. ^{1}H NMR ($CDCl_3$): δ = 1.22 - 1.62 (m, 12H); 1.99-2.29 (m, 4H); 4.94 (m, 2H); 5.73-6.28 (m, 2H); 6.67-6.86 (m, 1H); 7.26-7.58 (m, 3H); 7.85-8.00 (m, 1H). ^{13}C NMR ($CDCl_3$): δ = 28.35, 28.84, 28.92, 29.04, 29.27, 29.30, 29.36, 29.41, 33.13, 33.73, 114.05, 124.26, 124.35, 124.80, 124.91, 127.24, 127.54, 128.31, 131.81, 132.47, 132.70, 132.88, 133.32, 134.75, 136.86, 139.11, 147.63, 148.30. Anal. Calcd. for $C_{18}H_{25}NO_2$: C, 75.22; H, 8.77; N, 4.87. Found: C, 74.61; H, 8.76; N, 4.87.

2.2.4.3 1,22-Bis(2-nitrophenyl)-1,11,21-docosatriene. 1-(2-Nitrophenyl)-1,11-dodecadiene (1.00 g, 3.32 mmol) was combined with 14.0 mg of the ruthenium metathesis catalyst, $Ru(Cl)_2(P(C_6H_{11})_3)_2(CHC_6H_5)$, in a dry box. Regular bubbling began to occur within five minutes, which indicated the evolution of ethylene from the mixture. The reaction flask was then attached to a vacuum line and a vacuum was pulled on the solution while it was stirred at room temperature. After 72 h, the flask was opened to the atmosphere and toluene (5 mL) and silica (ca.0.5 g) were added to the flask. The solution was filtered and the silica was washed with toluene (3 x 5 mL). The toluene was removed under reduced pressure leaving 0.867 g of a light yellow oil. The yield was 95%. ^{1}H NMR($CDCl_3$) δ = 1.22 - 1.50 (m, 24H), 1.95 (bs, 4H), 2.04 - 2.29 (m, 4H), 5.37 (bs, 2H), 5.77 - 6.28 (m, 2H), 6.66 - 6.85 (m, 2H), 7.26 - 7.58 (m, 6H), 7.84 - 7.99 (m, 2H). ^{13}C NMR ($CDCl_3$)δ= 27.13, 28.34, 28.92, 29.05, 29.19, 29.29, 29.40, 29.54, 29.66, 32.51, 33.12, 124.25, 124.33, 124.76, 124.88, 127.22, 127.52, 128.30, 129.79, 130.25,

131.80, 132.46, 132.70, 132.86, 133.29, 134.74, 136.86, 147.60, 148.28. MS(FAB) exact mass calcd. (m +1): 547.3536, Found: 547.3555. Anal. Calcd. for $C_{34}H_{46}N_2O_4$: C, 75.22; H, 8.77; N, 4.87. Found: C, 74.61; H, 8.76; N, 4.87.

2.2.4.4 1,22-Bis(2-aminophenyl)docosane. 1,22-Bis(2-nitrophenyl)-1,11,21-docosatriene (0.817 g, 1.49 mmol) was placed in 15 mL of 95% ethanol with 0.20 grams of 10% palladium on carbon. The solution was stirred under a pure hydrogen gas atmosphere until no more hydrogen gas was consumed (4 days). The hydrogenation was carried out under normal atmospheric pressure and at room temperature. The mixture was filtered, the catalyst was washed with methylene chloride, the ethanol and methylene chloride solvents were combined, and the solvents were removed under reduced pressure yielding a white solid. Purification was carried out by column chromatography (silica/methylene chloride) and verified by gas chromatography (only one peak was observed). The melting point was 64.0 - 66.0 °C. The yield was 96% (0.703 g). ^{1}H NMR($CDCl_3$) δ = 1.25 (s, 36H), 1.60 (m, 4H), 2.47 (t, 4H), 3.56 (bs, 4H), 6.64 - 6.74 (m, 4H), 6.99 - 7.04 (m, 4H). ^{13}C NMR ($CDCl_3$) δ= 28.71, 29.54, 29.60, 29.67, 31.27, 115.44, 118.65, 126.75, 126.90, 129.35, 143.97. MS(FAB) exact mass calcd. (m +1): 493.4522. Found: 493.4585. Anal. Calcd. for $C_{34}H_{56}N_2$: C, 82.86; H, 11.45; N, 5.68. Found: C, 82.99; H, 11.43; N, 5.58.

2.3 Langmuir Film Preparation

The monolayer and polymerization studies were done on KSV 5000 Langmuir-Blodgett equipment (KSV Instruments, Finland). The surface area, pressure, and potential were recorded by an IBM compatible computer which ran the KSV 5000 software package. Experimental factors such as the molecular weight of the surfactant, solution concentration and volume, total interfacial area, and barrier speed were entered into the computer. The troughs used in these experiments were rectangular in shape and Teflon lined. Two Teflon barriers were used.

A Neslab RTE 250 circulating bath that was connected to a water-jacket just below the surface of the trough was used to maintain subphase temperature. The temperature was maintained to $\pm 0.1^{\circ}C$ and was determined by placing a digital thermometer just below the surface of the interface. The subphase was allowed to reach the desired temperature before the surfactants were added.

The water used for trough cleaning and subphase solution preparation was purified by a Millipore system($\geq$ 18 MΩ resistance). This system incorporates an activated carbon cartridge, two ion-exchange cartridges, and one Organex-Q cartridge. All water used in the experiments reported herein was Millipore water.

Before filling the trough with a subphase, the trough was cleaned using the following procedure: (1) the trough and the barriers were wiped with a chloroform soaked Kimwipe, (2) the trough was rinsed first with a dilute solution of ethanol and then twice with Millipore water.

The surfactant solutions were prepared in volumetric glassware using Fisher spectrograde chloroform. The surfactants were weighed on a Mettler AE240 balance. Solution concentrations ranged between 0.500 to 1.10 mg mL^{-1}. The solutions were deposited on the air-aqueous interface by careful dropwise addition with a microsyringe and then allowing the chloroform to evaporate.

2.4 Monolayer Characterization

2.4.1 Surface Pressure vs. Mean Molecular Area Isotherms

The monolayer films were prepared using the procedures and equipment described in Section 2.3. The surface pressure, π, vs. mean molecular area, A, isotherms were measured while compressing a film at a constant speed of ca. 4-6 $Å^2$ $molecule^{-1}$ min^{-1}. Reproducibility was insured by repeating experiments a minimum of three times until the onset areas of the π-A isotherms were within one $Å^2$ $molecule^{-1}$ of one another.

Surface pressure was measured using a Wilhelmy plate balance (KSV Instruments) equipped with a paper or platinum plate hung from a platinum wire. The paper plates were cut from P5 Fisherbrand filter paper to the dimensions of 19.5 x 10 mm, were cleaned between runs by soaking in water, and were replaced after four experiments. Platinum plates were cleaned by flaming and were stored between experiments in a mixture of ethanol and water. During the film experiments, the plate was placed near the center of the trough and was immersed half-way into the sub-phase.

The pressure onset area of the monolayer films was determined by the extrapolation of the linear portion of the π-*A* isotherm to zero π. If there was no linear portion in the π-*A* isotherm, the pressure onset area was assigned to the area where the surface pressure dramatically increased. The film collapse occurred when film's surface pressure was no longer stable upon compression.

2.4.2 Isobaric Stabilities

The isobaric stability measurements were performed by first depositing the surfactant as described in Section 2.3, and then compressing the film at a rate of ca. 4-6 $Å^2$ molecule^{-1} min^{-1} until a designated surface pressure was reached. The film was maintained at this surface pressure while the surface area was monitored over time.

2.4.3 Surface Potential vs. Mean Molecular Area Isotherms

The surface potential, ΔV, of the Langmuir films was measured with a vibrating plate surface potentiometer (KSV Instruments, Finland) that is based on a parallel plate capacitor.[22, 23, 136] This method uses two plates, one below and one above the interface, that are separated by the a distance, *d*. If the potential difference between the plates is Φ, then the charge residing on each plate is:

$$Q = C\Phi = \frac{A\epsilon_0\epsilon\Phi}{d} \qquad (2.1)$$

where *C* is the capacitance, and *A* is the area of the plates. Changing the distance between the plates, Δd, results in a change in the amount of charge on each plate, ΔQ. If

the two plates are connected by an external circuit, a charge will flow through the circuit while the distance between the plates is being changed. If the distance between the two plates is vibrated continuously at a specific frequency by a distance, Δd, then an alternating current will flow in the circuit at a frequency given by the following equation:

$$\Delta Q = -\frac{A\epsilon_0\epsilon\Phi}{d^2}\Delta d \qquad (2.2)$$

Figure 2.5 shows a schematic diagram of a vibrating plate potentiometer. A platinum plate is placed ca. 3 mm below the surface of the interface. A silver plate connected to a vibrating voice coil of a loudspeaker is placed less than 1 cm above the platinum plate. The contact potential between the plates, Φ, can be determined by the detection and amplification of the alternating current. An external bias in the circuit is used to adjust the circuit so the net potential difference is zero and no current flows when the plate is moved. This applied bias is V and equation 2.3 can be rewritten as

$$\Delta Q = -\frac{(\Phi + V)A\epsilon_0\epsilon}{d^2}\Delta d \qquad (2.3)$$

where ΔV is then the difference in external bias before and after the monolayer film has been applied to the surface of the interface, which is equivalent to the change in the contact potential at the interface.

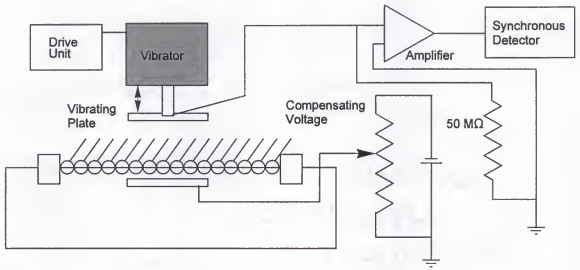

Figure 2.5. Surface potentiometer schematic (vibrating plate method) using the compensating voltage circuitry.

The surface potentiometer was calibrated against an external power source prior to use, which in this case was an AA battery whose exact voltage was determined with a voltmeter. Prior to the deposition of the monolayer on the subphase surface, the surface potentiometer's value was set to zero. After a surfactant was placed at the interface, the surface potential was allowed to come to equilibrium before the film was compressed (ca. 2 to 3 minutes).

The monolayer films were prepared using the procedures and equipment described in Section 2.3. ΔV and π vs. A isotherms were measured while compressing a film at a constant speed of ca. 4-6 $Å^2$ $molecule^{-1}$ min^{-1}.

2.5 Polymerization

The aniline monomers were polymerized at constant applied surface pressures and subphase temperatures on a subphase solution of 0.10 M sulfuric acid and 0.03 M ammonium peroxydisulfate unless otherwise noted. Sulfuric acid was used instead of simpler acids like HCl to be consistent with the previous literature on surfactant aniline polymerization.[93, 95, 99, 134, 155] The monolayer films were prepared using the procedures and equipment described in Section 2.3. The film was compressed at ca. 45 $Å^2$ $molecule^{-1}$ min^{-1} until the surface pressure was within 5 mN m^{-1} of the desired surface pressure; it was then compressed at ca. 15 $Å^2$ $molecule^{-1}$ min^{-1}. Once the target surface pressure was reached, there was a brief induction period, 15 to 60 seconds, when the change in area was slower. The end of this period was designated as the beginning of the reaction and the mean molecular area at this time is termed A_0. This short induction period is believed to be due to film stabilization after its rapid compression. The polymerization was monitored by the change in the mean molecular area of the surfactant at a constant applied surface pressure. The polymerization is considered complete when the change in mean molecular area, within experimental error, is zero. The polymerized Langmuir films were removed from the air-aqueous interface by passing the solution at the interface through a small glass frit, which collected the polymeric material. The polymers were washed with deionized water and dried under vacuum for a minimum of two hours.

The kinetic data was analyzed with the Microcal Origin software package. The curve fitting program within Origin used a least-square fit to determine the best fit for the

data presented. The average of at least three separate polymerizations was used to evaluate the kinetics.

2.6 Additional Characterizations Methods

2.6.1 UV-Vis

The polymer samples were collected from the surface of the trough by the technique outlined in Section 2.5. UV-vis data was collected on a Varian-Cary 5E UV-Vis-NIR Spectrophotometer. The solvent used for the UV-vis measurements was Fisher spectrograde chloroform.

2.6.2 Size Exclusion Chromatography

Size exclusion chromatography (SEC) molecular weight analysis was performed at room temperature using a Waters Associates liquid chromatography apparatus equipped with Phenomenex columns and a Kratos Analytical spectroflow 757 absorbance detector set at 254 nm and a Perkin-Elmer LC-25 refractive index detector. The mobile phase was tetrahydrofuran or chloroform and the instrument was calibrated with polystyrene standards. The mobile phase was passed through the columns at a rate of 1 mL min^{-1}.

2.6.3 FT-IR

The infrared measurements were performed on a Fourier transform infrared spectrometer (Bio-Rad FTS-40A) with a diffuse reflectance spectrometer accessory. The advantage of using the diffuse reflectance method of measuring the infrared spectrum is

that the small samples generated from Langmuir film polymerizations can be detected by this technique. The base forms of the polymer samples were prepared by dissolving a polymer sample in a small amount of chloroform, extracting several times with 0.10 M ammonium hydroxide and deionized water, and then mixing the polymer solution with a small amount of KBr powder. Once the chloroform had evaporated, the sample was dried under vacuum for two hours. The sample mixture was placed in the top half of the sample cup that was already filled with KBr powder.

2.6.4 Cyclic Voltammetry

The cyclic voltammetry measurements were carried out by Dr. Hiep Ly of the University of Florida. The measurements were performed on an EG&G Princeton Applied Research Model 273 potentiostat/galvanostat. The potentiostat/galvanostat was controlled by a Model 270/250 Research Electrochemistry Software package, version 4.30, that was loaded on a PC computer. The working electrode was a 0.006 cm^2 platinum button, the counter electrode was a platinum plate, and the reference electrode was Ag/Ag^+ (Ag wire in 0.1 M $AgNO_3$). The Ag/Ag^+ had a potential of +0.33 V vs. the SCE.[137] The scan rate was 50 mV sec^{-1}. The acetonitrile used in these experiments was refluxed and distilled over calcium hydride. The electrolyte compound used for all experiments was 0.10 M lithium perchlorate. The lithium perchlorate was not dried before use. The concentrations of the surfactant solutions were ca. 0.05 to 0.10 M. The platinum working electrode was cleaned between each scan and the voltammetry measurements were repeated a minimum of two times to ensure reproducibility. The anodic peak potential, E_{pa}, was determined to be at the point of maximum current flow.

CHAPTER 3

THE POLYMERIZATION AND SURFACE BEHAVIOR OF ALKYL SUBSTITUTED ANILINE SURFACTANTS AT THE AIR-AQUEOUS INTERFACE

3.1 Introduction

The advantage of studying polymerization kinetics in a Langmuir film is that the molecules can be held in a well-defined orientation at an interface while the polymerization kinetics can be observed in real time.[95] In past studies, the kinetics of Langmuir film polymerizations have been shown to be sensitive to applied surface pressure and temperature,[12, 15, 137-140] but the effect that the reactive group conformation has on the polymerization rate is still not well understood. This chapter addresses the effect that the surface pressure has on the relative orientation of the surfactant at the interface by comparing the surface pressure and potentials of *ortho*, *meta*, and *para* alkyl substituted aniline surfactants at the air-aqueous interface. A method which monitors the change in the mean molecular area of the surfactant at a constant applied surface pressure and predicts the concentrations of monomer and polymer and/or oligomer at the interface in order to determine the formation rate of poly(alkylaniline) is presented. The rate of

polymerization of 2- and 3-pentadecylaniline is expressed in terms of the concentration of the monomer and polymer at the interface. The autoacceleration effect for the polymerization of these aniline surfactants is also addressed.

3.2 Monolayer Characterization.

Figure 3.1 shows the surface pressure, π, vs. mean molecular area, A, isotherms of 2-, 3-, and 4-pentadecylaniline on an air-water interface. The π-A isotherm of 2-pentadecylaniline was previously reported and is the same within experimental error.[94] As

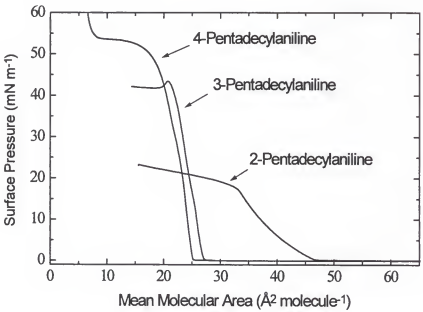

Figure 3.1. Surface pressure, π, vs. mean molecular area, A, isotherms of 2-, 3-, and 4-pentadecylaniline on deionized water at 25 °C.

shown in this graph, the onset areas of 3- and 4-pentadecylaniline are 27 and 25 $Å^2$ molecule^{-1} and collapse pressures are 43 and 50 mN m^{-1}, respectively. However, 2-pentadecylaniline had a much larger onset area, which was at 47 $Å^2$ molecule^{-1} and a collapse pressure of 18 mN m^{-1}. Up to the collapse pressure, both 3- and 4-pentadecylaniline had similar π-A isotherms when compared to that of 2-pentadecylaniline, but 3-pentadecylaniline was slightly more expanded. The onset area of 2-pentadecylaniline was ca. twice that of the onset area of 4-pentadecylaniline. It is assumed that the isomers are not ionized when they are on a water subphase; therefore, the differerences in the π-A isotherms are probably due to structural differences in the

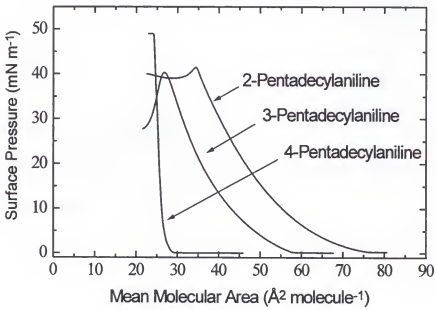

Figure 3.2. Surface pressure, π, vs. mean molecular area, A, isotherms of 2-, 3-, and 4-pentadecylaniline on 0.10 M H_2SO_4 at 25 °C.

molecules. The relatively large onset area of 2-pentadecylaniline is attributed to the position of the alkyl chain on the aromatic ring.

Figure 3.2 shows the π-A isotherms of 2-, 3-, and 4-pentadecylaniline on a 0.10 M H_2SO_4 subphase.[94, 100] As shown, 4-pentadecylaniline had an onset area of 27 $Å^2$ molecule^{-1} and a collapse pressure of 50 mN m^{-1} at 22 $Å^2$ molecule^{-1}. The steep pressure increase and low onset area suggests that this symmetric monomer formed a condensed monolayer film with little rearrangement between the onset and collapse pressures. The onset and collapse areas are considerably smaller than expected for an ionized monolayer as electrostatic repulsion between the positively charged head groups usually increases the surface area required by a film .[12] The lower onset and collapse areas may be explained by the divalent sulfate counter-ion in the subphase. Each sulfate ion near the interface is capable of forming an ion pair with two positively charged anilinium ions in the monolayer, allowing the surfactants to pack more tightly. The π-A isotherms of 2- and 3-pentadecylaniline are more expanded than that of 4-pentadecylaniline. The larger onset and collapse areas were previously attributed to the alkyl side chain of these unsymmetrical amphiphiles requiring larger areas at the interface as well as electrostatic repulsion between the positively charged monomers. [95,100]

The π-A isotherms of 2-pentadecylaniline on a 0.10 M H_2SO_4 subphase at temperatures between 10 to 40 °C have previously been reported.[144] This earlier study

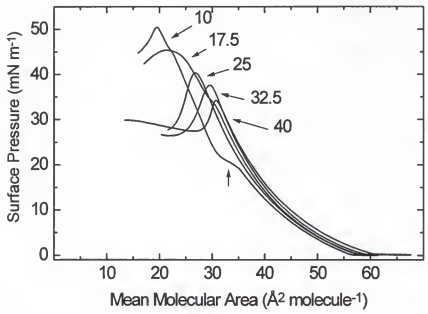

Figure 3.3. Surface pressure, π, vs. mean molecular area, *A*, isotherms of 3-pentadecylaniline on a H_2SO_4 subphase at 10, 17.5, 25, 32.5, 40 °C.

indicated that there was little change in the monolayer behavior at these temperatures. In a similar fashion, the π-*A* isotherms of 3-pentadecylaniline on a 0.10 H_2SO_4 subphase at temperatures of 10, 17.5, 25, 32.5, and 40°C were also recorded (Figure 3.3). The onset areas at the various temperatures were ca. 57 $Å^2$ $molecule^{-1}$. As with the data obtained from 2-pentadecylaniline, only a small increase in the onset mean molecular area was observed with increasing temperature.[141] However, the π-*A* isotherms of 3-pentadecylaniline at 10 and 17.5 °C show an apparent phase transition. At 10 °C, the π-*A* isotherm indicates that the film is more compact at pressures higher than 20 mN m^{-1} when compared to films at 25 to 40 °C, suggesting that the films are in two different

phases at these higher pressures.[12] The significance of this phase transition becomes important later in this chapter when a discussion on the Arrhenius plots for the polymerization of 3-pentadecylaniline is presented. The π-A isotherms of 4-pentadecylaniline on a 0.10 M H_2SO_4 subphase at temperatures between 10 to 40 °C were also recorded, and like 2-pentadecylaniline, the effects on the π-A isotherms of 4-pentadecylaniline were minimal.

A monolayer film at the air-aqueous interface can be treated as an assembly of molecular dipoles that can shift the potential across an interface.[12, 18] This potential shift, relative to a clean aqueous surface, is referred to as the surface potential of the

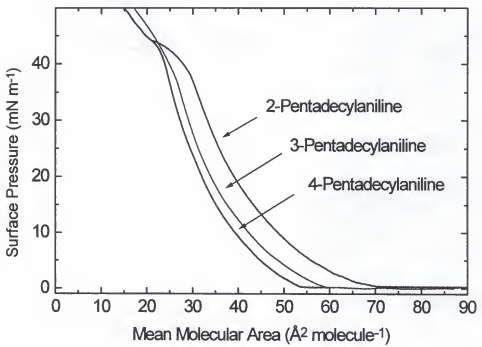

Figure 3.4. Surface Pressure, π, vs. mean molecular area, A, isotherms of 2-, 3-, and 4-pentadecylaniline on 0.20 M HCl at 25 °C.

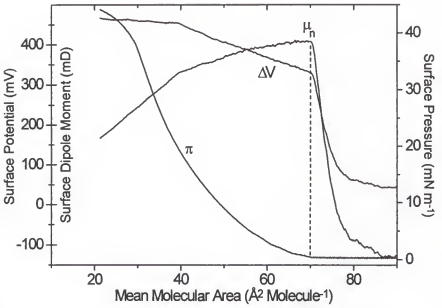

Figure 3.5. Surface pressure, π, potential, ΔV, and dipole moment, μ_n, vs. mean molecular area, A, for 2-pentadecylaniline on a 0.20 M HCl subphase at 25 °C.

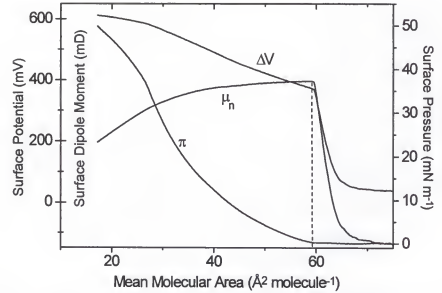

Figure 3.6. Surface pressure, π, potential, ΔV, and dipole moment, μ_n, vs. mean molecular area, A, for 3-pentadecylaniline on a 0.20 M HCl subphase at 25 °C.

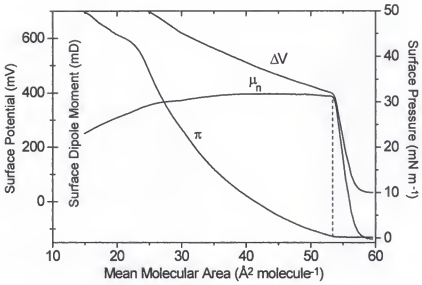

Figure 3.7. Surface pressure, π, potential, ΔV, and dipole moment, μ_n, vs. mean molecular area, A, for 4-pentadecylaniline on a 0.20 M HCl subphase at 25 °C.

monolayer, ΔV. To further characterize these monolayer films, surface potential measurements were done on the three isomers of pentadecylaniline. Using equations 1.5 and 1.6 the surface dipole moment, μ_n, of 2-, 3- and 4-pentadecylaniline can be calculated from ΔV.

To simplify the calculation of the double-layer potential, ψ_0, a 0.20 M HCl subphase (Figure 3.4) was used instead of a 0.10 M H_2SO_4 subphase. HCl has a monovalent anion which allows the use of equation 1.5 to calculate ψ_0. The degree of ionization, α, is assumed to be unity in all three cases. This is a good assumption as the pK_a values of 2-pentadecylaniline[142] and 4-hexadecylaniline[143] at the air-aqueous interface have previously been estimated at 4.6 and 3.6, respectively. Figures 3.5, 3.6, and 3.7 show the ΔV, μ_n, and π vs. A for 2-, 3-, and 4-pentadecylaniline, respectively.

The π-A isotherms of 2- and 3-pentadecylaniline on 0.20 M HCl were similar to those observed on 0.10 M H_2SO_4, while that of 4-pentadecylaniline was much more expanded. The π-A isotherm of 4-pentadecylaniline was similar to one previously reported for 4-hexadecylaniline on a 1.0 M HCl subphase, in which the onset pressure was ca. 60 $Å^2$ $molecule^{-1}$.[143] Ion pairing effects may contribute to the more condensed isotherm observed on 0.10 M H_2SO_4. Similar effects have been observed when comparing the π-A isotherms of stearic acid on a subphase containing a doubly charged ion.[144] A stearic acid monolayer on a cadmium chloride subphase was more compressed relative to that observed in the absence of the metal. This effect was attributed to the crosslinking action of the Cd^{2+}.

At an area approximately 10 $Å^2$ $molecule^{-1}$ greater than the pressure onset area, the calculated values of μ_n were negative even though the recorded ΔV at this A was positive. Upon compression, the value of μ_n increased dramatically for all three isomers and reached a maximum at ca. the same A as the onset pressure. As the film was compressed further, μ_n slowly decreased. It should be noted that Gouy-Chapman equation (equation 1.5) assumes that the monolayer consists of an impenetrable plane-layer of positive charge spread uniformly over the surface with the negative counter ions in the subphase just below this layer.[18] At higher surface areas, prior to the pressure onset area, the monolayer is not packed tightly and the counter-ions may penetrate the plane of the

charged head group, resulting in a higher approximation of ψ_0 and thus, a negative calculated value of μ_n. At areas below the pressure onset area, the Gouy-Chapman equation is believed to be a good approximation of ψ_0 as it assumes that the counter ion is no longer in the plane of the monolayer film.

When the values of μ_n of the three isomers at the corresponding pressures are compared, the largest decrease in μ_n was observed for 2-pentadecylaniline as the surface pressure was increased (Figure 3.8). The contribution to μ_n (equation 1.4) from the hydrophobic chain, μ_3, has been estimated to be positive when organized in a Langmuir

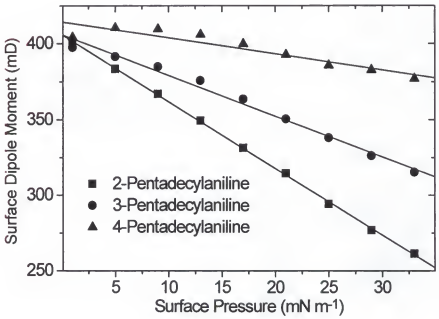

Figure 3.8. Plot of surface dipole moments (μ_n) of 2-, 3-, and 4-pentadecylaniline at their corresponding surface pressures (π).

film and relatively constant over the region measured ($\mu_3/\epsilon_3 \approx 116$ mD).[16] μ_2, the contribution of the anilinium head group, is predicted to be positive and largest when the C-N bond is approximately perpendicular to the interface. This prediction is based on surface potential measurements of an aliphatic ammonium ion, which also gave a large positive contribution to μ_n.[145] As the anilinium ion is rotated away from a perpendicular orientation, the value of μ_2 should approach zero as the dipole becomes closer to a parallel orientation at the interface. μ_2 is also affected by the position of the alkyl substituent on the anilinium ring, which adds uncertainty to the comparison of the μ_ns of the three isomers. A better use of the μ_n data would be the comparison of the slopes of the dipole change as the area per molecule was compressed. The slope of the lines in Figure 3.8, which are a measure of $(\delta\mu_n/\delta\pi)_T$, are -4.41, -2.68, and -1.05 mD m mN^{-1} for 2-, 3-, and 4-pentadecylaniline, respectively. As the surface pressure was increased, the change in μ_n of 2-pentadecylaniline was the greatest, which indicates a larger change in the relative orientation of the molecule compared to the two other isomers. As expected for a symmetric molecule, 4-pentadecylaniline showed little change in μ_n as the film was compressed. The change in μ_n for 3-pentadecylaniline (-2.68 mD m mN^{-1}) was in between that of the ortho and para substituted surfactant, which is an indication of orientational change, but not to the degree observed for 2-pentadecylaniline.

The differences in the surface behavior of the three isomers can be attributed to structural differences that affect their arrangement on the aqueous surface. These differences suggest that the conformation of the anilinium group at the air-aqueous interface is affected by the amount of surface area that confines the surfactants. In the

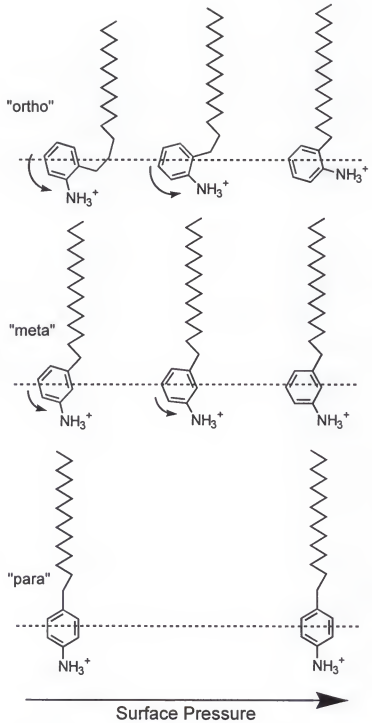

Figure 3.9. Predicted surface behavior of the head groups of 2-, 3-, and 4-pentadecylaniline at changing surface pressures. Arrows show the predicted conformation change of the anilinium head group when going from low to high surface pressures.

case of 2-pentadecylaniline, the alkyl chain had more space to occupy at larger areas, but as the area was decreased, the alkyl group was pushed away from the interface, thus reorienting the anilinium group. The surface potential and pressure measurements of 3-pentadecylaniline also suggest that the anilinium group reoriented to a lesser extent at the air-aqueous interface as the amount of surface area that confined the surfactant changed. The 4-pentadecylaniline data suggests that the anilinium group underwent little conformational change as the film was compressed to smaller surface areas. The observed surface behavior of the isomers is summarized by the cartoon in Figure 3.9.

Thermodynamic analysis of isothermal data is often used to quantitatively evaluate the interactions of surfactants in Langmuir monolayers.[146, 147] π-A isotherms can be viewed as 2-dimensional analogs of pressure-volume isotherm curves of 3-dimensional systems. In 3-dimensional systems, the change in Gibbs free energy, ΔG, of any pure material as it undergoes pressure changes at constant temperature can be determined by the integral:

$$\Delta G = \int_{p1}^{p2} V dp$$

Therefore, the ΔG of a surfactant molecule can be determined from the π-A isotherms between two different surface pressures using the following equation:

$$\Delta G = \int_{\pi 1}^{\pi 2} A d\pi$$

The calculated ΔGs of the three isomers between 0 and 10 mN m^{-1} on water, 0.10 M H_2SO_4 and 0.20 M HCl subphases are shown in Table 3.1.

Table 3.1. ΔG values determined from the π-A isotherms of 2-, 3-, and 4-pentadecylaniline between 0 and 10 mN m^{-1} surface pressure at 25 °C.

	ortho (kJ mol^{-1})	*meta* (kJ mol^{-1})	*para* (kJ mol^{-1})
water	2.5	1.6	1.4
0.10 M H_2SO_4	3.5	3.0	1.7
0.02 M HCl	3.5	3.0	2.7

The ΔG of the *ortho* and *meta* isomers on the acid subphases, within experimental error, had the same value, while 4-pentadecylaniline was different by 1.0 kJ mol^{-1}. The difference in value of the *para* isomer is attributed to the packing effect of the divalent ion sulfate ion. This change in film area on the different subphases was not observed for 2- and 3-pentadecylaniline. The ΔG values of the three isomers on water are smaller than on acid, which can be attributed to the electrostatic interactions between the charged surfactant molecules.

3.3 Polymerization of Pentadecylaniline

In theory, the polymerization of 2- and 3-pentadecylaniline should form the same product since the alkyl substituents on the monomers are equivalent in the polyaniline backbone, making the comparison of 2- and 3-pentadecylaniline particularly useful. It

should be noted that 4-pentadecylaniline did not polymerize under these conditions, so studies on this isomer were discontinued. Analysis of the polymerization product of 2-pentadecylaniline at the air-aqueous interface has been previously reported.[86] Due to the small amount of polymer produced during one polymerization (about 50 μg), size exclusion chromatography (SEC), UV-vis spectroscopy, and infrared spectroscopy were the most useful techniques for the analysis of the final polymer. SEC analysis of the polymerization product of 3-pentadecylaniline, poly(3-pentadecylaniline), produced two peaks of approximate equivalent intensity: one peak corresponded to high molecular

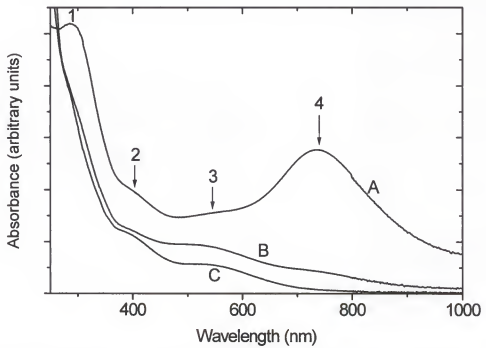

Figure 3.10. Absorption spectra of poly(2-pentadecylaniline) after completion of the polymerization reaction (spectrum A) and after the polymer is allow to remain at the interface for 4 h (spectrum B). Absorption spectrum of poly(3-pentadecylaniline) after completion of the polymerization reaction (spectrum C). Peaks 1, 2, 3, and 4 are 290, 405, 550, and 740 nm, respectively.

weight polymer and a second peak indicated lower weight oligomers. The first peak had a weight-average molecular weight (M_w) of ca. 740,000 g mol^{-1} and a number-average molecular weight (M_n) of ca. 250,000 g mol^{-1}. The polydispersity of the poly(3-pentadecylaniline) was 2.9. The previous analysis of poly(2-pentadecylaniline) found that M_w was 300,000 g mol^{-1} and the polydispersity was 2.0. Because very small amounts of impurities can have a large effect on the degree of reaction at an interface, little can be concluded from comparing the differences in the SEC data of the two isomers other than that polymerization occurred and that high molecular weight polymer was the result.[12]

Figure 3.10 shows the absorption spectra of 2- and 3-pentadecylaniline after polymerization. Poly(2-pentadecylaniline) was collected just after the reaction was complete (50 min). The resulting dark blue-green material had absorption maxima at 740 and 290 nm (Figure 3.10, spectrum A), which is similar to data that has been previously reported.[94] Further, the spectrum shows weak absorption maxima at 550 and 405 nm. Poly(3-pentadecylaniline) that was collected after the reaction was complete (4 hrs.) was a violet-blue material which had absorption maxima at 550 and 405 nm (Figure 3.10, spectrum C). The spectrum is similar to one previously reported by Lee et al. for polyaniline in the completely oxidized pernigraniline base form. Lee reported peaks at 296, 433, and 542 nm.[148] In the spectrum shown in Figure 3.10, the peak at 296 nm is believed to be hidden in the shoulder of the adjacent peak. From these spectra, it is believed that poly(3-pentadecylaniline) was in the pernigraniline base form at the end of the reaction and the strong absorption at 740 nm indicates that poly(2-pentadecylaniline) was probably in a lower oxidative state such as the emeraldine or nigraniline state. 2-

Pentadecylaniline normally reacts completely in less than one hour, while the polymerization of 3-pentadecylaniline is much slower. The polymerization product of 2-pentadecylaniline was allowed to remain under reactive conditions for four hours, then a second absorption spectrum was performed for comparison (Figure 3.10, spectrum B). This second spectrum of poly(2-pentadecylaniline) is similar to the spectrum of poly(3-pentadecylaniline), suggesting that they were both are in the perngraniline state after four hours. No significant area change was observed in the Langmuir film when poly(2-pentadecylaniline) was allowed to remain at the interface.

The infrared spectrum of the poly(2-pentadecylaniline) base is shown in Figure 3.11a. The asymmetrical stretching (ν_{as} CH_2) and the symmetrical stretching (ν_s CH_2) of the alkyl group occurred at 2928 and 2852 cm^{-1}, respectively, while the bending vibration of the methylene groups (δ_s CH_2) was observed at 1466 cm^{-1}. The characteristic carbon-carbon ring stretching of the polyaniline backbone are at 1590 and 1501 cm^{-1}. A second spectrum of poly(2-pentadecylaniline) was taken after the sample was allowed to remain at the interface for four additional hours after the completion of the polymerization (Figure 3.11b). This spectrum shows a decrease in the relative intensity of the peak at 1590 cm^{-1} and an increased peak at 1657 cm^{-1}. The peak at 1657 cm^{-1} is attributed to the carbonyl stretch on an alkyl substituted benzoquinone, which is the predicted product of the over oxidation of polyaniline.[133]

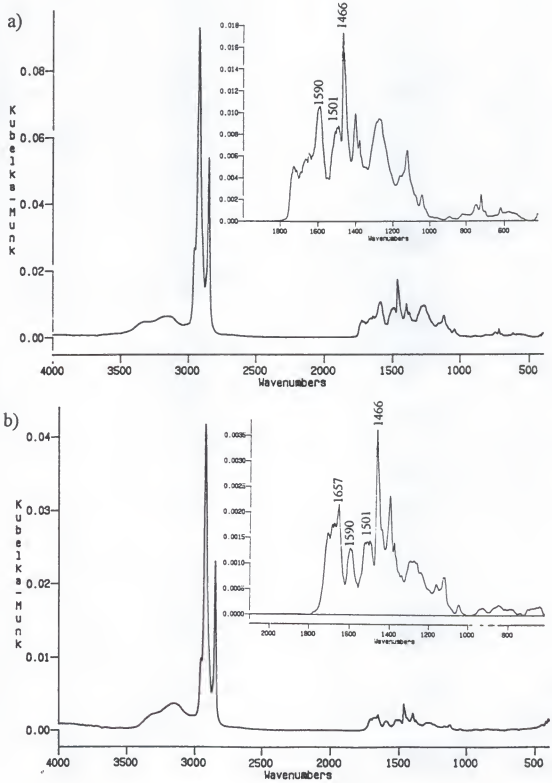

Figure 3.11 Infrared spectra of a) poly(2-pentadecylaniline) base and b) poly(2-pentadecylaniline) base after remaining on trough for five hours.

3.4 Kinetics of Polymerization

In order to study the kinetics of the polymerization of the isomers of pentadecylaniline, a method to determine the concentrations of monomer, [ANI], and polymer [PANI] at the interface was required and was developed using a surface balance technique. The initial concentration of aniline monomer in the monolayer film at the interface can be expressed by the following equation:

$$[ANI_0] = 1/A_0 \tag{3.1}$$

where A_0 is the mean molecular area of the surfactant at the beginning of the polymerization in $Å^2$ molecule^{-1}. In a similar manner, the concentration of the polymer expressed in repeat units at the end of the polymerization can be calculated in repeat units per $Å^2$:

$$[PANI_\infty] = 1/A_\infty \tag{3.2}$$

where A_∞ is the mean molecular area at the end of the reaction. As commonly assumed in monolayer film kinetics, the change in the mean molecular area of the monomer (A) is proportional to the fraction of surfactant that has reacted:[66, 88, 89]

$$\xi = (A_0 - A)/(A_0 - A_\infty) \tag{3.3}$$

where ξ is defined as the extent of reaction. By combining equations 3.1, 3.2, and 3.3 it is easily shown that the concentrations of the monomer and polymer at the interface can be expressed in terms of ξ:

$$[ANI] = (1/A)(1 - \xi) = (1/A)(A - A_\infty)/(A_0 - A_\infty) \tag{3.4}$$

$$[PANI] = (1/A)(\xi) = (1/A)(A_0 - A)/(A_0 - A_\infty) \tag{3.5}$$

Equations 3.4 and 3.5 allow the calculation of the monomer and polymer concentrations at any point during the course of the reaction if A, A_o, and A_∞ are known. Two assumptions were made in order for equation 3.4 and 3.5 to be valid. The first is that all of the monomer was consumed and formed polymer at the interface with no solubilization into the subphase. The second assumption made was that the mean molecular areas of the polymer and monomer surfactants are additive.

When calculating the rate of a reaction in solution chemistry, the volume of the reaction vessel is considered constant, which greatly simplifies the data interpretation. When there is a significant change in the volume during a reaction, the rate expression needs to be written to account for this change. Therefore, when the total area of a

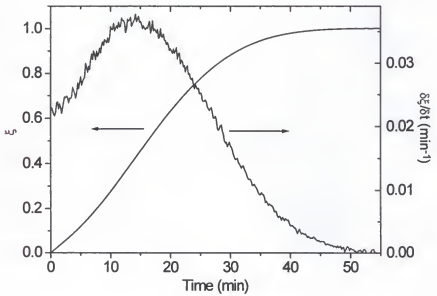

Figure 3.12. ξ and $d\xi/dt$ vs. time for the polymerization of 2-pentadecylaniline at an applied surface pressure of 10 mN m^{-1}. The temperature was held constant at 25 °C.

monolayer changes during the course of a reaction, this change must be accounted for when calculating the rate of the reaction in terms of the concentration of either the reactants or products. Most previous studies that determined rates of reactions from the change in A in a Langmuir film at constant surface pressure and temperature have not accounted for this change in the concentration of the surfactant at the interface, but have derived their rate expression from the change in area over time, dA/dt. Changes in the total area of a Langmuir film during the polymerization of 2-pentadecylaniline are considerable (ca. 40%). Therefore, the rate of reaction at the interface can be defined as

$$R_p = (1/\beta)(dn_p/dt) \tag{3.6}$$

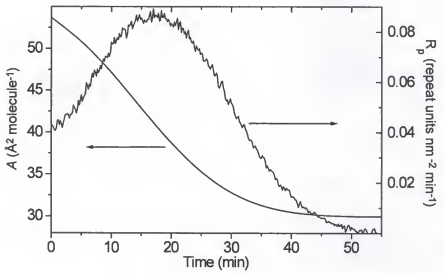

Figure 3.13. A and R_p vs. time for the polymerization of 2-pentadecylaniline at an applied surface pressure of 10 mN m^{-1}. The temperature was held constant at 25 °C.

where dn_p/dt is the rate of polymer formation in terms of repeat units vs. time and β is defined as the total area of the interface at any point in the reaction or more simply stated, $1/\beta$ is a correction factor for the change in the area of the film during the course of the polymerization. β can be calculated from the total initial area of the monolayer, β_0, times the fraction of change, A/A_0, during the course of the reaction. The amount of polymer, n_p, in area β can then be expressed as

$$n_p = [PANI](\beta) = \beta_0/A_0(\xi) \tag{3.7}$$

By substituting equation 3.6 into 3.7, the rate of polymer formation can be written as

$$R_p = (1/A)(d\xi/dt) = (1/A)(d((A_0 - A)/(A_0 - A_\infty))/dt) \tag{3.8}$$

Figure 3.12 shows the extent of reaction, ξ, and $d\xi/dt$ plotted against time for 2-pentadecylaniline at 10 mN m^{-1}. $d\xi/dt$ is calculated from the derivative of ξ over time. By substituting the values of $d\xi/dt$ into equation 3.8, the overall rate of the reaction can be calculated. Figure 3.13 shows a plot of A and R_p vs. time for 2-pentadecylaniline. Figure 3.14 shows ξ and $d\xi/dt$ plotted against time for 3-pentadecylaniline. Figure 3.15 shows a plot of A and R_p vs. time for 3-pentadecylaniline.

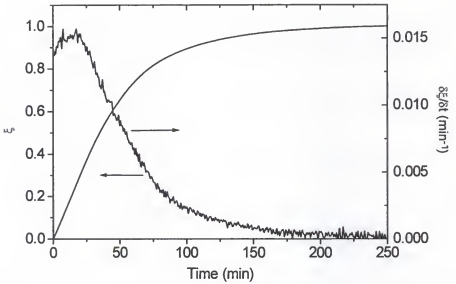

Figure 3.14. ξ and $d\xi/dt$ vs. time for the polymerization of 3-pentadecylaniline at an applied surface pressure of 10 mN m^{-1}. The temperature was held constant at 25 °C.

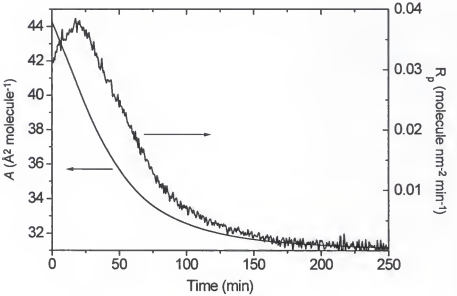

Figure 3.15. A and R_p vs. time for the polymerization of 3-pentadecylaniline at an applied surface pressure of 10 mN m^{-1}. The temperature was held constant at 25 °C.

Like the monomers of 2- and 3-pentadecylaniline, the ΔV of their polymeric films can be affected by μ_1, μ_2, μ_3, and ψ_0. Due to the complexity of the polymeric film's counter ion and subphase, a more convenient way of expressing the surface potential results is the surface potential per molecule (m), which is determined from ΔV divided by the number of molecules per cm^2 (n):[149]

$$m = \Delta V/n \tag{3.9}$$

It is predicted that as the monomer becomes incorporated into the polymer backbone that the value of μ_2 will decrease as compared to that of the monomer, therefore decreasing the value of m. Figure 3.16 shows a graph of m vs. π for the monomer and polymer. The change in the value of m with increasing pressure is more significant for the monomer (slope = -2.043×10^{-17} m π^{-1}) than for the polymer (slope = -0.4593×10^{-17} m π^{-1}). This difference is attributed to the larger orientational change of the monomer head group relative to that of the more rigid polymer.

Figures 3.17 and 3.18 show R_p vs. time for 2- and 3-pentadecylaniline at different applied surface pressures. These figures indicate that the overall polymerization rate was dependent on the applied surface pressure during the polymerization of 2-pentadecylaniline and was dependent to a lesser degree in the polymerization of 3-pentadecylaniline.

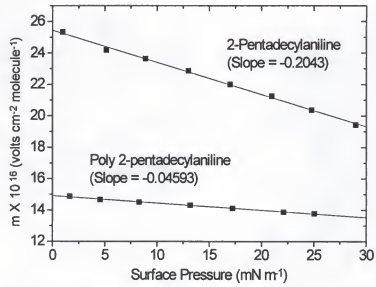

Figure 3.16. m vs. π for 2-pentadecylaniline on a 0.10 M H_2SO_4 subphase and poly(2-pentadecylaniline) on a 0.10 M H_2SO_4 and 0.03 M $(NH_4)_2S_2O_8$ subphase at 25 °C.

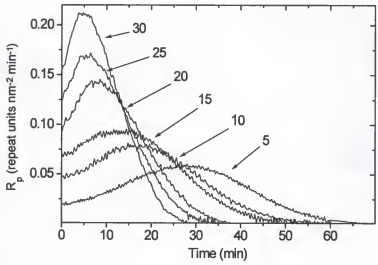

Figure 3.17. R_p vs. time for the polymerization of 2-pentadecylaniline at 5, 10, 15, 20, 25, 30 mN m^{-1} applied surface pressure. The temperature was held constant at 25 °C.

From studies of oxidatively polymerized aniline in solution, it was determined that R_p is first order in monomer concentration [ANI] at the initial point in the reaction[98] and can be expressed in terms of the concentration of monomer and oxidant:

$$R_p = k^{app}[ANI][OX] \tag{3.10a}$$

where k^{app} is the apparent first order rate constant and [OX] is the concentration of oxidant. The concentration of the ammonium peroxydisulfate in a solution polymerization normally ranges from 0.5 to 2 equivalents per mole of aniline.[150] In a Langmuir film polymerization, the amount of monomer is 0.1-0.5 μmoles, so in order to have a concentration of ammonium peroxydisulfate in the subphase that is high enough to polymerize the film, a very large excess is needed. The ratio of ammonium

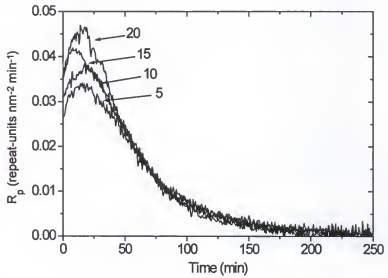

Figure 3.18. R_p vs. time for the polymerization of 3-pentadecylaniline at 5, 10, 15, 20 mN m^{-1} applied surface pressure. The temperature was held constant at 25 °C.

peroxydisulfate to aniline surfactant is ca. 150,000:1. Due to the large excess of oxidant, its concentration is considered constant during the course of the polymerization. Therefore, equation 3.10a can be simplified and rewritten as:

$$R_p = k^{app}[ANI] \quad (3.10b)$$

Upon further examination of Figures 3.13 and 3.15, it can be determined that R_p increased from its initial rate until it reached a maximum value and then decreased as the remaining monomer is consumed. The values of k^{app} are plotted against the amount of

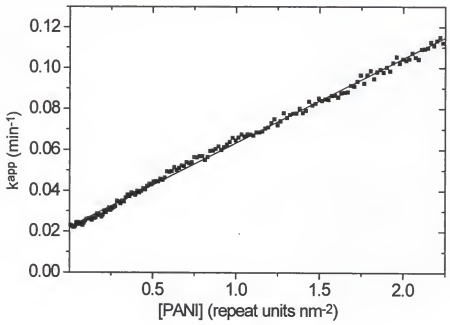

Figure 3.19. k^{app} vs. poly(2-pentadecylaniline) concentration at the air-aqueous interface. The plot shows up to 80 % conversion. k was determined from the slope of the linear plot and k' was determined from the y-intercept of the line.

poly(2-pentadecylaniline) formed, as calculated by Equation 3.5, to quantitatively evaluate the effect that polymer formation has on k^{app}. Figure 3.19 shows the linear correlation that occurs between the increase in k^{app} and polymer concentration. k^{app} can now be rewritten in terms two rate constants (k and k') and [PANI]:

$$k^{app} = k[PANI] + k' \tag{3.11}$$

where k' is the reaction rate constant in the absence of polymer and is determined from the intercept of the line in Figure 3.19 and k is the observed autoacceleration reaction rate constant when polymer is present and is determined from the slope of this line. By combining equations 3.10b and 3.11, the polymerization rate law can be rewritten as:

$$R_p = k[ANI][PANI] + k'[ANI] \tag{3.12}$$

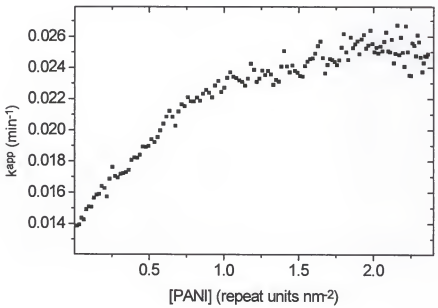

Figure 3.20. k^{app} vs. poly(3-pentadecylaniline) concentration at the air-aqueous interface. The plot shows up to 80 % conversion.

Similar rate expressions have been derived for the oxidative polymerization of aniline by chemical[98] and electrochemical[97] means.

Figure 3.20 is a plot of k^{app} vs. polymer concentration for the polymerization 3-pentadecylaniline. This figure shows that after an initial linear increase, k^{app} follows a nonlinear correlation with polymer concentration at the interface. In order to calculate the values of k' and k at different surface pressures in the case of 3-pentadecylaniline, only the linear portion of the plot (at low polymer concentrations) was used. Figure 3.21 shows an example of a linear fit of k^{app} at low polymer concentrations.

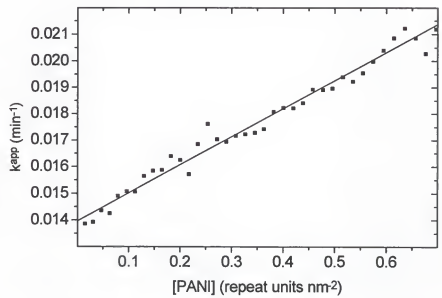

Figure 3.21. k^{app} vs. poly(3-pentadecylaniline) concentration at the air-aqueous interface. The plot shows up to 15 % conversion. k was determined from the slope of the linear plot and k' was determined from the y-intercept of the line.

Table 3.2 shows the values of k' and k for the interfacial polymerizations of 2- and 3-pentadecylaniline at surface pressures of 5, 10, 15, 20, 25, and 30 mN/m. Figure 3.22 shows a plot of ln k' vs. ln π, which indicates that at low pressures (~5 mN/m) the rate constants for both 2- and 3-pentadecylaniline were similar. Because both isomers had a similar k' at 5 mN/m, the initial rates of reaction (R_p at time = 0) at this applied surface pressure were also similar. As the applied surface pressure was increased, 2-pentadecylaniline had a linear increase in ln k', while 3-pentadecylaniline did not. This observation may be explained by the behavior of the monomers on acidic subphases. Not only was the concentration of the surfactant at the air-aqueous interface increased by increasing the applied surface pressure, but a conformational change of the anilinium moiety was probably induced and may have contributed to the effect that surface pressure had on k'. In Figure 3.8, μ_n for 2- and 3-pentadecylaniline are similar at high surface areas and deviate as the monolayer was compressed. The same effect is shown in Figure 3.22 for k'. As illustrated in Figure 3.9, the compression of the film of 2-pentadecylaniline has the effect of orienting the anilinium group such that the amine group and the *para* position on an adjacent surfactant molecule are better aligned for polymerization. This conformational change of the reactive group at higher applied surface pressures should make the reaction with a neighboring monomer more thermodynamically favorable, as it is assumed that the polymer backbone is also oriented parallel to the surface of the interface. In the case of 3-pentadecylaniline, the effect of

surface pressure on the rate constant k' is less dramatic, which is probably due to a less significant change in the conformation of the reactive group upon compression and hence, little effect on the polymerization rate.

Table 3.2. k and k' for 2- and 3-pentadecylaniline at different surface pressures.

	2-Pentadecylaniline		3-Pentadecylaniline	
π (mN m^{-1})	k' (min^{-1})	k (repeats units nm^{-2} min^{-1})	k' (min^{-1})	k (repeat units nm^{-2} min^{-1})
5	0.0119	0.0425	0.0130	0.0132
10	0.0239	0.0364	0.0154	0.0152
15	0.0319	0.0358	0.0166	0.0158
20	0.0499	0.0374	0.0146	0.0140
25	0.0618	0.0399	-	-
30	0.0741	0.0407	-	-

As shown in Table 3.2, k remains nearly constant for both 2- and 3-pentadecylaniline as the surface pressure was varied. The value of k, in the case of 2-pentadecylaniline, was about three times greater than that of 3-pentadecylaniline. If the orientation of the anilinium ion at the interface had an effect on the value of k, the increasing applied surface pressures would have increased the value of k for the *ortho* isomer. Different head group conformations of the isomers are then ruled out as a reason for the different values of k. However, the electrochemical differences in the monomers may provide an explanation.

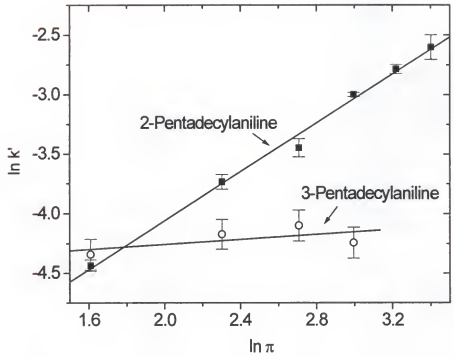

Figure 3.22. ln k' vs. ln π for the formation of poly(2-pentadecylaniline) and poly(3-pentadecylaniline) at 25 °C.

The anodic peak potentials, E_{pa}, in acetonitrile were 0.72 and 0.85 V vs. Ag/Ag^+ for 2- and 3-pentadecylaniline, respectively. It is felt that even though these oxidation potentials were determined in an acetonitrile solution, these measurements would give the relative order of the oxidation potentials at the air-aqueous interface. According to Shim and Park,[97] the autoacceleration step of the polymerization involves the oxidation of the monomer by the polymer (Section 1.4.2). If this is the case, then it is reasonable to assume that if the monomer has a lower oxidation potential, the oxidation rate would be faster and the value of k would be larger. As the potentials indicate, the *ortho* monomer has a lower oxidation potential, suggesting that it is more readily

oxidized by the polymer, causing its value of k to be higher. The *ortho* monomer may be more easily oxidized by the polymer because of the position of the electron donating alkyl group on the aniline ring compared to that of the *meta* isomer.

The values of k' at low surface pressures and the values of k at low and high pressures were much smaller in the case of 3-pentadecylaniline, suggesting that the total amount of time to complete the polymerization would be much longer. Because of the long reaction time and the large excess of ammonium peroxydisulfate in the subphase, over oxidation must be considered when evaluating the kinetic data of this polymerization. It was found that if the polymer was allowed to remain on the ammonium

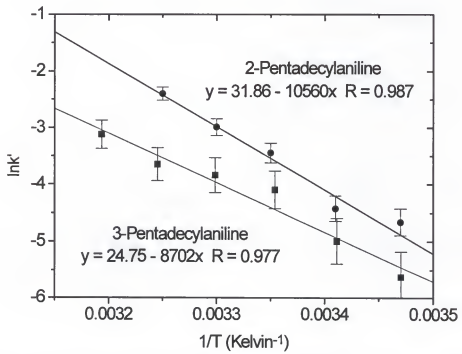

Figure 3.23. lnk' vs. 1/T plot for the polymerization of 2- and 3-pentadecylaniline at 15 mN m^{-1}.

peroxydisulfate subphase for more than 24 hours, the polymer decomposed. Over oxidation of the polymer is most likely the reason for polymer decomposition and may explain why k^{app} (Figure 3.20) is not linear at higher polymer concentrations.

The activation energies were calculated for the polymerization of 2- and 3-pentadecylaniline at 15 mN m^{-1} and temperatures of 15, 20, 25, 30, 35 and 40 °C using the Arrhenius equation:

$$\ln k = \ln A - (E_a/RT) \tag{3.13}$$

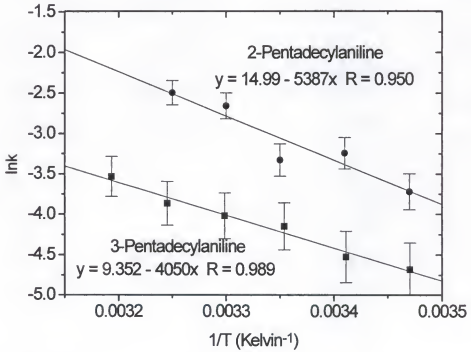

Figure 3.24. lnk vs. 1/T plot for the polymerization of 2- and 3-pentadecylaniline at 15 mN m^{-1}.

where k is the rate constant, A is the collision frequency factor, E_a is the activation energy, R is the gas constant, and T is the absolute temperature. Figures 3.23 and 3.24 are the Arrhenius plots for k' and k, respectively. Because of the phase transitions that were observed above 15 mN m^{-1} in the isotherms of 3-pentadecylaniline at 10 and 17.5 °C (Figure 3.3), 15 mN m^{-1} was chosen as the highest surface pressure used for this temperature study. The calculated E_as for k' were 88 and 74 kJ mol^{-1} and for k were 45 and 34 kJ mol^{-1} for 2- and 3-pentadecylaniline, respectively. For both k and k', the activation energy is slightly larger for 2-pentadecylaniline than for 3-pentadecylaniline. One possible reason for the differences in E_a of the two isomers at the interface is the steric effect of the alkyl group, which is the same reason that 2-pentadecylaniline occupies more surface area than 3-pentadecylaniline at the same surface pressure. In the case of 2-pentadecylaniline at higher surface pressures, k' is higher because of the favorable conformation of the reactive group. At lower surface pressures (5 mN m^{-1}), k' is lower, which can be explained by the similar conformations of the anilinium ions at the interface and the differences in E_a.

3.5 Conclusion

The 2-dimensional polymerization of alkyl substituted aniline at the air-aqueous interface has been presented and the rates of polymer formation were determined by monitoring the mean molecular area change at a constant applied surface pressure. The polymerization of the *meta* alkyl derivative, which is reported here for the first time, was

compared to the *ortho* derivative. In both cases, the initial rate of the polymerization was shown to be dependent on the applied surface pressure. For 2-pentadecylaniline, the initial rate of polymerization increased as the applied surface pressure was increased, but for 3-pentadecylaniline the effect was less significant. This observed effect is explained by the differences in the conformation of the reactive group at the interface and activation energies. As the pressure was increased, the conformational change at the interface favored faster polymerization. The rate constant for autoacceleration (k) stayed relatively constant as the applied surface pressure changed, but is about three times smaller in the case of the 3-pentadecylaniline, which may be due to the higher oxidation potential of the *meta* isomer. It is this slower rate of polymer formation in the case of the 3-pentadecylaniline that is used to explain why the overall rate of the reaction falls off significantly as the reaction proceeds.

In this chapter, it was shown that the rate of the polymerization of an aniline containing surfactant was dependent on the conformation of the reactive group at the interface. If a monomers orientation could be more effectively controlled at the interface, then there would be more control over reactivity. In Chapter 4, new aniline containing surfactants are presented that may allow for better control over interfacial orientation and hence, reactivity. Their surface and polymerization behavior are presented and compared with the results in this chapter. It was felt that this new monomer, 2-(1-octadecynyl)aniline, would be more reactive than its alkyl counter-part because of a more favorable orientation for polymerization.

CHAPTER 4

SURFACE BEHAVIOR AND POLYMERIZATION OF 2- AND 3-(OCTADECYNYL)ANILINE AT THE AIR-AQUEOUS INTERFACE

4.1 Introduction

As discussed in Chapters 1 and 3, the orientation of a monomer's reactive group in a Langmuir film can affect the rate at which it polymerizes. For example, 2-pentadecylaniline was more reactive at higher surface pressures than at lower surface pressures. It was hypothesized that the monomer's orientation at higher surface pressures was closer to that of the resulting polymer; therefore, the monomer was more reactive. Thus, if the orientation of the reactive group on a surfactant could be more effectively controlled, its reactivity may also be controlled.

One way of achieving a desired orientation may be to synthesize a molecule with a structure more conducive to polymerization. For an aniline containing monomer, this might be accomplished by designing a surfactant with an inflexible component, such as an acetylene, on the aliphatic chain adjacent to the anilinium group. The length of the rigid acetylene unit is estimated to be ca. 4.27 Å (two single and one triple bond), compared to that of a single C-C bond (1.54 Å). An inflexible triple bond in the aliphatic

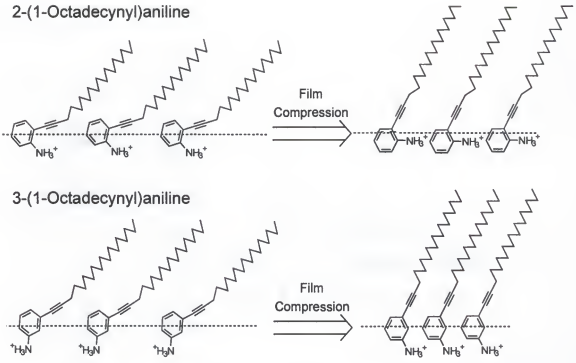

Figure 4.1. Cartoon of the predicted conformational change of 2- and 3-(1-octadecynyl)aniline at the air-aqueous interface during compression.

chain should alter the orientation of the anilinium group in the Langmuir film, which should also change the monomer's reactivity.

Figure 4.1 shows a cartoon of the predicted relative conformation of the anilinium group. When the *ortho* substituted aniline is compressed, it is proposed that the amino group will be favorably aligned for polymerization with the *para* position on an adjacent anilinium group. The hydrophobic chain with the triple bond may assist in orienting the monomer at the interface. The reactivity of the *meta* substituted surfactant may also be affected by the presence of the triple bond, but the anticipated outcome is less predictable.

The work presented in this chapter explored the polymerization of 2- and 3-(1-octadecynyl)aniline at the air-aqueous interface. The surface behavior and

polymerization kinetics of these monomers are compared with the results presented in Chapter 3.

4.2 Monolayer Characterization

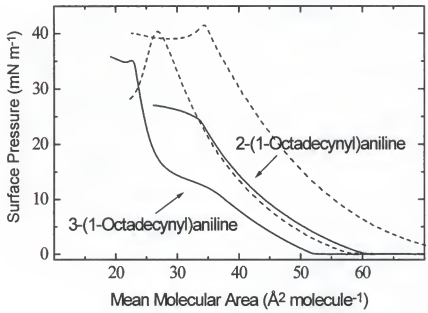

Figure 4.2. Surface pressure, π, vs. mean molecular area, A, isotherm of 2- and 3-(1-octadecynyl)aniline on 0.10 M H_2SO_4 at 25 °C. The dotted lines are the π-A isotherms of 2- and 3-pentadecylaniline.

The π-A isotherms of 2- and 3-(1-octadecynyl)aniline on a 0.10 M H_2SO_4 subphase at 25 °C are shown in Figure 4.2. For comparison, the π-A isotherms 2-, 3-

pentadecylaniline under the same conditions are also shown. The isomers of (1-octadecynyl)aniline have lower pressure onset areas suggesting the formation of a more tightly packed film. The surface area of 2-(1-octadecynyl)aniline more closely matches that of 3-pentadecylaniline. For 2-(1-octadecynyl)aniline, the pressure onset area was at 60 $Å^2$ $molecule^{-1}$ and its collapse pressure at 24 mN m^{-1} was near 34 $Å^2$ $molecule^{-1}$. Though this collapse pressure was 16 mN m^{-1} lower than that recorded for 2-pentadecylaniline, both had similar collapse areas at ca. 34 $Å^2$ $molecule^{-1}$. In contrast, 3-(1-octadecynyl)aniline had a pressure onset area of. 52 $Å^2$ $molecule^{-1}$ and a collapse

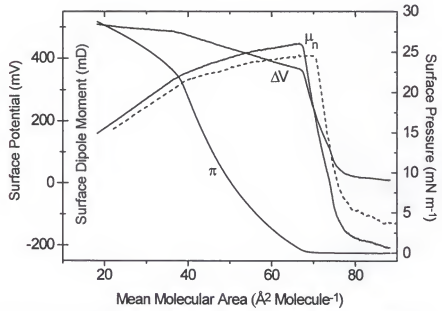

Figure 4.3. Surface pressure, π, potential, ΔV, and dipole moment, μ_n, vs. mean molecular area, *A*, for 2-(1-octadecynyl)aniline on a 0.20 M HCl subphase at 25 °C. The dotted line is μ_n for 2-pentadecylaniline under similar conditions.

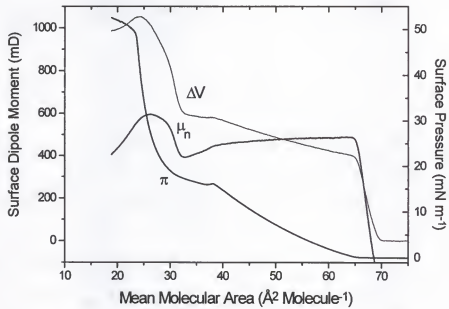

Figure 4.4. Surface pressure, π, potential, ΔV, and dipole moment, μ_n, vs. mean molecular area, *A*, for 3-(1-octadecynyl)aniline on a 0.20 M HCl subphase at 25 °C.

pressure of 35 mN m^{-1} at 23 $Å^2$ $molecule^{-1}$. Between the onset and collapse areas, there appears to be a phase transition, which occurred at ca. 37 $Å^2$ $molecule^{-1}$ and at a surface pressure of ca.14 mN m^{-1}. In the π-*A* isotherms of 3-pentadecylaniline, phase transitions were only observed at temperatures of 10.0 and 17.5 °C (Figure 3.2).

The surface potential was studied in order to better understand the effect of surface pressure on the relative orientation of the head groups of 2- and 3-(1-octadecynyl)aniline at the air-aqueous interface. Figures 4.3 and 4.4 show the plots of π, surface potential, ΔV, and surface dipole moment, μ_n vs. *A* on a 0.20 M HCl subphase at 25 °C for the *ortho* and *meta* isomers, respectively. In contrast to the π-*A* isotherms on H_2SO_4, the pressure onset areas were larger at 66 and 60 $Å^2$ $molecule^{-1}$. The π-*A* isotherm

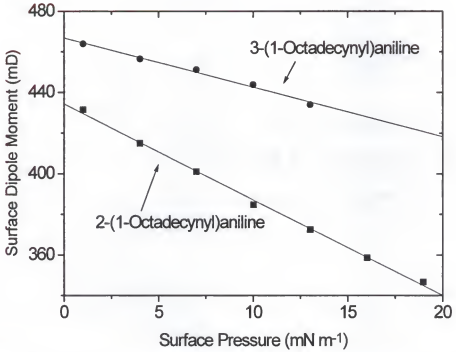

Figure 4.5. Plot of surface dipole moments, μ_n, of 2- and 3-(1-octadecynyl) aniline at their corresponding surface pressures, π.

on a 0.20 M HCl subphase of 3-(1-octadecynyl)aniline showed a phase transition, which was similar to that on H_2SO_4.

The μ_n was calculated from ΔV using equations 1.5 and 1.6. The degree ofionization, α, (equation 1.5) was assumed to be unity for both 2- and 3-(1-octadecynyl)aniline. As in the case of 2- and 3-pentadecylaniline, the maximum μ_n occurred at the same molecular area as the pressure onset and slowly decreased as the film was compressed. In the case of 3-(1-octadecynyl)aniline, μ_n increased in value as the film was compressed past the phase transition. Figure 4.5 shows a plot of μ_n vs.π of 2- and 3-(1-octadecynyl)aniline. Only the values below the phase transition are shown.

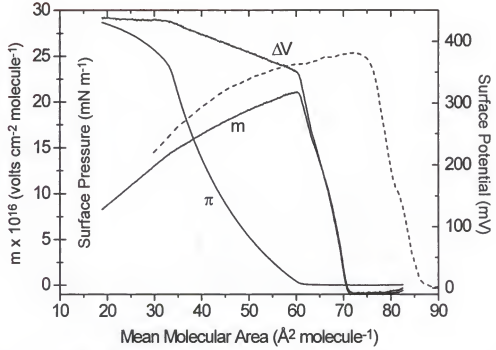

Figure 4.6. Surface pressure, π, potential, ΔV, and normalized surface potential, m, vs. mean molecular area, A, for 2-(1-octadecynyl)aniline on a 0.10 M H_2SO_4 subphase at 25 °C. The dotted line is the value of m for 2-pentadecylaniline.

In contrast to the values obtained from the three isomers of pentadecylaniline, which have similar μ_n at low surface pressures, the values of μ_n for the alkynyl isomers at 1 mN m^{-1} differ by 34 mD (2-(1-octadecynyl)aniline at 431 mD and 3-(1-octadecynyl)aniline at 463 mD).

The study of the electrical properties of the isomers on the polymerization subphase, 0.10 M H_2SO_4, was necessary because the monolayers were more condensed on H_2SO_4 as compared to HCl according to the isotherms. Figures 4.6 and 4.7 show the π and ΔV vs. A isotherms of 2- and 3-(1-octadecynyl)aniline on a 0.10 M H_2SO_4 subphase at 25 °C. The normalized value of the surface potential, m, which was calculated using equation 3.9, is displayed for the alkynyl isomers and for 2-pentadecylaniline (Figure

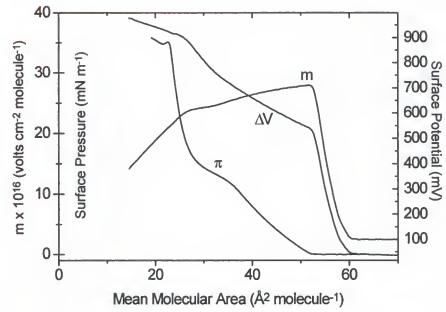

Figure 4.7. Surface pressure, π, potential, ΔV, and m vs. mean molecular area, A, for 3-(1-octadecynyl)aniline on a 0.10 M H_2SO_4 subphase at 25 °C.

4.8). Like μ_n, m is an indication of the dipole moment of a surfactant relative to the interface; m also includes the effect on the surface potential per surfactant due to the double-layer potential, ψ_0. Since the two isomers are structurally similar, comparing the electronic properties of the two may provide some insight into the effect of different mean molecular areas on the orientation of the anilinium group at the interface.

For both alkynyl isomers, the values of m increased dramatically prior to andreached maximum values near the pressure onset areas. As the film was compressed further, m slowly decreased. Figure 4.8 shows the change in the value of m at different surface pressures for the two alkynyl isomers and for 2-pentadecylaniline. At a surface pressure of 1 mN m^{-1}, the *ortho* and *meta* alkynyl isomers had m values of 21 and 28 x 10^{16} V cm^{-2} $molecule^{-1}$, respectively, while 2-pentadecylaniline had a value of 25 x 10^{16} V

cm^{-2} $molecule^{-1}$. In Chapter 3, the effect that the different positions of the hydrophobic chain had on the value of μ_n at low surface pressures was uncertain. However, in this case, the relatively large difference in the values of m and μ_n may be a result of a difference in the orientation of the head groups.

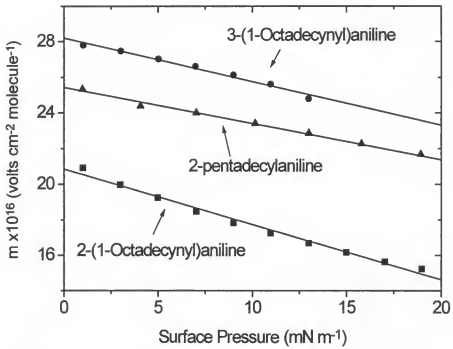

Figure 4.8. Plot of m for 2- and 3-(1-octadecynyl)aniline and 2-pentadecylaniline at their corresponding surface pressures, π.

The surface behavior of the alkynyl isomers can be attributed to structural differences which affect their arrangement at the interface. As illustrated in Figure 4.1, 2-(1-octadecynyl)aniline is more favorably oriented for polymerization than its alkyl counter-part, even at low surface pressures. From the surface pressure and potential measurements, it is proposed that the alkynyl isomers underwent an orientational change

as the film was compressed, which is similar to that of 2-pentadecaniline. However, the relative orientation of the two alkynyl isomers appear to be affected to a greater degree by film compression.

4.3 Polymerization and Polymer Characterization

The monomers in this study were polymerized by the method described in Chapter 2. The films were analyzed by size exclusion chromatography (SEC), UV-vis and infrared spectroscopy.

The product of the chemical oxidation of 2-(1-octadecynyl)aniline had a M_w of 16 000 g mol^{-1} and a M_n of 2800 g mol^{-1}. According to SEC data, only low molecular weight oligomer was recovered from the monolayer polymerization of 3-(1-octadecynyl)aniline. The M_w was 2800 g mol^{-1} (5 to 6 repeat units) with a polydispersity of 1.4.

The materials produced by the polymerizations were violet and dark brown for 2- and 3-(2-octadecynyl)aniline, respectively. Poly[2-(1-octadecynyl)aniline] had absorption maxima at 300, 410, and 595 nm (Figure 4.9). The spectrum was similar to that previously reported by Lee et al.(peaks at 296, 433, and 546 nm) for polyaniline in the completely oxidized pernigraniline base form.[148] Therefore, this spectrum implies that poly[2-(1-octadecynyl)aniline] was in the pernigraniline oxidative state.

Figure 4.10 shows the infrared spectrum of poly[2-(1-octadecynyl)aniline] in its base form. The vibrational bands at 2923 and 2852 cm^{-1} correspond to the asymmetric

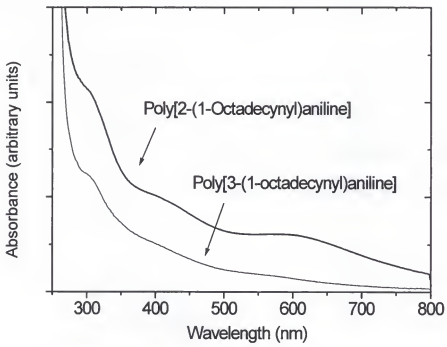

Figure 4.9. The absorption spectra of the polymerization products of 2- and 3-(1-octadecynyl)aniline.

and symmetric C-H stretching and the band at 1465 cm^{-1} is assigned to the C-H bending of the long hydrophobic chain. The vibrational band at 1581 cm^{-1} is assigned to the C=N and C=C stretching of the quinoid diimine unit, while the band at 1511 cm^{-1} is attributed to the C-C aromatic ring stretching of the benzenoid diamine unit of the polymer backbone.[113, 150] A very weak band at 2224 cm^{-1} is attributed to the C≡C stretching band of the acetylene on the alkyl chain.

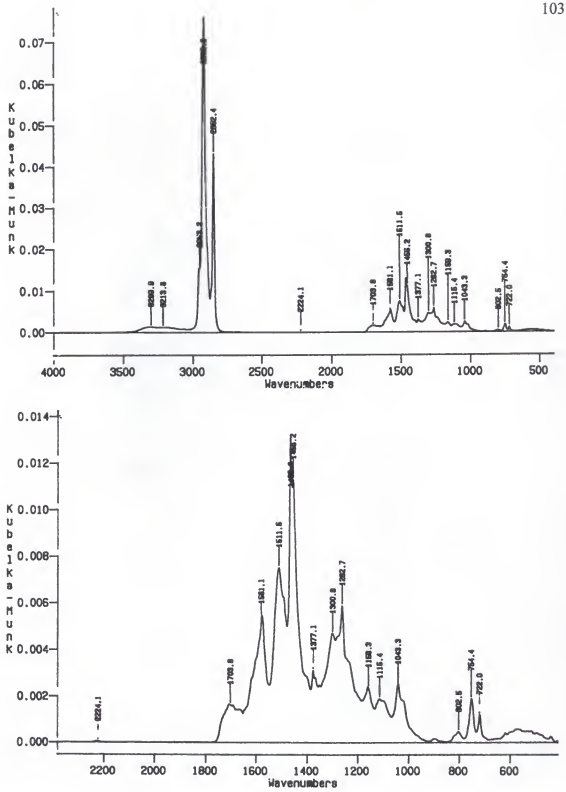

Figure 4.10. Infrared spectra of poly[2-(octadecynyl)aniline] base.

4.4 Polymerization Kinetics

As outlined in Chapter 3, the polymerization rate, R_p, can be calculated from the mean molecular areas at constant temperature and pressure during the reaction (equation 3.8). Figures 4.11 and 4.12 show R_p and A vs. time for the reaction of 2- and 3-(1-octadecynyl)aniline on a 0.03 M $(NH_4)_2S_2O_8$ and 0.10 M H_2SO_4 subphase at an applied surface pressure of 5 mN m^{-1}. R_p was at a maximum at the beginning of the reactions and then decreased as the reactions proceeded. Autoacceleration was not apparent in the polymerization of 2-(1-octadecynyl)aniline. However, autoacceleration was observed

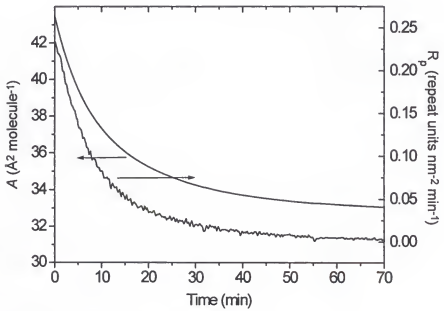

Figure 4.11. A and R_p vs. time for the polymerization of 2-(1-octadecynyl)aniline at an applied surface pressure of 5 mN m^{-1}. Temperature held constant at 25 °C.

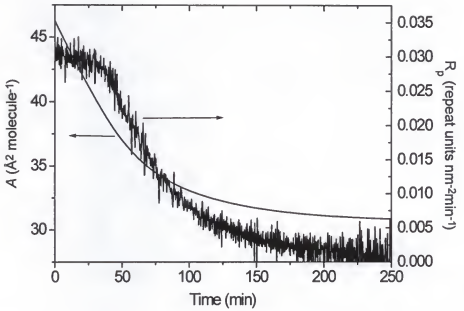

Figure 4.12. *A* and R_p vs. time for the polymerization of 3-(1-octadecynyl)aniline at an applied surface pressure of 5 mN m^{-1}. Temperature held constant at 25 °C.

during the reaction of 3-(1-octadecynyl)aniline, as indicated by the S shape of the plot of R_p vs. time.

The autoacceleration rate constant, k, and the true rate constant (detected at the beginning of the reaction when no polymer is present), k', can be determined from a plot of the apparent rate constant, k^{app}, vs. polymer/oligomer concentration, [PANI] (Figures 4.13 and 4.14). k^{app} was calculated from R_p divided by the monomer concentration. Similar to the polymerization of 2- and 3-pentadecylaniline, the k^{app} for 3-(1-octadecynyl)aniline increased as the [PANI] increased, which is attributed to the autoacceleration of the polymerization. By fitting the observed rate data to the rate

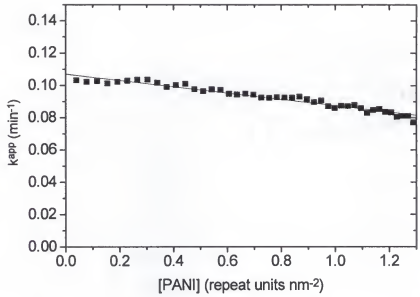

Figure 4.13. k^{app} vs. poly[2-(1-octadecynyl)aniline] concentration at the air-aqueous interface. The plot shows polymerization up to 50 % completion.

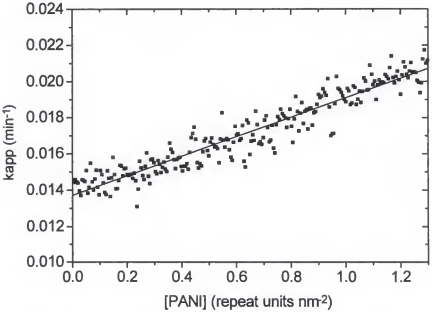

Figure 4.14. k^{app} vs. poly[3-(1-octadecynyl)aniline] concentration at the air-aqueous interface. The plot shows polymerization up to 50 % completion.

expression for the polymerization of aniline (equation 3.12), k and k' were determined. Tables 4.1 and 4.2 show the calculated rate constants of 2- and 3-(1-octadecynyl)aniline.

Table 4.1. The rate constant k' for 2-(1-octadecynyl)aniline at surface pressures of 5, 10, and 15 mN m^{-1} and at 25°C.

Surface Pressure (mN m^{-1})	k' (min^{-1})
5	0.119
10	0.173
15	0.182

Table 4.2. The rate constants k' and k for 3-(1-octadecynyl)aniline at surface pressures 5 and 10 mN m^{-1} and at 25°C.

Surface Pressure (mN m^{-1})	k' (min^{-1})	k (repeats units nm^{-2} min^{-1})
5	0.0158	0.00538
10	0.0213	0.00570

Figure 4.14 shows that autoacceleration was not observed in the polymerization of 2-(1-octadecynyl)aniline and k^{app} decreased as the polymerization proceeded, which may be explained by the large value of k' and the low molecular weight material obtained for this polymerization. The rate constant, k', of 2-(1-octadecynyl)aniline was ca. 6 to 10 times greater than that of 2-pentadecylaniline at surface pressures between 5 and 15 mN m^{-1}, and as in the case 2-pentadecylaniline, k' increased with increasing surface pressure. To illustrate this observation, the half-lives of the reactions at 10 mN m^{-1} were calculated and it was determined that 2-(1-octadecynyl)aniline and 2-pentadecylaniline had half-

lives of ca. 3½ and 17 minutes, respectively. Therefore, because k' was so large, autoaccleration was hard to detect.

If the autoacceleration were significant, then the plot of k^{app} vs. [PANI] would have a positive slope. However, this plot had a slightly negative slope, which may be explained by the following argument. High molecular weight polymer was produced early in the reaction of 2-pentadecylaniline, indicating a chain type polymerization and kinetics.[95] When high molecular weight material is produced, R_p is assumed to be nearly equal to the propagation rate since there are relatively few monomers participating in the initiation step (the formation of 4-aminophenylamine). This assumption is valid for the polymerization of 2- and 3-pentadecylaniline as high molecular weight material was produced. However, low molecular weight material was produced in the reaction of 2-(1-octadecynyl)aniline, so a more accurate expression for the polymerization is:

$$-d[ANI]/dt = R_p + R_{ADPA}$$

where R_{ADPA} is formation rate of 4-aminophenylamine, which is a function of the rate of the following bimolecular reaction:

R_{ADPA} is dependent on the monomer and oxidant concentrations. The oxidant concentration is constant during the reaction and does not need to be included in the rate expression. Therefore, the expression for R_{ADPA} can be written as

$$R_{ADPA} = 2k_1[ANI]^2$$

where k_1 is the rate constant for the formation of 4-aminophenylamine. The rate expression and k^{app} can now be rewritten as

$$-d[ANI]/dt = R_p + R_{ADPA} = k[PANI][ANI] + k'[ANI] + 2k_1[ANI]^2$$

and

$$k^{app} = k[PANI] + k' + 2k_1[ANI]$$

The results suggest that values of k' and k_1 are significantly larger than k in the polymerization of 2-(1-octadecynyl)aniline and account for the decrease in k^{app} at low monomer concentrations (due to the complexity of the polymerization kinetics and the difficulty of separating k and k_1, precise determination of k_1 for this reaction is beyond the scope of this dissertation). Therefore, the slope of the plot of k^{app} vs. [PANI] is slightly negative because the rate of disappearance of monomer is attributed not only to propagation of the polymerization, but also to dimer formation. It is believed that the low molecular weight material produced in the reaction of 2-(1-octadecynyl)aniline can be attributed to a high initiation rate, R_{ADPA}, which leads a high number of polymer chains

with few repeat units per chain. This observation is similar to that of radical chain polymerizations in which the chain length of the resulting polymer is affected by the rate of initiation. The larger the rate of initiation compared to the rate of propagation, the lower the kinetic chain length, ν, of the polymer. The kinetic chain length can be determined from the ratio of R_p to R_{ADPA}:

$$\nu = \frac{R_p}{R_{ADPA}}$$

Oxidation potential may also explain the differences in reactivities of the two *ortho* monomers as it affects the ease of formation of the cation radical intermediate that leads to polymer. The oxidation potentials of the 2-(1-octadecynyl)aniline and 2-pentadecylaniline were 0.75 and 0.72 mV (Table 4.3), respectively, suggesting that the alkyl aniline was slightly more easily oxidized. Since 2-(1-octadecynyl)aniline reacts faster than its alkyl counterpart, it is unlikely that oxidation potential is the reason for the difference in k'.

Table 4.3. Oxidation potentials of aniline containing surfactants in acetonitrile.

2-Pentadecylaniline	0.72 mV
3-Pentadecylaniline	0.85 mV
2-(1-Octadecynyl)aniline	0.75 mV
3-(1-Octadecynyl)aniline	0.86 mV
Aniline	0.83 mV

The reactivities of 3-pentadecylaniline and 3-(1-octadecynyl)aniline were similar at the beginning of the reaction and both monomers had similar k' values at a surface pressure of 5 mN m^{-1}. However, the k values for 3-(1-octadecynyl)aniline were about a third of those calculated for 3-pentadecylaniline. As in the case of the polymerization of 2-(1-octadecynyl)aniline, the low k value can be explained by the low molecular weight material that was produced in this reaction and the effect that R_{ADPA} had on the reaction.

4.5 Conclusions

The surface behavior of 2- and 3-(1-octadecynyl)aniline on acidic subphases was characterized using surface pressure and potential measurements. It was determined that the triple bond affected the conformation of the surfactants at the interface.

A Langmuir polymerization study of the two alkynyl isomers at the aqueous interface was presented. Low molecular weight material was produced in the polymerization of 3-(1-octadecynyl)aniline, while high molecular weight material was

produced in the polymerization of 2-(1-octadecynyl)aniline. The polymerization rates of the alkynyl isomers were determined and compared to the rates of 2- and 3-pentadecylaniline polymerization. It was found that 2-(1-octadecynyl)aniline polymerized at a faster rate than 2-pentadecylaniline, and that autoacceleration was not observed. The differences in the rates are attributed to the relative orientation of the monomers at the air-aqueous interface. Further, both monomers were found to be sensitive to surface pressure. The rate constant, k', was similar for the two meta isomers.

The polymerization of aniline surfactants at the aqueous interface behaved like chain polymerization in which the molecular weight of the polymer was affected by the rate of the initiation step. If the initiation rate is relatively large, the molecular weight of the polymer will decrease. The low molecular weight material produced in the polymerization of 2-(1-octadecynyl)aniline suggests that the formation rate of the propagating dimer is faster than in the case of 2-pentadecylaniline, which is probably due to orientational differences.

CHAPTER 5

DIPOLAR ANILINE SURFACTANTS

5.1 Introduction

In order to obtain high molecular weight polyaniline, the solution polymerization of monomeric aniline is normally carried out in a strong acidic aqueous solution, but when polymerization is carried out under neutral conditions, only low molecular weight oligomers are normally obtained. However, Yan and co-workers reported the polymerization of 2-aminobenzoic acid in an aqueous solution of ammonium peroxydisulfate with no additional acid added.[152] The poly(2-aminobenzoic acid) was then heated to 240°C to drive off carbon dioxide and produce polyaniline in 26% yield.

The original objective of this study was to synthesize a surfactant that was both an acid and an anilinium and to polymerize this molecule in a Langmuir film without the addition of acid to the subphase. It was hoped that the acid group would affect the surface pH and facilitate the production of high molecular weight polymer. The molecule that was selected for this purpose was 17-(2-aminophenyl)heptadecanoic acid.

Preliminary results showed that only very low molecular weight oligomers were produced in the Langmuir film polymerization on water. However, this dipolar molecule

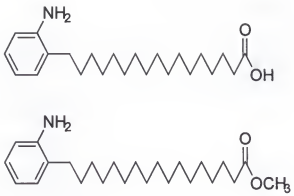

Figure 5.1. Structures of the dipolar molecules 17-(2-aminophenyl)heptadecanoic acid and methyl 17-(2-aminophenyl) heptadecanoate.

has interesting surface behavior and it was felt that it would be useful to study the surface behavior of this molecule.

There are few examples in the literature that examine the effects that dipolar surfactants have on Langmuir film behavior and even fewer known reports on the polymerization of such molecules. This chapter presents a study of monomers with hydrophilic groups on opposite ends of an alkyl chain. Novel monomers were synthesized and then studied in a Langmuir environment in order to gain insight into their surface behavior and reactivity. The two molecules (Figure 5.1) that were prepared and used in this study were 17-(2-aminophenyl)heptadecanoic acid and methyl 17-(2-aminophenyl)heptadecanoate.

5.2 Synthesis

Methyl 17-(2-aminophenyl)heptadecanoate and 17-(2-aminophenyl)heptadecanoic acid were synthesized via a five and six step synthetic route outlined in Figure 2.3. The first step in this synthesis involved the protection of 16-hydroxyhexadecanoic acid by an acid catalyzed esterification to form methyl 16-hydroxyhexadecanoate. In order to prevent the coupling of the hydoxyl and acid group on the molecule, this step was carried out in a dilute solution of methanol. Next, 16-hydroxyhexadecanoate was brominated with carbon tetrabromide and triphenylphosphine. The halide was then refluxed in acetonitrile with triphenylphosphine to form the Wittig salt, (carbomethoxy) pentadecyltriphenylphosphonium bromide, which was then coupled with 2-nitrobenzaldehyde to make methyl 17-(2-nitrophenyl)-16-heptadecenoate. The double bond produced in this coupling was a mixture of *cis* and *trans* isomers. This coupled product was then catalytically reduced to produce methyl 17-(2-aminophenyl) heptadecanoate. The acid form of this surfactant, 17-(2-aminophenyl) heptadecanoic acid, was obtained from methyl 17-(2-aminophenyl)heptadecanoate by the acid promoted hydrolysis of the ester.

5.3 Monolayer Characterization

The π-*A* isotherms of 17-(2-aminophenyl)heptadecanoic acid and methyl 17-(2-aminophenyl)heptadecanoate on a water subphase at 25 °C are shown in Figures 5.2 and

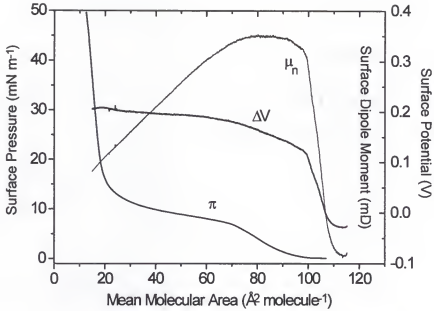

Figure 5.2. Surface pressure, π, potential, Δ V, and dipole moment, μ_n, vs. mean molecular area, *A*, for 17-(2-aminophenyl)heptadecanoic acid on water subphase at 25 °C

.

5.3, respectively. Also shown are the surface potentials, Δ V, and the surface dipole moments, μ_n, of these two dipolar molecules. The surface dipole moments were calculated from the surface potential using Helmholtz equation (equation 1.3).

5.3.1 π-A isotherms. The analysis of the π-*A* isotherms of 17-(2-aminophenyl)heptadecanoic acid and methyl 17-(2-aminophenyl)heptadecanoate show that these monolayer films were more expanded at lower surface pressures than monopolar molecules like 2-pentadecylaniline,[94] stearic acid,[12] and methyl stearate,[145] which have pressure onset areas on a water subphase of ca. 43, 25, and 21 Å^2 molecule^{-1}, respectively. Higher pressure onset areas have been recorded for surfactants that have shorter hydrophobic chains, such as pentadecanoic acid, which had a pressure onset area

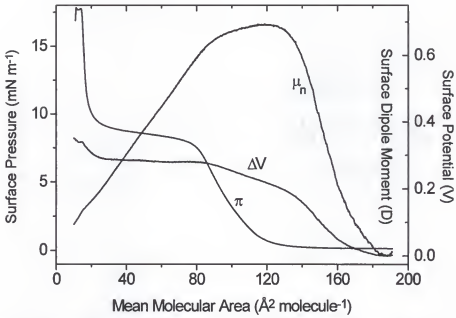

Figure 5.3. Surface pressure, π, potential, ΔV, and dipole moment, μ_n, vs. mean molecular area, A, for methyl 17-(2-aminophenyl)heptadecanoate on water subphase at 25 °C.

of ca. 47 Å^2 molecule^{-1}. However, this area is still less than that determined for these dipolar molecules. The pressure onset areas of these two monolayer films on water, which were determined from an extrapolation of the linear portion of the π-A isotherm to a surface pressure of zero, were ca. 94 and 112 Å^2 molecule^{-1} for 17-(2-aminophenyl)heptadecanoic acid and methyl 17-(2-aminophenyl)heptadecanoate, respectively. The larger pressure onset areas are typical of surfactants that have polar groups on the opposites ends of a long hydrocarbon chain. For example, it was reported by Kellner and Cadenhead that 16-hydroxyhexadecanoic acid[153] and methyl 16-hydroxyhexadecanoate[154] on a 3 M NaCl subphase at 22 °C had onset areas of 100 and 177 Å^2 molecule^{-1}, respectively. The larger surface areas were attributed to the adsorption

of both of the polar groups to the interface. Since the molecules in this study display such high onset areas, it is also believed that both the polar groups were adsorbed to the interface at low surface pressures. The summation of the onset pressure areas of the two monopolar surfactants, 2-pentadecylaniline (47 $Å^2$ $molecule^{-1}$) and pentadecanoic acid (47 $Å^2$ $molecule^{-1}$), has a value of 94 $Å^2$ $molecule^{-1}$, which is similar to that recorded for 17-(2-aminophenyl)heptadecanoic acid.

Both of the dipolar molecules in this study exhibit inflection points in their π-*A* isotherms that were at ca. 75 and 80 $Å^2$ $molecule^{-1}$. These inflection points occur at a surface pressure of ca. 8 mN m^{-1} for both isomers. At the inflection point, the films appear to undergo a phase transition in which the surface pressure of the film increased at a slower rate as the film was compressed further. As the films were compressed to lower areas, this transition ended and the films exhibited the behavior of a condensed film. This condensed region of the film behaved like that of a 2-dimensional solid and is characterized by a sharp increase in the surface pressure with little change in the surface area. Condensed monolayer films are those in which the molecules are oriented nearly upright with the terminal polar groups in the water and the hydrophobic chains closely packed.[12] For a single hydrophobic chain that is closely packed, the area is about 20 $Å^2$. When the condense regions of the π-A isotherms of these films were extrapolated to zero surface pressure, the mean molecular areas were found to be at ca. 22 and 23 $Å^2$ $molecule^{-1}$ for the acid and ester, respectively.

The collapse pressures of the two dipolar molecules in the condensed state are significantly different at ca. 17 and 45 mN m^{-1} for the ester and acid, respectively. When

the acid compound was compressed above 45 mN m^{-1}, the surface pressure continued to increase; however, a small inflection occurred in the π-*A* isotherm and the film was highly unstable upon further compression, which indicated that the film had collapse at 45 mN m^{-1}. The difference in the collapse pressures may be a reflection of the difference in hydrophilic character of the two surfactants. The acid, which is more hydrophilic than a methyl ester, would be expected to form a more stable film and have a higher collapse pressure. It is possible that other factors, which will be discussed in section 5.3.2, also contributed to a more stable film.

5.3.2 Surface potential. The ΔV and μ_n of the surfactants are shown in Figures 5.2 and 5.3. ΔV of both films increased in value prior to the pressure onset area. After the onset area was reached, ΔV increased at a slower rate, and after the inflection point in the π-*A* isotherm, the rate of increase was reduced further. The surface dipole moments of both surfactants increased prior to the pressure onset area and decreased as the monolayers were compressed past the inflection point.

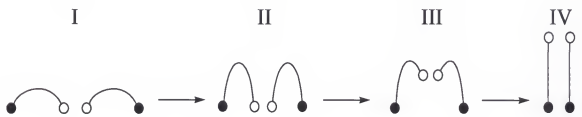

Figure 5.4. The proposed surface behavior of 17-(2-aminophenyl)heptadecanoic acid and methyl 17-(2-aminophenyl)heptadecanoate on a water surface at different surface areas.[157]

Figure 5.4 shows a schematic representation of the proposed molecular conformations of the monomers at the air-aqueous interface during the course of the monolayer compression. This schematic representation was also proposed by Kellner and Cadenhead for the dipolar molecule 16-hydroxyhexadecanoic acid.[153] At areas larger than the pressure onset area, the two polar ends of the molecules are adsorbed to the surface (I). As the film is compressed, the surface area begins to decrease and the hydrocarbon chain begins to be forced up and away form the water surface (II). At the point of inflection in the π-A isotherm, one of the polar groups on each surfactant begins to be pushed out of the aqueous phase (III). Upon further compression, one of the polar groups is completely desorbed from the surface and a condensed film is formed(IV).

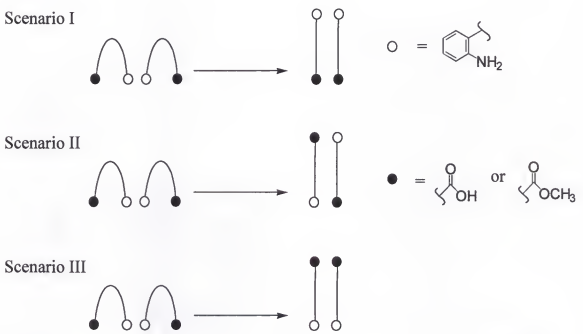

Figure 5.5. Three proposed mechanisms for the phase transition of the dipolar compounds 17-(2-aminophenyl)heptadecanoic acid and methyl 17-(2-aminophenyl)heptadecanoate on water.

There are three possible scenarios by which the phase transition (Figure 5.4, III) could occur. Scenario I and III involve the expulsion of either all of the anilinium or carboxyl groups from the water while the opposite polar groups remain at the surface. Scenario II involves the expulsion of a mixture of end groups from the water interface while a mixture of the two groups remains adsorbed to the surface. Figure 5.5 shows a cartoon of the possible scenarios that are involved in the phase transition of the two dipolar molecules.

According to Scenario III, the anilinium group remains at the surface of the water interface and the ester or acid group is pushed away from the surface as the film is

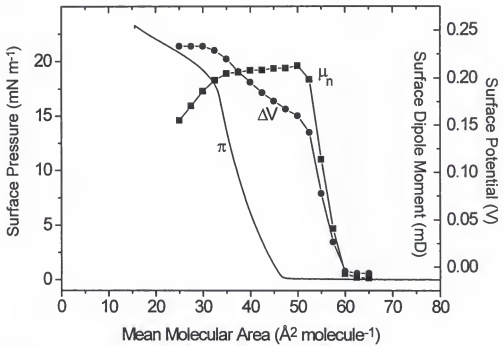

Figure 5.6. Surface pressure, π, potential, ΔV, and dipole moment, μ_n, vs. mean molecular area, *A*, for 2-pentadecylaniline on water subphase at 25 °C.[160]

compressed. The pressure onset area of a film of 2-pentadecylaniline on a water subphase is ca. 46 $Å^2$ $molecule^{-1}$, which is double the area of the compressed region observed for 17-(2-aminophenyl)heptadecanoic acid and methyl 17-(2-aminophenyl)heptadecanoate. If only the anilinium group remained adsorbed to the water surface, the compressed region of the π-*A* isotherms of the acid and methyl ester surfactants would probably be more expanded due to the larger area requirement of the anilinium group. Further, small molecules with carboxylic acid and methyl ester functionalities are more water soluble than those with anilinium groups. For example, acetic acid and methyl acetate are completely miscible in water, while 29 mL of water is required to solubilize one gram of aniline. Therefore, it is believed that a carboxylic acid and methyl ester are more hydrophilic than an anilinium group and would have a stronger affinity for the aqueous interface. This knowledge, together with the isotherm data, leads to the elimination of Scenario III as a possible mechanism for the compression of 17-(2-aminophenyl) heptadecanoic acid and methyl 17-(2-aminophenyl)heptadecanoate.

The surface potentials of stearic acid and methyl stearate have been previously reported.[139] In that report, the surface potentials of the stearic acid and methyl stearate were +275 and +592 mV in the condensed phase (~20 $Å^2$ $molecule^{-1}$), respectively. The surface pressure, surface potential, and surface dipole moment of 2-pentadecylaniline on water are shown in Figure 5.6.[155] As this plot shows, the change in μ_n was ca. 210 mD between the onset and collapse pressures. The surface dipole moment of 2-pentadecylaniline was lower on water than on a 0.2 M HCl subphase, which was probably due to the uncharged anilinium species making the double-layer potential effect

insignificant. As in the case 2-pentadecylaniline on a 0.2 M HCl subphase, there was no large decrease in the dipole moment between the onset and collapse pressures as μ_n remained ca. 210 mD over this entire region, which is an indication there was little conformational change of the surfactant as it was compressed. Stearic acid and methyl stearate also show little change in μ_n between their collapse and onset areas, making the comparison of their surface properties useful when evaluating the electrical properties of 17-(2-aminophenyl)heptadecanoic acid and methyl 17-(2-aminophenyl)heptadecanoate.

Table 5.1. Comparison of the electrical properties of 17-(2-aminophenyl) heptadecanoic acid and methyl 17-(2-aminophenyl)heptadecanoate.

Expanded Region				
	Area/molecule (Å^2)	ΔV (mV)	μ_n (mD)	$\Delta\mu_n$ (mD)
Acid	197	127	327	364
Ester	123	211	691	
Inflection Point				
	Area/molecule	ΔV	μ_n	$\Delta\mu_n$
Acid	73	177	344	248
Ester	80	278	592	
Condensed Region				
	Area/molecule	ΔV	μ_n	$\Delta\mu_n$
Acid	19.2	208	106	56
Ester	20	307	162	

A comparison of the electrical properties of 17-(2-aminophenyl)heptadecanoic acid and methyl 17-(2-aminophenyl)heptadecanoate is provided in Table 5.1. If Scenario I holds true for both surfactants on water, the difference between the μ_n in the compressed region should equal the difference between the contribution of one methyl ester and one carboxylic acid at the water surface as both films have the same anilinium tail group oriented away from the subphase. It was reported by Vogel and Möbius [145] that the contributions of a carboxylic acid and methyl ester on a water subphase at 18°C in the compressed state (~20 mN m^{-1}) were -200 and -50 mD, respectively. Using these two values to evaluate the surfactants in this study, the difference between the two surface dipole moments, $\Delta\mu_n$, in the compressed state would then be ca. 150 mD. The $\Delta\mu_n$ obtained in this study was ca. 56 mD, which indicates that at least one of the surfactants did not follow Scenario I. Since the carboxylic acid containing molecule should have a more negative surface dipole moment on a water surface than the methyl ester molecule by ca. 150 mD, it is unlikely that 17-(2-aminophenyl)heptadecanoic acid follows Scenario I. Therefore, the likely pathway for 17-(2-aminophenyl)heptadecanoic acid through the phase transition is Scenario II. The pK_as of an anilinium ion[142] and carboxylic acid[156] at a water-air interface have been estimated to be 4.6 and 5.0, respectively. The similarities in the pK_as of these two functional groups suggest that some acid-base interaction could occur. It is hypothesized that the transition of 17-(2-aminophenyl)heptadecanoic acid involves the formation of acid-base pairs which may explain why 17-(2-aminophenyl)heptadecanoic acid appears to follow Scenario II, even

though the carboxylic acid is more hydrophilic than the anilinium group. The formation of acid-base pairs may also explain the film stability at higher surface pressures.

Strong acid-base interactions are unlikely between the end groups of the methyl 17-(2-aminophenyl)heptadecanoate and the methyl ester is more hydrophilic than the anilinium group; therefore, this molecule probably follows Scenario I.

The π-A isotherms of the surfactants were measured on a 0.10 M H_2SO_4 subphase at 25 °C. As in the case of the film on a water subphase, a surface pressure was recorded as soon as a small amount of material was placed at the interface, suggesting that the monolayer film behaves like a two-dimensional gas at large areas[12] and that both polar

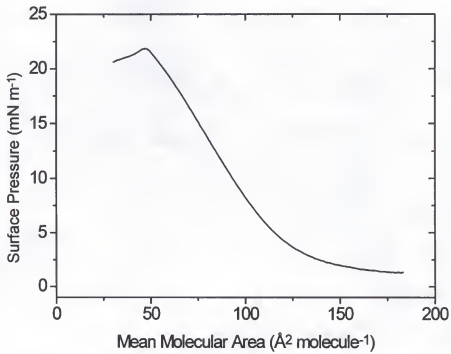

Figure 5.7. Surface pressure, π, vs. mean molecular area, A, isotherm of methyl 17-(2-aminophenyl)heptadecanoate on 0.10 M H_2SO_4 subphase at 25 °C.

groups are adsorbed to the subphase at low surface pressures. As the film was compressed to lower surface areas, no phase transition was observed, which indicates that the monolayer film has both groups at the interface until collapse at 22 mN m^{-1} and 49 $Å^2$ $molecule^{-1}$ (Figure 5.7). 17-(2-Aminophenyl)heptadecanoic acid did not form a stable monolayer film on 0.10 M H_2SO_4 at 25 °C, which was probably due to the increased solubility of the ionized anilinium group.

5.4 Polymerization

Methyl 17-(2-aminophenyl)heptadecanoate formed a stable monolayer on a 0.10 M H_2SO_4 subphase; however, when the monomer was subjected to polymerization conditions, only low molecular weight oligomer was collected. At an applied surface pressure of 5 mN m^{-1}, an oligomer with a M_n of 1600 g mol^{-1} and a M_w of 2200 g mol^{-1} (SEC) was produced.

The π-A isotherm results of methyl 17-(2-aminophenyl)heptadecanoate on 0.10 M H_2SO_4 indicate that the methyl ester functionality occupied ca. 60 $Å^2$ per molecule and the 2-pentadecylaniline polymerization results indicate that the polymer repeat unit occupied ca. 33 $Å^2$ per molecule. Therefore, a larger portion of the interfacial area should be occupied by the methyl ester group, which is unable to diffuse away from the anilinium group or the growing polymer chains. Thus, the polymerization is hindered and the production of high molecular weight polymer is prevented (Figure 5.8). This theory could be tested by polymerizing mixed monolayer films that contain varying

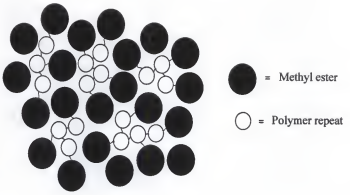

Figure 5.8. Cartoon of the methyl 17-(2-aminophenyl)heptadecanoate polymerization.

concentrations of 2-pentadecylaniline. If the molecular weight of the resulting polymer increased with increased 2-pentadecylaniline concentration, it would indicate that the methyl ester group was inhibiting polymerization. When the polymerization was carried out at higher surface pressures, no polymerization occurred, further indicating that the anilinium group was oriented away from the aqueous subphase.

17-(2-Aminophenyl)heptadecanoic acid was unstable on an acidic subphase, so polymerization studies were not performed on this surface. However, the polymerization was studied on a 0.03 M ammonium peroxydisulfate subphase at high and low surface areas (5 and 25 mN m^{-1}). Figure 5.9 shows that there is a greater change in surface area at 5 mN m^{-1}, which is attributed to the oligomerization of the monomer. Due to the lack of high molecular weight polymer product, these polymerization studies were discontinued.

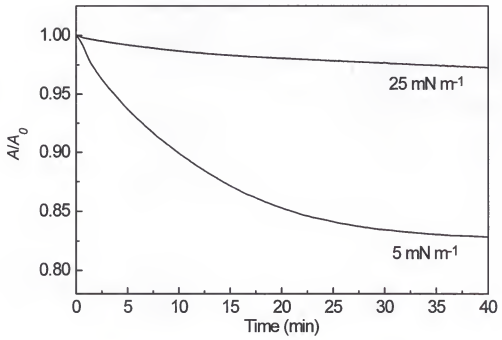

Figure 5.9. Change of surface area for the polymerization of 17-(2-aminophenyl)heptadecanoic acid monolayer at 5 and 25 mN m^{-1}.

5.5 Conclusions

The surface behavior of 17-(2-aminophenyl)heptadecanoic acid and methyl 17-(2-aminophenyl)heptadecanoate on water and 0.10 M H_2SO_4 subphases was presented. It was proposed that these dipolar molecules undergo a phase transition during the compression of the molecular film. It is believed that before the phase transition, the two polar ends of the molecules were adsorbed onto the water surface and at the end of the phase transition, only one of the polar groups from each molecule was adsorbed to the subphase. Surface potential data was used to determine the relative orientation of the

surfactants. It was proposed that in the condensed phase 17-(2-aminophenyl)heptadecanoic acid was oriented such that a mixture of anilinium and carboxylic acid groups were adsorbed to the subphase and that this unusual conformation was facilitated by a strong interaction between the anilinium and acid functional groups. Methyl 17-(2-aminophenyl)heptadecanoate is believed to orient such that the anilinium groups are away from the aqueous interface when the film is in the condensed state. The greater hydrophilic nature of the methyl ester, compared to the anilinium group, is felt to contribute to this result.

Results on the surface behavior and polymerization of the dipolar molecule, 1,22-bis(2-aminophenyl)docosane, are presented in Chapter 6. It will be shown that the surface behavior of that film will mirror some of the characteristics presented in this chapter.

CHAPTER 6

LANGMUIR FILM POLYMERIZATION OF 1,22-BIS(2-AMINOPHENYL)DOCOSANE

6.1 Introduction

One of the major disadvantages of using Langmuir and LB films in most technical applications is the requirement that the film is mechanically, thermally, and chemically stable under environmental conditions.[87] One way of stabilizing monolayer films is by producing a 2-dimensional network or crosslinked polymer system. Network polymers in 3-dimensions are generally more stable to thermal and physical stress than their non-crosslinked counterparts and it was felt that a polymer of this type produced in 2-dimensions would also have greater stability. There have been only a few published reports in the literature that deal with Langmuir films that are capable of forming 2-dimensional network polymers.[157-161] A study of the surface behavior and Langmuir film polymerization of a new polymerizable surfactant, 1,22-bis(2-aminophenyl)docosane, that is unique in that it has four reactive sites and is capable of forming crosslinked polymer is presented in this chapter.

Together with Mr. Mark Watson, a novel synthetic approach that is relatively short (6 steps) and high yielding was developed. The synthesis of this disubstituted

aniline monomer is outlined and discussed in detail and its surface behavior is presented and compared with the monosubstituted alkyl aniline surfactant, 2-pentadecylaniline. Further, this monomer was polymerized at the air-aqueous interface and results are presented that suggest that this monomer formed a 2-dimensional network polymer. The reactivities of the monopolar and dipolar surfactants are presented and the differences in the reaction rates are compared.

6.2 Synthesis of 1,22-Bis(2-aminophenyl)docosane

Figure 6.1. 1,22-Bis(2-aminophenyl)docosane.

Figure 6.1 shows the structure of 1,22-bis(2-aminophenyl)docosane and Figure 2.4 shows the synthetic route by which the monomer was prepared. The first step in this synthesis was the preparation of a phosphonium salt from 11-bromo-1-undecene and triphenylphosphine. 1-(2-Nitrophenyl)-1,11-dodecadiene was made by coupling 2-nitrobenzaldehyde with the phosphonium salt via a Wittig reaction. Two molecules of this diene were then coupled together at the terminal olefin position by a metathesis reaction using the Ruthenium catalyst shown in Figure 6.2.[162]

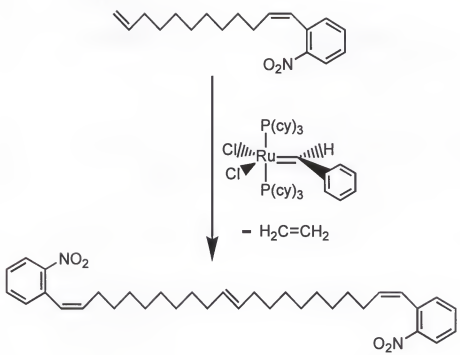

Figure 6.2. Ruthenium alkylidene catalyzed methathesis coupling of 1-(2-nitrophenyl)-1,11-dodecadiene.

One of the concerns about this metathesis coupling was that the starting material, 1-(2-nitrophenyl)-1,11-dodecadiene, contains two non-aromatic double bonds, both of which could possibly undergo self-metathesis. If this reaction was not selective toward the terminal olefin, a mixture of coupled products and/or polymer could result. However, because the two olefins of 1-(2-nitrophenyl)-1,11-dodecadiene are not equivalent and since the olefin adjacent to the nitrophenyl is both sterically hindered and electron poor, it was hypothesized that self-metathesis would selectively occur at only the terminal olefin. Published results show that the reactivity of a metathesis mediated exchange of an alkylidene unit between olefins can be very sensitive to steric and electronic factors in the

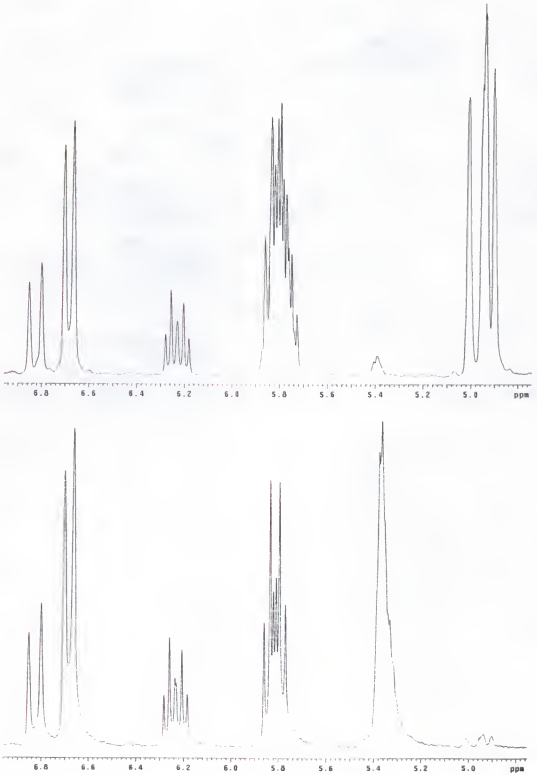

Figure 6.3. ^{1}H NMR spectra a 1-(2-nitrophenyl)-1,11-dodecadiene (top) and 1,22-bis(2-nitrophenyl)-1,11,21-docostriene (bottom) between 4.8 and 7.0 ppm.

olefin.[163, 164] ^{1}H NMR data clearly show that the reaction was selective toward the terminal olefin.

Figure 6.3 shows the ^{1}H NMR spectra between 5.0 and 7.0 ppm of 1-(2-nitrophenyl)-1,11-dodecadiene and its self-metathesis product. There are chemical shift peaks centered at ca. 4.96 and 5.81 ppm in the ^{1}H NMR of the starting material that represent the protons on the terminal olefin. These peaks decrease in intensity during the reaction while a multiplet centered at 5.37 ppm, which is a chemical shift that is expected for a disubstituted alkyl internal olefin, appears. The doublets at 6.68 and 6.82 ppm and the multiplets at 5.81 and 6.24 ppm are assigned to the double bonds (*cis* and *trans*, respectively) next to the aromatic rings. The integration of the peaks at 6.24, 6.68, and 6.82 ppm was unchanged by the reaction conditions, but the peak at 5.81 ppm (a combination of terminal and internal double bond) was reduced in relative intensity, indicating that the reaction was highly selective toward coupling at the terminal olefin. Once the metathesis reaction was complete, the nitro group and the three nonaromatic double bonds were reduced by catalytic hydrogenation, giving the final disubstituted aniline surfactant.

An alternative route to the synthesis of 1,22-bis(2-aminophenyl)docosane is outlined in Figure 6.4. One of the disadvantages of this route over the one discussed above is that the route is longer and involves two Wittig reactions, which in this case produced low yields. Once the synthetic route involving the Ruthenium alkylidene catalyst showed promise, this route was abandoned.

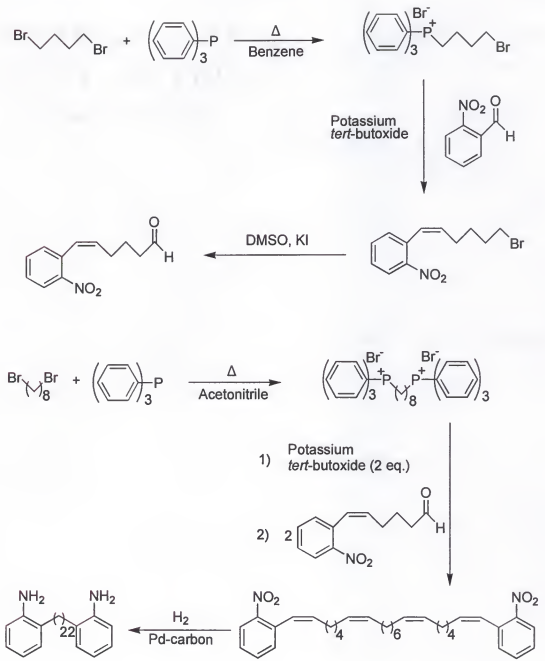

Figure 6.4. An alternative route for the synthesis of 1,22-bis(2-aminophenyl) docosane.

6.3 Monolayer Characterization

The π-A isotherms of 1,22-bis(2-aminophenyl)docosane and 2-pentadecylaniline are shown in Figure 6.5. The pressure onset areas of 2-pentadecylaniline and 1,22-bis(2-aminophenyl)docosane on 0.10 M H_2SO_4 were 74 and 150 $Å^2$ molecule^{-1}, respectively. The dotted line on Figure 6.5 shows the π-A isotherm of 1,22-bis(2-aminophenyl) docosane per anilinium group up to the first collapse pressure. As expected, the pressure onset area of 1,22-bis(2-aminophenyl)docosane was about twice that of the 2-

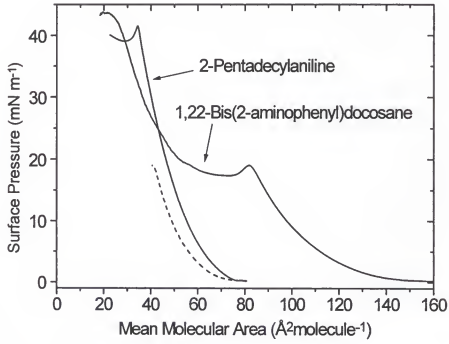

Figure 6.5. Surface pressure (π) vs. mean molecular area (A) isotherm of 2-pentadecylaniline and 1,22-bis(2-aminophenyl)docosane on 0.10 M H_2SO_4 at 25 °C. The dotted line is the π-A isotherm of 1,22-bis(2-aminophenyl) docosane per anilinium group up to the first collapse pressure.

pentadecylaniline, indicating that both of the anilinium groups were adsorbed to the interface with the long chain oriented away from the surface. The collapse pressure of 1,22-bis(2-aminophenyl)docosane occurred at ca. 19 mN m^{-1} and at a mean molecular area of 82 $Å^2$ $molecule^{-1}$, which was lower than that observed for 2-pentadecylaniline. This lower collapse pressure, which was less than half of that of 2-pentadecylaniline, implies that the monolayer of this molecule may be less stable at higher surface pressures and may indicate that the looping alkyl chains impede this monomer's ability to pack efficiently at the interface.

As 1,22-bis(2-aminophenyl)docosane was compressed past this first collapse pressure, a second increase in the surface pressure was observed. The film apparently has a second collapse pressure of ca. 40 mN m^{-1} at 37 $Å^2$ $molecule^{-1}$. The cause of this second increase is unclear, but it is possible that at this point in the isotherm, the surfactant is oriented such that only one anilinium group is adsorbed to the interface. More work needs to be done in this area to better understand this observation.

Isobaric creep experiments show that this film is more stable over time on a 0.10 M H_2SO_4 subphase than 2-pentadecylaniline under similar conditions. At a surface pressure of 15 mN m^{-1}, the monolayer film creeped at ca. 0.048 $Å^2$ anilinium $unit^{-1}$ min^{-1}, while under the same conditions, 2-pentadecylaniline had a film creep of 0.30 $Å^2$ anilinium $unit^{-1}$ min^{-1}.[148] This difference suggests that even though the molecule has two polar groups, a stable film is formed.

The 2-dimensional compressibility, C_s, of a Langmuir film at an area A can be calculated directly from the π-A isotherms of a film and is defined by the equation:[12, 18]

$$C_s = -\frac{1}{A}\left(\frac{\delta A}{\delta \pi}\right)_T$$

Even though the C_s is a useful way of expressing compressibility of a Langmuir film, a more convenient term is the surface compressional modulus, C_s^{-1}. C_s^{-1} is a physical measurement of the state that the Langmuir film is in and increases as the film becomes more condensed. According to Davies and Rideal,[18] the following states should have the corresponding C_s^{-1}: liquid expanded, 12.5 - 50 mN m^{-1}; liquid condensed, 100 - 250 mN m^{-1}; and solid condensed, 1000 - 2000 mN m^{-1}. Table 6.1 shows the C_s^{-1}s of 2-pentadecylaniline and 1,22-bis(2-aminophenyl)docosane at different surface pressures. The values C_s^{-1} of these two monolayers indicate that both films are in the liquid expanded state.

Table 6.1. The surface compressional modulus at surface pressures of 2, 5, 10, and 15 mN m^{-1} for 2-pentadecylaniline and 1,22-bis(2-aminophenyl)docosane on a 0.10 M H_2SO_4 subphase at 25 °C.

Surface Compressional Modulus, C_s^{-1} (mN m^{-1})		
Surface Pressure (mN m^{-1})	2-Pentadecylaniline	1,22-bis(2-aminophenyl)docosane
2	22.3	17.1
5	35.1	29.8
10	49.2	44.2
15	59.2	57.8

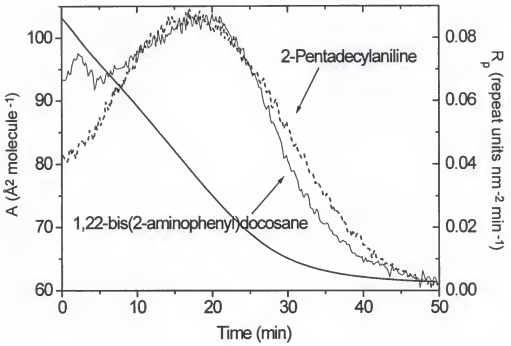

Figure 6.6. *A* vs. time for the polymerization of 1,22-bis(2-aminophenyl)docosane and R_p vs. time for the polymerization of 1,22-bis(2-aminophenyl)docosane and 2-pentadecylaniline at 10 mN m^{-1} and 25 °C.

6.4 Polymerization

The polymerization of 1,22-bis(2-aminophenyl)docosane was carried out as described in Chapter 2 and was monitored by the change in the mean molecular area with time at a specific applied surface pressure. The change in the molecular area can then be converted to a reaction rate using equation 3.8. However, because there are two anilinium groups for each surfactant, this rate equation is multiplied by two (equation 6.1).

$$R_p = \left(\frac{2}{A}\right)\left(\frac{d\xi}{dt}\right) = \left(\frac{2}{A}\right)\left(\frac{d((A_0 - A)/(A_0 - A_\infty))}{dt}\right) \qquad (6.1)$$

Figure 6.6 shows the mean molecular area change and polymer formation rate with time. The rate of polymer formation of 2-pentadecylaniline is also shown in Figure 6.6. As in the case of 2-pentadecylaniline, the polymerization of 1,22-bis(2-aminophenyl)docosane undergoes autoacceleration. The reaction rate runs parallel to that of 2-pentadecylaniline under similar conditions except at low conversion, where the reaction rate appears to be faster. This difference may be due to the incorporation of one aniline unit of the monomer into the polymer backbone while the other unit remains unreacted. The area that an insoluble molecule occupies at an interface is dependent not only on its molecular size, but also on intermolecular attractive and repulsive forces. This unreacted portion of the monomer would have its mobility in the monolayer hindered, causing it to occupy a smaller portion of the interface. Therefore, since the reactivity of the monomer was measured by the change in the surface area of the reactive groups, the rate would appear to be greater at lower conversions. If this were true, then at higher conversions the change in area would appear to be less than that observed for the polymerization of 2-pentadecylaniline and the polymerization rate, R_p, would be smaller at higher conversions. This is in fact what was observed and is illustrated in Figure 6.6.

As in the polymerization of 2- and 3-pentadecylaniline at the air-aqueous interface, the amount of area that the polymer occupies compared to the monomer is much less. This area change is due to the incorporation of the anilinium group into the backbone of a polymer, which takes up less area. Figure 6.7 shows the π-A isotherm of poly(1,22-bis[2-aminophenyl]docosane), which had a pressure onset area of ca. 70 $Å^2$ molecule^{-1} or 35 $Å^2$ repeat unit^{-1}. The figure also shows the π-A isotherm of poly(2-pentadecylaniline). From the π-A isotherms of the polymers, it is apparent that the two polymers at low surface pressure are very similar in character, with both having pressure

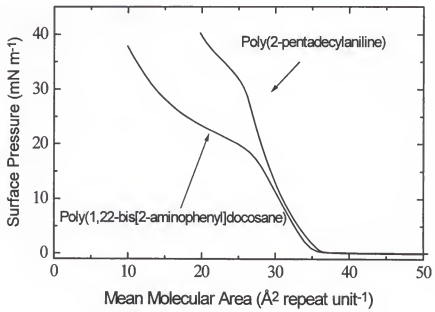

Figure 6.7. Surface pressure (π) vs. mean molecular area (A) isotherm of poly(1-22-bis[2-aminophenyl]docosane) and poly(2-pentadecylaniline) on 0.10 M H_2SO_4 and 0.03 M $(NH_4)_2S_2O_8$ subphase at 25 °C.

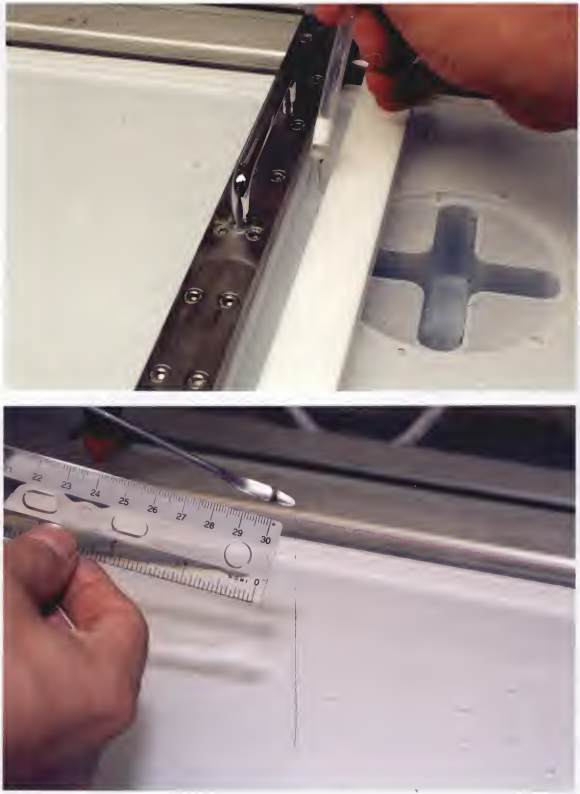

Figure 6.8. Top: the removal of poly(1,22-bis[2-aminophenyl]docosane) from the trough's surface. Bottom: a single fiber of poly(1,22-bis[2-aminophenyl]docosane).

onset areas of ca. 35 $Å^2$ repeat $unit^{-1}$. As in the case of the π-A isotherms of the monomers on 0.10 M H_2SO_4, the polymer of the dipolar compound has a lower collapse pressure when compared to that of poly(2-pentadecylaniline).

Once the polymerization was complete, the polymer was removed from the interface. The material was collected by first compressing the trough barriers to ca. 2 cm and then a glass frit connected to vacuum was used to pull the material from the aqueous surface (Figure 6.8). Unlike poly(2-pentadecylaniline), this material was gel like and was collected essentially in one piece. The material was insoluble in the solvents that usually solubilize polyaniline (N-methyl pyrrolidinone and sulfuric acid) and in the solvents

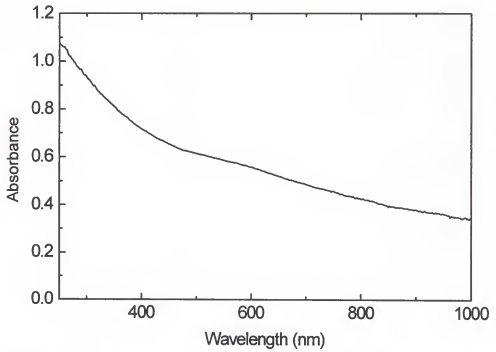

Figure 6.9. Absorption spectra of poly(1,22-bis[2-aminophenyl]docosane film on a quartz slide.

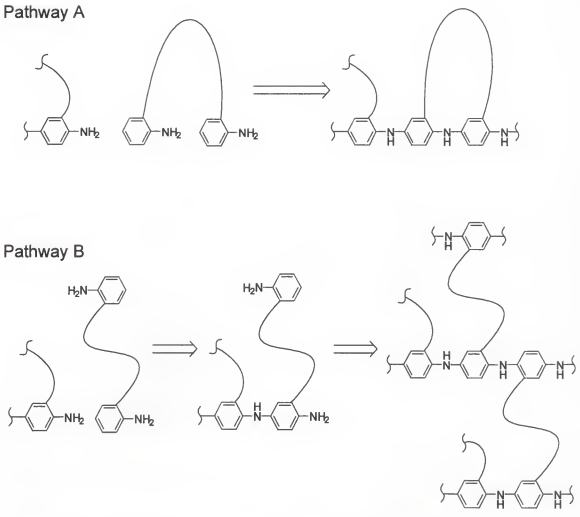

Figure 6.10. Two possible polymerization pathways of 1,22-bis(2-aminophenyl)docosane.

typically used for poly(2-pentadecylaniline) (chloroform and tetrahydrofuran). Further, no solvent was found that would solubilize this polymer, which made analysis by GPC and FT-IR impossible.

The only characterization available was UV-vis. Therefore, the polymer was transferred to a quartz slide and an absorption spectrum of the material was recorded (Figure 6.9). This very dark blue material had a broad absorbance over the region

between 250 and 1000 nm. A dark blue material is characteristic of the material that is produced in the polymerization of 2-pentadecylaniline in a Langmuir film.

Due to the two reactive anilinium groups of 1,22-bis(2-aminophenyl)docosane, there are several ways of ordering the anilinium group in the backbone of the polymer (Figure 6.10). One possible pathway (A) involves incorporating the anilinium groups such that connected groups are next to each other in a single polymer chain. This pathway would probably lead to a material with properties similar to those of poly(2-pentadecylaniline). A second possible pathway (B) would incorporate connected anilinium groups into the backbones of different polyaniline chains. It is this pathway that would lead to crosslinked polyaniline. It is also possible that both pathways could occur simultaneously. This third option would also lead to a network polymer, but to a lesser degree. The insolubility of the material and the fact that it could be lifted from the aqueous interface in one piece suggests that pathway B is occurring to some extent and that a 2-dimensional polymer was formed.

6.5 Conclusions

Preliminary results show that 1,22-bis(2-aminophenyl)docosane can be polymerized to form a novel, stable, insoluble material in a Langmuir film. The surface behavior of this dipolar molecule is analogous to the behavior of 2-pentadecylaniline under similar conditions as described in Chapter 3. The onset pressure area of 1,22-bis(2-aminophenyl)docosane on a 0.10 M H_2SO_4 was approximately double that of 2-

pentadecylaniline, and the collapse pressure was lower by 20 mN m^{-1}. It was concluded from the comparison of the π-*A* isotherms that both of the polar anilinium ions of 1,22-bis(2-aminophenyl)docosane were adsorbed to the aqueous surface with the hydrophobic hydrocarbon chain oriented away from the surface. A similar effect was observed at high surface areas for methyl 17-(2-aminophenyl) heptadecanoate and 17-(2-aminophenyl) heptadecanoic acid (Chapter 5).

The Langmuir film polymerization kinetics of 1,22-bis(2-aminophenyl)docosane were similar to that presented for 2-pentadecylaniline; however, at the beginning of the reaction, the rate appeared to be faster. It was hypothesized that the surface area occupied by an unreacted anilinium group attached to one that has been incorporated into the polymer backbone may be decreased, giving the appearance of an increased rate.

Since 1,22-bis(2-aminophenyl)docosane has two polymerizable groups adsorbed to the interface, the Langmuir polymerization resulted in a two-dimensional network polymer. Though more study of this polymer is needed, it is apparent that this material has stability that is rarely observed in films of this type. This stability could lead to a wider acceptance of highly ordered LB films in technical applications.

CHAPTER 7

CONCLUSIONS

Chapter 7 is a brief summary of the surface behavior and Langmuir polymerization of the aniline surfactants presented in this dissertation. Further, experiments are suggested that may give additional insight into the chemistry herein.

The surface behavior of 2-, 3-, and 4-pentadecylaniline was investigated using surface pressure and potential measurements in Langmuir films. The results suggest that the relative orientation of the head group changes with increased surface pressure to accommodate smaller areas and is dependent on the structure of the molecule. For example, the orientational change of the symmetric 4-pentadecylaniline was insignificant, while 2-pentadecylaniline changed considerably.

The polymerization rate of 2-pentadecylaniline was sensitive to applied surface pressure while 3-pentadecylaniline was less sensitive, which indicates that the *ortho* isomer reoriented with changing area. The overall rate constant of the polymerization was attributed to two constants; k, is the rate at the beginning of the reaction and can be called the true rate constant , and k' is the rate attributed to autoacceleration. The oxidation potential of the monomer affected k, and k' was sensitive to surface pressure.

The faster reaction rate of the *ortho* isomer was attributed to a lower oxidation potential and a more favorable alignment for polymerization.

The surface behavior of 2- and 3-(1-octadecynyl)aniline was investigated and compared to the alkyl monomers. The initial polymerization rates of 2-(1-octadecynyl)aniline increased as much as ten fold when compared to the rates of 2-pentadecylaniline at the same surface pressures, but no autoacceleration was observed. Since the initiation rates of the *ortho* alkynyl monomer were much greater than that of the *ortho* alkyl isomer, a useful experiment to investigate molecular weight control might be to polymerize mixed monolayers the two. Adding small amounts of the alkynyl surfactant to the film may speed the reaction but adding greater amounts may reduce molecular weight.

The results presented in Chapters 3 and 4 suggest that optimum orientation for Langmuir polymerization of the aniline surfactants occurs when the amino group and the *para* position of adjacent surfactant molecules are aligned. Kinetic results suggest that the *ortho* isomers react much faster than the *meta* isomers, which indicates that alignment may be better in the former case.

There have been few published reports on the study of dipolar surfactants in Langmuir films. Films of these types of molecules may find use as model compounds for the study of the surface behavior of preformed polymers with hydrophilic moieties as they may mimic the behavior of the more complex polymers.

Methyl 17-(2-aminophenyl)heptadecanoate and 17-(2-aminophenyl)heptadecanoic acid are dipolar surfactants that were studied in a Langmuir environment. At large

surface areas, both polar ends of the molecules were adsorbed to the water surface. Upon film compression, an apparent phase transition was observed in the π-A isotherms, which probably resulted from the desorption of one polar group from the interface. In the case of 17-(2-aminophenyl)heptadecanoic acid, surface potential data suggested that the aminophenyl and carboxylic acid ends of the molecule were leaving (and remaining at) the surface as ion pairs, forming a unique monolayer film. Methyl 17-(2-aminophenyl) heptadecanoate also had a transition during its compression, but the data indicated that only the aminophenyl group was desorbed while the methyl ester groups remained at the surface.

A surface behavior study of 1,22-docosanedioic acid and dimethyl 1,22-docosanedioate (a disubstituted carboxylic acid and a disubstituted methyl ester, respectively) would provide additional insight into the monolayers discussed in Chapters 5 and 6. These symmetric, dipolar molecules could be easily prepared using the synthetic methodology described in Chapter 6. By comparing surface pressure and potential data from these systems, a more accurate determination of the surface areas and dipole moments could be assigned.

The polymerization of methyl 17-(2-aminophenyl)heptadecanoate produced low molecular weight oligomer, which was attributed to hindrance from the methyl ester groups that were unable to diffuse away from the growing polymer chains. This theory could be tested by polymerizing mixed monolayer films that contain varying concentrations of 2-pentadecylaniline. If the molecular weight of the resulting polymer

increased with increased 2-pentadecylaniline concentration, it would indicate that the methyl ester group was inhibiting polymerization.

1,22-Bis(2-aminophenyl)docosane was synthesized via a ruthenium alkylidene catalyzed methathesis coupling and polymerized in a Langmuir film. Surface characterization showed that both anilinium ends were at the aqueous surface at lower surface pressures and its polymerization kinetics mirrored that of 2-pentadecylaniline. Upon polymerization, this molecule formed a unique, 2-dimensional, network polymer that was insoluble in common organic solvents and could be lifted from the trough in one piece. The mechanical stability and insolubility that made this polymer so unique also made charaterization by the usual techniques impossible. The study of the polymerization of mixed monolayers of 1,22-bis(2-aminophenyl)docosane and a monopolar aniline surfactant like 2-pentadecylaniline may lead to materials that are lightly crosslinked and have added stability, but are still soluble and could be characterized.

The results presented in this dissertation have lead to a better understanding of how molecular structure affects molecular orientation, which can affect reactivity. If the reactivity of surfactants in Langmuir films can be controlled, properties, such as molecular weight, may also be optimized. By designing surfactants with desired reactivity and pendant side chain functionality, highly oriented Langmuir and Langmuir-Blodgett films may be developed and find use in applications like corrosion inhibition, sensors, and lithography.

LIST OF REFERENCES

1. Giles, C. H.; Forrester, S. D.; Roberts, G. G. In Langmuir-Blodgett Films, Roberts, G. G., Ed.; Plenum Press: New York, 1990; Chapter 1.

2. Franklin, B., Philos. Trans. R. Soc. London, 64, 445 (1774).

3. Lord Rayleigh, Proc. R. Inst. London, 47, 281 (1890).

4. Lord Rayleigh, Proc. R. Inst. London, 47, 364 (1890).

5. Lord Rayleigh, Proc. R. Inst. London, 13, 85 (1890).

6. Lord Rayleigh, Proc. R. Inst. London, 48, 127 (1890).

7. Lord Rayleigh, Philos. Mag., 30, 386 (1890).

8. Lord Rayleigh, Philos. Mag., 48, 321 (1899).

9. Pockels, A., Nature (London), 43, 437 (1891).

10. Pockels, A., Nature (London), 46, 418 (1892).

11. Pockels, A., Nature (London), 48, 152 (1893).

12. Ganies, G. L., Insoluble Monolayers at Liquid-Gas Interfaces; Interscience Publishers: NewYork, 1966.

13. Langmuir, I., J. Am. Chem. Soc., 39, 1848 (1917).

14. Castellan, G. W., Physical Chemistry, 3rd Ed., Addison-Wesley: Reading, MA, 1983; Chapter 18.

15. MacRitchie, F., Chemistry at Interfaces, Academic Press: San Diego, 1990.

16. Oliveira, O. N.; Taylor, D. M.; Lewis, T. J.; Salvagno, S.; Stirling, C. J. M., J. Chem. Soc. Faraday Trans. 1, 85, 1009 (1989).

17. Davies, J. T.; Rideal, E. K., Can. J. Chem., 33, 947 (1955).

18. Davies, J. T.; Rideal, E. K., Interfacial Phenomena, 2nd Ed., Academic Press: New York, 1963.

19. Demchak, R. J.; Tomlinson, F., J. Colloid Interface Sci., 46, 191 (1974).

20. Gouy, J., Phys. Radium., 9, 457 (1910).

21. Oliveira, O. N.; Taylor, D. M.; Morgan, H., Thin Solid Films, 210/211, 76 (1992).

22. Thomas, W., Phil. Mag., 46, 82 (1898).

23. Zisman, W. A., Rev. Sci. Instrum., 3, 367 (1932).

24. Venselaar, J. L. M.; Kruger, A, J.; Verbakel, L. M. H.; Poulis, J. A., J. Colloid Inst. Sci., 70, 149 (1979).

25. Jacobs, J. C.; Buuron, A. J. M.; Render, P. J. M.; Snik, A. F. M., J. Colloid Int. Sci., 84, 270 (1981).

26. Schulman, J. H.; Hughes, Proc. Roy. Soc., A138, 430 (1932).

27. Schulman, J. H.; Rideal, E. K., Proc. Roy. Soc., A130, 270 (1931).

28. Adam, N. K.; Harding, J. B., Proc. Roy. Soc., A138, 411 (1932).

29. Langmuir, I *Trans.,* Faraday Soc., 15, 74 (1920).

30. Blodgett, K. B., J. Am. Chem. Soc., 56, 495 (1934).

31. Blodgett, K. B., J. Am. Chem. Soc., 57, 1007 (1935).

32. Langmuir, I; Schaefer, V. K. Sobotka, H., J. Am. Chem. Soc., 59, 1751 (1937).

33. Petty, M. C.; Barlow, W. A. In Langmuir-Blodgett Films, Roberts, G., Ed.; Plenum Press: New York, 1990; Chapter 3.

34. Tsibouklis, J., J. Mater. Chem., 1, 819 (1991).

35. Baniel, A.; Frankel, M.; Friedrich, I.; Katchalsky, A., J. Org. Chem., 13, 791 (1948).

36. Ringsdorf, H.; Bader, H.; Dorn, K.; Hupfer, B., Adv. Polym. Sci., 64, 1 (1985).

37. Shimidzu, T., Reactive Polymers, 11, 177 (1989).

38. Shimidzu, T.; Iyoda, T.; Ando, M.; Kaneko, T.; Ohtani, A.; Honda, K., Langmuir, 3, 1169 (1987).

39. Shimidzu, T.; Ando, M.; Watanabe, Y.; Iyoda, T.; Honda, K., Thin Solid Films, 179, 225 (1989).

40. Tieke, B. In Polymerization in Organized Media, Paleos, M., Ed.; Gordon and Breach Science: Philadelphia, 1992; Chaper 2.

41. Bain, C. D.; Whitesides, G. M., Angew. Chem. Int. Ed. Engl., 28, 506 (1989).

42. Sagiv, J., J. Am. Chem. Soc, 102, 92 (1980).

43. Hong, H.; Jang, M.; Sligar, S. G.; Bohn, P. W., Langmuir, 10, 153 (1994).

44 Nakagawa, T.; Ogawa, K.; Kurumizawa, T., Langmuir, 10, 525 (1994).

45. Porter, M. D.; Bright, T. B.; Allara, D. L.; Chidsey, C. E. D., J. Am. Chem. Soc., 109, 3559 (1987).

46. Bain, C. D.; Troughton, E. B.; Tao, Y.; Evall, J.; Whitesides, G. M.; Nuzzo, R. G., J. Am. Chem. Soc., 111, 321 (1989).

47. Weisshaar, D. E.; Lamp, D. E.; Porter, M. D., J. Am. Chem. Soc., 114, 5860 (1992).

48. Weisshaar, D. E.; Walczak, M. M.; Porter, M. D., Langmuir, 9, 323 (1993).

49. Zhong, C.; Porter, M. D., J. Am. Chem. Soc , 116, 11616 (1994).

50. Chambrier, I.; Cook, M. J.; Russell, D. A., Synthesis, 1283 (1995).

51. Mumbauer, P. D.; Carey, D. H.; Ferguson, G. S., Chem. Mater., 7, 1303 (1995).

52. Takehara, K.; Takemura, H., Bull. Chem. Soc. Jpn., 68, 1289 (1995).

53. Nuzzo, R. G., Allare, D. L., J. Am. Chem. Soc., *105*, 4481 (1983).

54. Shinkai, S.; Inuzuka, K.; Miyazaki, O., J. Am. Chem. Soc., 107, 3950 (1985).

55. Biebuyck, H. A.; Whitesides, G. M., Langmuir, 9, 1766 (1993).

56. Takemi, T.; Delamarche, B. M., Gerber, C.; Wolf, H.; Ringsdorf, H., Langmuir, 11, 3876 (1995).

57. Allara, D. L.; Nuzzo, R. G., Langmuir, 1, 45 (1985).

58. Ogawa, H.; Chihera, T. Taya, K., J. Am. Chem. Soc., 107, 1365 (1985).

59. Schlotter, N. E.; Porter, M. D.; Bright, T. B.; Allara, D. L., Chem. Phys. Lett., 132, 93 (1986).

60. Ulman, A., An Introduction to Ultrathin Organic Films; Academic Press: Boston, 1991.

61. Ulman, A., Characterization of Organic Thin Films; Butterworth-Heinemann: Boston, 1995.

62. Marsden, J.; Rideal, E. K., J. Chem. Soc., 1163 (1938).

63. Mittelmann, R.; Palmer, R. C., Trans. Faraday Soc., 38, 506 (1942).

64. Davies, J. T., Trans. Faraday Soc. 38, 506, (1949).

65. Alexander, A. E.; Schulman, J. H., Proc. Roy. Soc., *A161*, 115 (1937).

66. Gee, G., Faraday Trans., 32, 187 (1936).

67. Hatada, M.; Nishii, M.; Hirota, K., Macromolecules, 8, 19 (1975).

68. Dubault, A.; Casagrande, C.; Veyssie, M., J. Phys. Chem., 21, 2254 (1975).

69. Rolandi, R.; Paradiso, R.; Xu, S. Q.; Palmer, C.; Fendler, J. H., J. Am. Chem. Soc., 111, 5233 (1989).

70. Peltonen, J. P. K.; Pingsheng, H.; Rosenholm , J. B., Thin Solid Films, 210/211, 372 (1992).

71. Peltonen, J. P. K.; Pingsheng, H.; Linden, M.; Rosenholm , J. B., J. Phys. Chem., 98, 12403, (1994).

72. Parodi, M. T.; Bonfiglio, A.; Bianco, B.; Ruggeri, G.; Ciardelli, F., Thin Solid Films, 295, 234 (1997).

73. Tan, Y. Y. In Comprehensive Polymer Science, Pergamon Press, Inc.: New York, 1989, vol. 3, 245.

74. Kabanov, V. A. In Polymerization in Organized Media, Paleos, M., Ed.; Gordon and Breach Science: Philadelphia, 1992; Chaper 7.

75. Percec, V.; Jonsson, H.; Tomazos, D. In Polymerization in Organized Media, Paleos, M., Ed.; Gordon and Breach Science: Philadelphia, 1992; Chaper 1.

76. Paleos, C. M. In Polymerization in Organized Media, Paleos, M., Ed.; Gordon and Breach Science: Philadelphia, 1992; Chaper 3.

77. Candau, F. In Polymerization in Organized Media, Paleos, M., Ed.; Gordon and Breach Science: Philadelphia, 1992; Chaper 4.

78. Lando, J. B.; O'Brien, K. C.; Rogers, C. E., Thin Solid Films, 102, 131 (1983).

79. Lando, J. B.; O'Brien, K. C.; Long, G., Langmuir, 1, 514 (1985).

80. Girling, I. R.; Kolinsky, P. V.;Cade, N. A.; Earls, J. D.; Peterson, I. R., Opt. Commun. , 55, 289 (1985).

81. Neal, D. B.; Petty, M. C.; Roberts, G. G.; Ahmad, M. M.; Feast, W. J.; Girling, I. R.; Cade, N. A.; Kolinsky, P. V.; Peterson, I. R., Electron. Lett., 22, 460 (1986).

82. Roberts, G. G., Adv. Phys., 34, 475 (1985).

83. Roberts, G. G., Sensors and Actuators, 4, 131 (1984).

84. Novotny, V.; Swalen, J. D.; Rabe, J. P., Langmuir, 5, 485 (1989).

85. Arndt, T.; Schupp, H.; Schrepp, W., Thin Solid Films, 178, 319 (1989).

86. Barraud, A., Thin Solid Films, 99, 317 (1983).

87. Fuchs, H.; Ohst, H.; Prass, W., Adv. Mat., 3, 10 (1991).

88. Gee, G., Proc. Roy. Soc., (London), A153, 116 (1935).

89. Gee, G., Proc. R. Soc. London A, CLIII, 129 (1936).

90. Hatada, M.; Nishii, M.; Hirota, K., J. Colloid Interface. Sci., 45, 502 (1973).

91. Tamura, H.; Mino, N.; Ogawa, K., Thin Solid Films, 179, 33 (1989).

92. Folda, T.; Gros, L.; Ringsdorf, H., Makromol. Chem. Rapid Commun., 3, 167 (1982).

93. Duran, R. S.; Zhou, H. C., Polymer, 33, 4019 (1992).

94. Zhou, H.; Stern, R.; Batich, C.; Duran, R. S., Makromol. Chem., Rapid Commun., 11, 409 (1990).

95. Bodalia, R. R.; Duran, R. S., J. Am. Chem. Soc., 115, 11467 (1993).

96. Wei, Y.; Sun, Y; Tang, X., J. Phys. Chem., 93, 4878 (1989).

97. Shim, Y. B.; Park, S. M., Synth. Met., 29, E169 (1989).

98. Tzou, K.; Gregory, R. V., Synth. Met , 47, 267 (1992).

99. Bodalia, R; Manzanares, J. Reiss, H. Duran, R., Macromolecules, 27, 2002 (1994).

100. Kloeppner, L. J; Nguyen, C. K.; Duran, R. S., Polym. Prepr., Am. Chem. Soc. Div Polym. Chem., 36(1), 580 (1995).

101. Shirakawa, H.; Louis, E. J.; MacDiarmid, A. G.; Chiang, C. K.; Heeger, A. J., J. Chem. Soc., Chem. Commun., 578 (1977).

102. Chiang, C. K.; Park, Y. W.; Heeger, A. J.; Shirakawa, H.; Louis, E. J.; MacDiarmid, A. G., Phys. Rev. Lett., 39, 1098 (1977).

103. Chiang, C. K.; Druy, M. A.; Gau, S. C.; Heeger, A. J.; Louis, E. J.; MacDiarmid, A. G.; Park, Y. W.; Shirakawa, H., J. Am. Chem. Soc., 100, 1013 (1978).

104. Syed, A. A., Talanta, 38, 815 (1991).

105. Reynolds, J. R.; Childs, A. D.; Gileselman, M. B. In Kirk-Othmer Encyclopedia of Chemical Technology; Vol. 9, John Wiley & Sons, 1994, 61.

106. MacDiarmid, A. G., Synth. Met., 84, 27 (1997).

107. Letheby, H., J. Chem. Soc., 15, 161 (1862).

108. Willstätter, R.; Dorogi, S., Chem. Ber., 42, 4118 (1909).

109. Willstätter, R.; Majima, R., Chem. Ber., 43, 2588 (1910).

110. Green, A. G.; Woodhead, A. E., J. Chem. Soc., Trans., 97, 2388 (1910).

111. Green, A. G.; Woodhead, A. E., J. Chem. Soc., Trans., 101, 1117 (1912).

112. Lux, F., Polymer, 35, 2915 (1994).

113. Wudl, F.; Angus, R. O.; Lu, F. L.; Allemand, P. M.; Vachon, D. J.; Nowak, M.; Liu, Z. X.; Heeger, A. J. J. Am. Chem. Soc., 109, 3677 (1987).

114. Vachon, D.; Angus, R. O.; Lu, F. L.; Nowak, M.; Liu, Z. X. Schaffer, H.; Wudl, F.; Heeger, A. J., Synth. Met., 18, 297 (1987).

115. Wilbur, J. M.; Snadreczki, T. C.; Brown, I. M.; Leopold, D. J.; Mohite, S., Synth. Met., 82, 175 (1996).

116. Chiang, J. C.; MacDiarmid, A. G., Synth. Met., 13, 193 (1986).

117. Genies, E. M.; Syed, A. A.; Tsintavis, C., J. Electroanal. Chem., 195, 109 (1985).

118. Geines, E. M.; Tsintavis, C., J. Electroanal. Chem., 195, 109 (1985).

119. Mohilner, D. M.; Adams, R.N.; Argersinger, W. J., J. Am. Chem. Soc., 84, 3618 (1962).

120. Breitenbach, M; Heckner, K. -H., J. Electroanal. Chem., 29, 309 (1971).

121. Breitenbach, M.; Heckner, K. -H., J. Electroanal. Chem., 33, 45 (1971).

122. Breitenbach, M; Heckner, K. -H., J. Electroanal. Chem., 43, 267 (1973).

123. Hand, R. L.; Nelson, R. F., J. Am. Chem. Soc., 96, 850 (1974).

124. Hand, R. L.; Nelson, R. F., J. Electrochem Soc., 125, 1059 (1978).

125. Genies, E. M.; Lapkowski, M., J. Electoanal. Chem., 236, 189 (1987).

126. Bacon, J.; Adams, R. N., J. Am. Chem. Soc., 90, 6596 (1968).

127. Wei, Y.; Jang, G.; Chan, C.; Hsueh, K. F.; Hariharan, R.; Patel, S. A.; Whitecar, C. K., J. Phys. Chem., 94, 7716 (1990).

128. Wei, Y.; Hariharan, R.; Patel, S. A., Macromolecules, 23, 758 (1990).

129. Duic, L.; Mandic, Z.; Kovac, S., Electochimica Acta., 40, 1681 (1995).

130. Genies, E. M.; Tsintavis, C., J. Electroanal. Chem., 195, 109 (1985).

131. Kobayashi, T.; Yoneyama, H.; Tamura, H., J. Electroanal. Chem., 161, 419, (1984).

132. Reynolds, J. R.; Poropatic, P. A.; Toyooka, R. L., Macromolecules, 20, 958 (1987).

133. Pud, A. A., Synth. Met., 66, 1 (1994).

134. Bodalia, R.; Stern, R.; Batich, C.; Duran, R., J. Polym. Sci., Polym. Chem. Ed., 31, 2123 (1993).

135. Sonogashira, K.; Tohda, Y.; Hagihara, N., Tetrahedron Lett., 4467 (1975).

136. Evans, S. D. In Characterization of Organic Thin Films, Ulman, A., Ed.; Butterworth-Heinemann: Boston, 1995; Chapter 6.

137. Adams, R. N., Electrochemistry at Solid Electrodes; Marcel Dekker: New York, 1969.

137. Letts, S.A.; Fort, T.; Lando, J. B., J. Colloid Interface Sci., 56, 64 (1976).

138. Gee, G., Proc. R. Soc, 32, 39 (1935).

139. Fukuda, K.; Shibasaki, Y.; Nadahara, H., J. Macromol. Sci. Chem., A15, 999 (1981).

140. Shibata, A; Oasa, A.; Hashimura, Y.; Yamashita, S.; Ueno, S.; Yamashita, T., Langmuir , 6, 217 (1990).

141. Bodalia, R. Ph.D. Dissertation, Univerisity of Florida, Dec. 1993.

142. Herod, T. Ph.D. Dissertation, Univerisity of Florida, Dec. 1997.

143. Zhao, X.; Subrahmanyan, S.; Eisenthal, K. B., Chem. Phys. Lett., 171, 558 (1990).

144. Hann, R. A. In Langmuir-Blodgett Films, Roberts, G. G., Ed.; Plenum Press: New York, 1990; Chapter 2.

145. Vogel, V.; Möbius, D., J. Colloid Interface Sci., 126, 408, (1988).

146. Baglioni, P.; Dei, L.; Gabrielli, G.; Innocenti, F. M.; Niccolai, A.,Colloid and Polym. Sci., 266, 783 (1988).

147. Caminati, G.; Gabrielli, G.; Puggelli, M.; Ferroni, E.,Colloid and Polym. Sci., 267, 237 (1989).

148. Lee, J. Y.; Ong, L. H.; Chuah, G. K., J. Appl. Electrochem., 23, 1031 (1993).

149. Harkins, W. D.; Fischer, E. K., J. Chem. Phys., 1, 852 (1933).

150. Genies, E. M.; Boyle, A.; Lapkowski, M.; Tsintavis, C., Synth. Met., 36, 139 (1990).

151. Harada, I.; Furukawa, Y.; Ueda, F., Synth. Met., 29, E303 (1989).

152. Yan, H.; Wang, H.; Adisasmito, S.; Toshima, N., Bull. Chem. Soc. Jpn., 69, 2395 (1996).

153. Kellner, B. M. J.; Cadenhead, D. A., J. Colloid Interface Sci., 63, 452 (1978).

154. Kellner, B. M. J.; Cadenhead, D. A., Chem. Phys. Lipids, 23, 41 (1979).

155. Duran, R. S.; Zhou, H. C., Thin Solid Films, 210/211, 356 (1992).

156. Spink, J. A., J. Colloid Sci., 18, 512 (1963).

157. Steitz, R.; Peterson, I. R.; Voigt-Martin, I.; Möhwald, H., Thin Solid Films, 178, 289 (1989).

158. Dubault, C.; Casagrande, M.; Veyssie, M., J. Phys. Chem., 79, 2254 (1975).

159. Rosilio, C.; Ruaudel-Teixier, A.; J. Polym. Sci. Polym. Chem. Ed. 13, 2459, (1975).

160. Emmerling, W. N.; Pfannemüller, B., Colloid and Polym. Sci., 261, 677 (1983).

161. Porteu, F.; Palacin, S.; Ruaudel-Teizier, A.; Barraud, A., Makromol. Chem., Macromol. Symp., 46, 37 (1991).

162. Schwab, P.; France, M. B.; Ziller, J. W.; Grubbs, R. H., Angew. Chem., Int. Ed., 34, 2039 (1995).

163. Crowe, W. E.; Zhang, Z. J., J. Am. Chem. Soc., 115, 10998 (1993).

164. Crowe, W. E.; Goldberg, D. R., J. Am. Chem. Soc., 117, 5162 (1995).

BIOGRAPHICAL SKETCH

The author was born in St. Cloud, Minnesota, on the 12th of January 1964. As the fifth child of eight, he spent many long days working on the family farm in central Minnesota. In 1982, the author started undergraduate studies at St. Cloud State University and majored in photographic science and engineering, with a minor in chemistry. After graduation, he took a job in a wholesale photofinishing lab as an assistant manager. After two years, he returned to St. Cloud State University and obtained his B.S. in chemistry. Completing his degree in 1991, the author started graduate school at the University of Rochester. At Rochester, he conducted research in organic photochemistry under the advisement of Dr. David Whitten. In 1993, he obtained his M.S. in organic chemistry and moved to Florida to continue graduate studies of the University of Florida. At the University of Florida, the author conducted research in organic polymer science under the advisement of Dr. Randy Duran. While at the University of Florida, the author met and married his wife, Jennifer who also is a graduate student in the university chemistry department.

I certify that I have read this study and that in my opinion it conforms to acceptable standards of scholarly presentation and is fully adequate, in scope and quality, as a dissertation for the degree of Doctor of Philosophy.

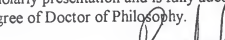

Randolph S Duran, Chairman
Associate Professor of Chemistry

I certify that I have read this study and that in my opinion it conforms to acceptable standards of scholarly presentation and is fully adequate, in scope and quality, as a dissertation for the degree of Doctor of Philosophy.

John R. Reynolds
Professor of Chemistry

I certify that I have read this study and that in my opinion it conforms to acceptable standards of scholarly presentation and is fully adequate, in scope and quality, as a dissertation for the degree of Doctor of Philosophy.

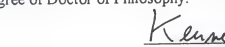

Kenneth B. Wagener
Professor of Chemistry

I certify that I have read this study and that in my opinion it conforms to acceptable standards of scholarly presentation and is fully adequate, in scope and quality, as a dissertation for the degree of Doctor of Philosophy.

Kirk S. Schanze
Professor of Chemistry

I certify that I have read this study and that in my opinion it conforms to acceptable standards of scholarly presentation and is fully adequate, in scope and quality, as a dissertation for the degree of Doctor of Philosophy.

Dinesh O. Shah
Charles A. Stokes Professor of Chemical Engineering

This dissertation was submitted to the Graduate Faculty of the Department of Chemistry, in the College of Liberal Arts and Sciences and to the Graduate School and was accepted as partial fulfillment of the requirements for the degree of Doctor of Philosophy.

December, 1998

_____

Dean, Graduate School